VOLUME 33 SEPTEMBER 1955 NUMBER 9

Canadian Journal of Chemistry

Published by THE NATIONAL RESEARCH COUNCIL

OTTAWA CANADA

CANADIAN JOURNAL OF CHEMISTRY

(*Formerly Section B, Canadian Journal of Research*)

Under the authority of the Chairman of the Committee of the Privy Council on Scientific and Industrial Research, the National Research Council issues THE CANADIAN JOURNAL OF CHEMISTRY and six other journals devoted to the publication, in English or French, of the results of original scientific research. Matters of general policy concerning these journals are the responsibility of a joint Editorial Board consisting of: members representing the National Research Council of Canada; the Editors of the Journals; and members representing the Royal Society of Canada and four other scientific societies.

The Chemical Institute of Canada has chosen the Canadian Journal of Chemistry and the Canadian Journal of Technology as its medium of publication for scientific papers.

Manuscripts for publication should be submitted to Dr. Léo Marion, Editor-in-Chief, Canadian Journal of Chemistry, National Research Council, Ottawa 2, Canada.
(For instructions on preparation of copy, see **Notes to Contributors** (inside back cover).)

Proof, correspondence concerning proof, and orders for reprints should be sent to the Manager, Editorial Office (Research Journals), Division of Administration, National Research Council, Ottawa 2, Canada.

Subscriptions, renewals, requests for single or back numbers, and all remittances should be sent to Division of Administration, National Research Council, Ottawa 2, Canada. Remittances should be made payable to the Receiver General of Canada, credit National Research Council.

The journals published, frequency of publication, and prices are:

Canadian Journal of Biochemistry and Physiology	Bimonthly	$3.00 a year
Canadian Journal of Botany	Bimonthly	$4.00 a year
Canadian Journal of Chemistry	Monthly	$5.00 a year
Canadian Journal of Microbiology*	Bimonthly	$3.00 a year
Canadian Journal of Physics	Monthly	$4.00 a year
Canadian Journal of Technology	Bimonthly	$3.00 a year
Canadian Journal of Zoology	Bimonthly	$3.00 a year

The price of single numbers of all journals is 75 cents.

*Volume 1 will combine three numbers published in 1954 with six published in 1955 and will be available at the regular annual subscription rate of $3.00.

Reprinted in entirety by photo-offset.

Canadian Journal of Chemistry

Issued by THE NATIONAL RESEARCH COUNCIL OF CANADA

VOLUME 33 SEPTEMBER 1955 NUMBER 9

LONDON – VAN DER WAALS ATTRACTIVE FORCES BETWEEN GLASS SURFACES[1]

BY P. G. HOWE,[2,3] D. P. BENTON,[2] AND I. E. PUDDINGTON

ABSTRACT

The attractive force between a pyrex glass bead and plate has been measured using a sensitive pendulum-type apparatus. The force required for separation of the bead from the plate has been shown to be strongly time dependent, a phenomenon which appears not to have been reported previously for adhesions in gaseous media. The observed results have been shown to be consistent with the theoretical London – van der Waals interaction. The estimated value of the London force constant is compared with that obtained by other workers.

INTRODUCTION

Many workers have shown the existence of attractive forces between solid surfaces. Tomlinson (11) demonstrated the adhesion between quartz fibers and between equal glass spheres. Bradley (1) confirmed this adhesion between quartz spheres and improved the method to measure the adhesion between sodium pyroborate spheres and quartz spheres of unequal size. He also established experimentally the theoretical dependence of adhesion on the ratio of the bead diameters. McFarlane and Tabor (9) attempted to measure the interaction between a suspended glass bead and a glass plate by means of a pendulum-type apparatus. With this apparatus adhesions as low as 10^{-6} *g* could theoretically be measured but in clean dry air no adhesion was observed. Courtney-Pratt (3) found considerable adhesion when freshly cleaved mica sheets were placed in contact. Spaarnay and Overbeek (10) found the existence of long range attractive forces between highly polished parallel glass plates and that the calculated force constant was of the expected magnitude. Derjaguin (4) has also shown the existence of adhesion between various glasses but disagrees with the magnitude of those obtained by Spaarnay and Overbeek. In this paper the existence of time-dependent attractive forces between glass surfaces has been demonstrated. These have been attributed to London – van der Waals attractive forces and have been shown to be consistent with theoretical considerations.

[1]*Manuscript received March 24, 1955.*
Contribution from the Division of Applied Chemistry, National Research Council, Ottawa, Canada. Issued as N.R.C. No. 3669.
[2]*N.R.L. Postdoctorate Fellow, 1953–55, National Research Council, Ottawa, Canada.*
[3]*Present address: American-Marietta Company, Adhesives and Resin Division, Seattle 4, Washington, U.S.A.*

EXPERIMENTAL

Measurements have been made of the adhesion between pyrex glass surfaces using various pendulum-type apparatuses, both *in vacuo* and in small pressures of nitrogen. In the main these apparatuses have consisted of a glass bead, about 1 mm. diameter, formed on the end of a very fine pyrex fiber which was suspended by sealing into a 25 mm. pyrex tube. Contact surfaces were variously a flame-polished glass plate, a convex surface drawn in from the wall of the container tube and approximately equivalent to a sphere of radius 25 mm., or the concave inner wall of the glass tube itself, preheated to the melting point of the glass. Both bead and contact surfaces were formed just prior to assembly and evacuation of the apparatus. The apparatus was then degassed at about 350°C. and mounted on an electrically driven slow-motion rotor arm. When not continuously attached to the vacuum line, the apparatus was sealed off or closed with a vacuum stopcock. Some tubes were coated externally with electrically conducting silver paint and effectively earthed.

The measurement of adhesion was carried out as follows. The bead was allowed to make contact with the plate for a certain time and then the deflection, α, of the bead suspension from the vertical at the break point was measured. As the fiber suspensions used were practically weightless compared with the weight of the bead, calculation of the adhesion was made assuming a rigid pivoted assembly, using the equation

$$F = mg. \sin \alpha \qquad [1]$$

where m is the weight of the bead.

The results obtained show that adhesion exists but that the interaction is strongly time dependent. Very large instantaneous adhesions were found with the freshly degassed apparatus. The time of contact required for maximum adhesion increased, while the maximum adhesion itself fell, as the initial hard vacuum decayed in the closed system to *ca.* 10^{-3} mm. The adhesion then fell off more slowly over a period of days until some reproducible lower maximum was obtained.

Fig. 1 shows the *typical* slow build-up of the adhesion which was consistently encountered. The decay of adhesion after separation of the bead from the plate was very rapid, as is also shown in Fig. 1. Measurement of this decay of adhesion was carried out as follows. After a required separation time a quick measurement of adhesion was made within the minimum time necessary to bring the bead up to the plate and rotate to find the angle of break. The contact time required for this operation was about 10 sec. and the residual adhesion in the decay curve is due to this short contact time. This is also shown in Fig. 2, which is essentially a detail from Fig. 1. Fig. 2 further shows the reproducibility of the adhesion build-up in successive determinations.

DISCUSSION

1. The time dependency is possibly determined by the viscous flow of the gaseous or adsorbed medium from the gap between the approaching bead and plate, since with the freshly degassed surfaces the adhesion is very large and

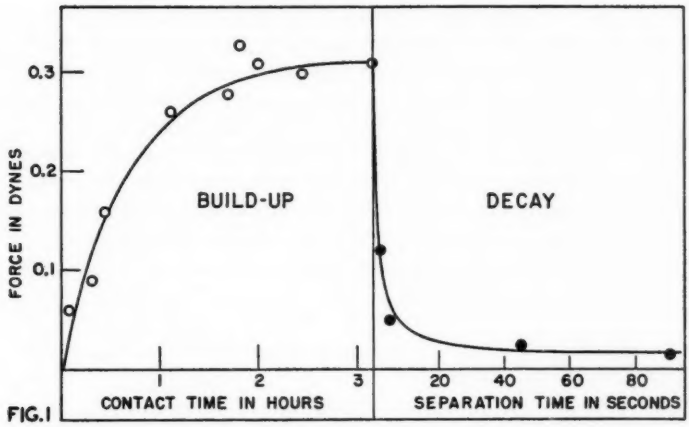

FIG. 1

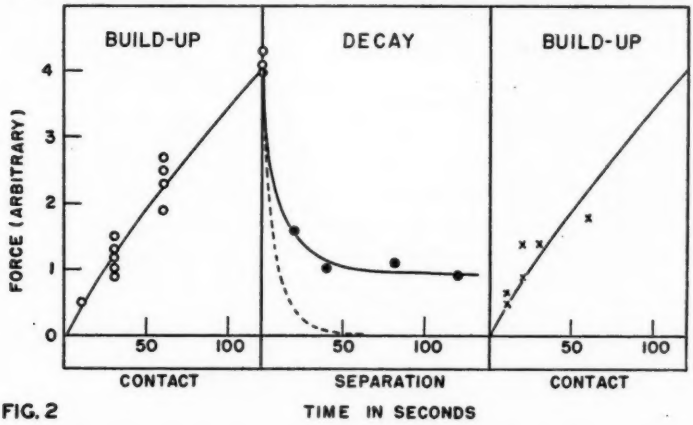

FIG. 2

FIG. 1. Adhesion build-up and decay for 0 7 mm. diameter bead and convex surface in decayed vacuum.

FIG. 2. Adhesion build-up and decay for 0.7 mm. diameter bead and convex surface in decayed vacuum. Residual adhesion of decay curve is due to short contact times required for force measurement.

instantaneous. If the movement over molecular distances of the bead towards the plate is responsible for the increase in adhesion with time, the time dependency of the decay may be explained by the reorientation of the molecules adsorbed on the surface. The initial rapid fall off in the maximum adhesion may be caused by this adsorption on the glass surface. The subsequent gradual fall off in the maximum adhesion might be attributed, in part, to the shock abrasion of the surfaces by repeated impact of the bead. Fig. 3 shows the decrease in the maximum adhesion over a period of several days in an apparatus containing 1 mm. of dry nitrogen. No very large adhesions were observed in atmospheres of nitrogen. The time required for the maximum adhesion

was very similar to that observed in a decayed vacuum although much greater than that required in freshly evacuated systems. This is consistent with the observed fall of the large maximum adhesions observed with freshly degassed and evacuated systems. The lower adhesions in atmospheres of nitrogen and the time dependence of the adhesion build-up might explain why McFarlane and Tabor (9) found no adhesion between glass surfaces in air. It is interesting to note that the adhesion kinetics reported in this paper are similar to those found by Derjaguin (4) for the interaction between quartz fibers in aqueous solution. The significance of this phenomenon in relation to the properties of suspensions is discussed elsewhere (7).

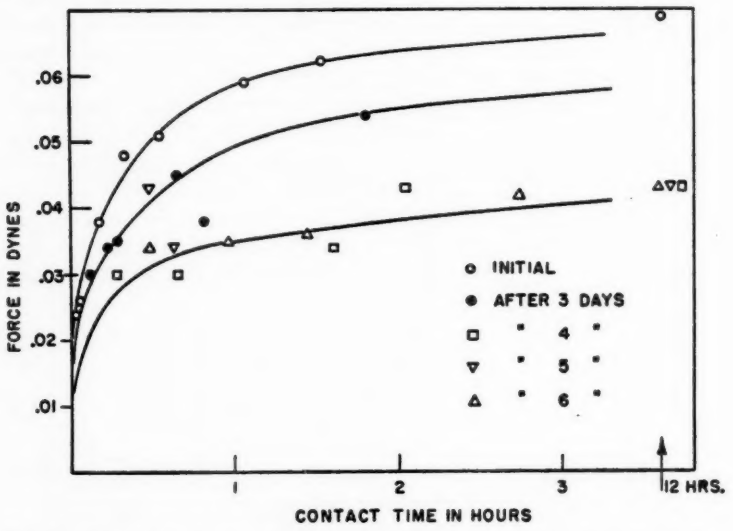

FIG. 3. Adhesion in 1 mm. nitrogen; 0.5 mm. diameter bead and convex surface.

In the course of the various experiments over a period of one year it was noted that the behavior of the bead was considerably affected by the induction of electrostatic charges. However, these decayed fairly rapidly and the consistent reproducibility of the adhesion and the adhesion kinetics points to the existence of attractive forces inherent in the system rather than spurious electrostatic charges. It seems unlikely that the mere 'contact' of the bead with the plate should induce electrostatic charge build-up. Also, the order of magnitude of the adhesion was found to be consistently the same in all experiments and with the various apparatuses used. In connection with this point it is interesting to refer to the behavior of glass spheres in anhydrous toluene (8). Agitation of the glass spheres in toluene apparently induces electrostatic charges which cause the beads to adhere to one another. Quite vigorous or prolonged agitation of the beads is required to produce agglomeration at room temperatures and the agglomerate collapses fairly rapidly in this temperature

region. Agitation of the beads alone, *in vacuo*, did not give any agglomeration, showing that the motion of the beads due to the supporting medium is important. In itself, this suggests that the contact of a bead with a plate is not sufficient to cause the build-up of an electrostatic attractive force. Furthermore, no indication of any increase in interparticle adhesion with time was obtained in the case of the uncharged sediments of glass spheres in various anhydrous liquids and with the glass beads *in vacuo*. If the observed time-dependent adhesion with the bead and the plate were electrostatic in origin, such an increase, of considerable magnitude, might be expected.

When the bead was brought into contact with the plate, it was allowed to rest under a small positive force. The application of larger positive forces did not seem to affect the observed adhesions. However, this was difficult to ascertain owing to the experimental difficulty of bringing the bead to the same position on the contact surface, since very small tangential forces would cause the bead to move in an arc, dictated by the fiber suspension, on the contact surface. Derjaguin (4) also observed the small dependence of the adhesion on the applied pressure in aqueous media.

McFarlane and Tabor (9) have shown that the elastic forces in the solid are important and that as the applied force is removed, contact points causing adhesion can break one by one. The measured adhesion is then the same as that without any applied load. In the above experiments it did not appear that elastic recovery prevented the measurement of adhesion. This is not surprising for two reasons; in the first place it is doubtful, except in the case of rigorously outgassed and freshly evacuated systems, whether the surfaces of the bead and plate in the above experiments ever were in true contact (continuous lattice formation) and secondly, elastic recovery at contact points implies an interaction between two irregular surfaces whereas in this case contact between the opposing lattices would be virtually at a single 'point' of molecular dimensions, if it occurred at all. It will be shown that the observed adhesion is consistent with the theoretical interaction expected for the close approach of the bead and the contact surface.

2. For the London – van der Waals force of interaction between a sphere and a plate Hamaker (5) obtains

$$F = AD/12d^2 \qquad [2]$$

where F is the force in dynes, $A = \pi^2 q^2 \lambda$, λ is the London constant, D is the diameter of the sphere in cm., d is the shortest distance of separation between the sphere and the plate in cm., and q is the number of atoms per cm^3.

This expression is not greatly affected by the curvature of the contact surface (the 'plate') as long as the radius of curvature of the plate is large compared with that of the bead. In the above experiments the curvature ratio was about 50 and any correction is of negligible importance, Fig. 4 shows the variation of F with d for a 1 mm. diameter bead, calculated from equation [2]. For a mean distance of close approach of 3–10 Å, which may be considered a reasonable range to assume for the approach between fused glass surfaces, it is seen that the attractive force would be in the vicinity of 10–100

dynes, taking the value of the A constant as 10^{-11} to 10^{-12} erg. This is consistent with the observation that the force of adhesion between freshly formed and rigorously degassed surfaces was well beyond the upper limit of force measurement of the apparatus which was about 1 dyne. The maximum adhesion measured with surfaces aged after evacuation and in atmospheres of nitrogen was generally of the order 0.1–0.2 dyne for beads of 1 mm. diameter. Taking the theoretical value of 10^{-12} for the force constant A, this corresponds

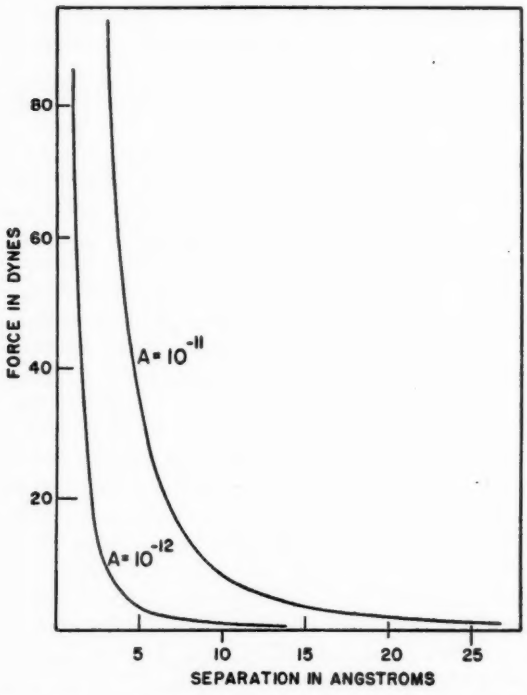

FIG. 4. Calculated interaction for 1 mm. diameter bead and plate.

to a distance of separation of 20–29 Å. This is a reasonable order for the effective separation in the presence of adsorbed foreign molecules in view of the separation considered *in vacuo*, and the fact that two solid surfaces are involved.

Table I shows the calculated variation in d, the closest distance of approach for perfect surfaces using the observed *maximum residual* forces of interaction. Using these values the selection of a value for the force constant A, which is consistent with the experimental evidence, will be considered. These residual forces were at least 10–100-fold less than the forces observed with freshly prepared and degassed systems *in vacuo*. This implies that the lower values of A, viz. 10^{-13} and 10^{-14}, can probably be eliminated since a 10–100-fold

TABLE I

CALCULATED SEPARATION BETWEEN 1 MM. DIAMETER BEAD AND PLATE FOR SELECTED VALUES OF THE A CONSTANT

A constant (ergs)	Separation d (Å)	
	$F = 0.1$ dyne	$F = 0.2$ dyne
10^{-10}	290	200
10^{-11}	91	65
10^{-12}	29	20
10^{-13}	9	7
10^{-14}	3	2

increase in the adhesion from the residual value would lead to a very unlikely value for the distance of closest approach, i.e., to within less than the diameter of an adsorbed gas molecule. Also, although fused glass surfaces are among the smoothest types of solid surfaces that can be obtained, surface undulations and discontinuities will possibly be of the order of 10–20 Å and this will tend to reduce the interaction. Calculated values of d will therefore tend to be too high, which favors the elimination of the lower values of the force constant.

For the residual adhesion it appears that the bead and the plate may be separated by adsorption products which prevent their approaching to within an atomic distance. It is unlikely that this adsorbed layer of gas could extend to over 50 Å from the surface of the solid, i.e., 10 or more molecular diameters. In view of this it is suggested that the values of 10^{-10} and 10^{-11} for A are too high. Adsorption studies in general indicate that after a few monolayers, adsorption energies are weak for physically adsorbed gases and approach normal bulk gaseous interactions. The observed results are therefore consistent with the adsorption of gaseous material and, with due allowance made for surface irregularities, the most favorable value of the A constant is about 10^{-12}, which agrees very well with the theoretical value.

3. The magnitude of the London – van der Waals interaction will depend on the value of the London constant, λ, which is included in the constant A. The direct experimental verification of the value of A is exceptionally difficult and the experimental results of different workers are conflicting. Table II shows the estimated values of A from the experimental data of other workers. These vary from about 10^{-10} to 10^{-14}, scattering about the theoretical estimate (2, 12) of 10^{-12} erg. For close approach between the surfaces a value of about 10^{-12} is general but Spaarnay and Overbeek (10) and Derjaguin (4), for wider distances of separation, give values which differ very considerably from one another. Unfortunately, the extreme sensitivity of the attraction to small changes of separation at close approach does not allow for a precise estimation of the force constant owing to the indeterminancy of the actual distance of separation, quite apart from other factors involved.

Derjaguin has suggested that the results of Spaarnay and Overbeek are too high owing to the inadequate removal of electrostatic mosaics from the glass surfaces. If this were the case it would seem surprising that the presence of water vapor or the coating of the glass plates with an evaporated silver layer

TABLE II

Author	Gaseous medium	Material	Minimum separation (Å)	A constant (ergs) ($\times 10^{12}$)
Bradley	Vacuum	Borate spheres	Close approach (3)	4.7*
	Vacuum	Quartz spheres	Close approach (3)	2.2*
Courtney-Pratt (3)	Air	Cleaved mica	Close approach (5–25)	0.1–10†
Spaarnay and Overbeek	Air	Glass plates 1	Close approach (200)	0.01–22
		Glass plates 2	Close approach (200)	0.015–15
		Glass plates 1	2500	1.1–30
		Glass plates 2	5000	60–230
		Quartz plates	3000	11–30
		Silvered quartz	8000	39–78
Derjaguin (4)	Air	Quartz sphere and plate	1000	0.05
Present authors	Vacuum and nitrogen	Pyrex glass bead and plate	Close approach	0.1–10†
Theoretical (2, 12)	Vacuum			1

After Hamaker (6).
†Estimates only. Calculated by present authors.*

did not affect the measured interaction. It appears that the important question of the electrical neutrality of the surface, either on a molecular or on a macro scale, has not yet been settled. If a charge mosaic were capable of stable existence on such surfaces then it might be expected that such a phenomenon might also be a dominant factor in many types of suspensoidal systems. For glass type solids, the major part of the London interaction has been attributed to the highly polarizable oxygen atoms. In view of this, it is perhaps surprising that freshly sheared dispersions of paraffin wax in methanol coagulate spontaneously on standing. Vold (13) has offered an explanation of the interparticle adhesion in soap greases based on the polarizability of the oxygen atoms in the predominantly hydrocarbon fiber matrix. It is interesting to note, however, that comparable interparticle attraction apparently exists in polyethylene greases, in which the solid particles are totally hydrocarbon in composition and are embedded in a hydrocarbon liquid. This might suggest that such attractions are predominantly electrostatic in nature rather than London-type interactions. Alternatively, the application of the London additivity theorem to the interaction between solids might be inadequate, as suggested by Spaarnay and Overbeek, and much higher interactions than calculated from the London theory might be possible. Apart from the possibility of charged surface mosaics, the existence of induced like charges on two interacting glass-type surfaces might also be possible and thus account for the reduced interactions observed by Derjaguin. However, the present authors obtained reproducible adhesions in systems where there was no introduction of ionizing contaminants. The reproducibility of the observed adhesions suggests that the attractive force is an inherent property of the system and not due to electrostatic forces. The observed adhesion kinetics support this inference and are, in themselves, extremely important in the understanding and evaluation of colloidal and other aggregative phenomena.

REFERENCES

1. BRADLEY, R. S. Phil. Mag. 13: 853. 1932.
2. CASIMIR, H. B. G. and POLDER, D. Phys. Rev. 73: 360. 1948.
3. COURTNEY-PRATT, J. S. Proc. Roy. Soc. (London), A, 202: 505. 1950.
4. DERJAGUIN, B. V. *et al.* Discussions Faraday Soc. No. 18: 24. 1954.
5. HAMAKER, H. C. Physica, 4: 1058. 1937.
6. HAMAKER, H. C. Rec. trav. chim. 57: 61. 1938.
7. HOWE, P. G. and BENTON, D. P. To be published.
8. HOWE, P. G., BENTON, D. P., and PUDDINGTON, I. E. Can. J. Chem. 33: 1189. 1955.
9. MCFARLANE, J. S. and TABOR, D. Proc. Roy. Soc. (London), A, 202: 224. 1950.
10. OVERBEEK, J. T. G. and SPAARNAY, M. J. Discussions Faraday Soc. No. 18: 12. 1954.
11. TOMLINSON, G. A. Phil. Mag. 6: 695. 1928.
12. VERWEY, E. J. W. and OVERBEEK, J. T. G. Theory of the stability of lyophobic colloids. Elsevier Publishing Co., Inc., New York. 1948. p. 32.
13. VOLD, M. J. N.L.G.I. Spokesman, 19: 24. April, 1955.

THE MESOMORPHIC BEHAVIOR OF ANHYDROUS SOAPS

PART I. LIGHT TRANSMISSION BY ALKALI METAL STEARATES[1]

By D. P. Benton,[2] P. G. Howe,[2] and I. E. Puddington

ABSTRACT

The anhydrous salts of the long chain fatty acids are known to pass through a number of well-defined mesomorphic forms between the true crystalline solid and the isotropic liquid. The nature of some of these mesomorphic forms has been investigated by a study of their optical properties, electrical conductivity, density, and viscosity. In this paper, results obtained by an optical method are presented for phase transition temperatures of the alkali metal stearates and a number of sodium stearates having substituents in the hydrocarbon chain.

INTRODUCTION

The extensive and varied studies that have been made, in the past two or three decades, of the mesomorphic forms of salts of the long chain fatty acids have included a number of optical methods. The majority of the optical work has involved the use of hot stage microscopes; many photographs have been made of the different mesomorphic forms, particularly with the use of polarized light (10). The "hot wire" technique, used by Vold (7), has been very useful in the determination of phase transition temperatures. Relations between the transitions in different soaps have been investigated by Vold by a systematic microscopic study of the mesomorphic forms of the sodium salts of the *n*-fatty acids containing an even number of carbon atoms from C_6 to C_{22} (9) and also those of the series of alkali metal palmitates (11).

The optical methods have depended, in general, on the visual observation of change in appearance, usually by transmitted light, produced by the transition from one mesomorphic form to another. The experimental technique to be described here consists essentially of following the changes in intensity of light transmitted through the material under investigation, as a function of temperature, by means of a sensitive photometer. Besides confirming transitions which are observable to the eye without difficulty, this technique has enabled many less well defined changes from one mesomorphic form to another to be followed easily and speedily without camera work and without uncertainties caused by eye fatigue.

In this paper are given results obtained by the application of the light transmission technique to a study of the phase transitions in the alkali metal stearates and in a number of sodium stearates having substituents in the hydrocarbon chain. The density, viscosity, and electrical conductivity of these soaps have also been investigated in some detail and the results will be presented in subsequent papers in this series.

EXPERIMENTAL

Apparatus

The apparatus is shown diagrammatically in Fig. 1. The cell (*A*) consisted of a 3 in. length of precision molded Pyrex tubing, rectangular in cross-section,

[1]*Manuscript received March 24, 1955.*
Contribution from the Division of Applied Chemistry, National Research Council, Ottawa, Canada. Issued as N.R.C. No. 3673.
[2]*National Research Council Postdoctorate Fellow, 1953–55.*

supplied by H. S. Martin & Co. It was sealed at the lower end and fitted with a standard ground glass joint, for connection to the vacuum line, at the upper end. The internal dimensions of the cell were 10 mm. × 2 mm. The cell fitted into a dural block furnace (*F*) which was bored so that light entering the tube (*B*) passed through the 2 mm. dimension of the cell. The block was

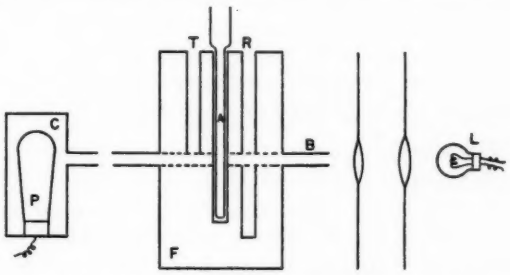

FIG. 1. Arrangement of apparatus (diagrammatic).

also bored to receive a thermocouple or thermometer at *T* and a mercury regulator at *R*. It was heated electrically by a Chromel winding and heavily lagged with asbestos. Temperature control was better than ±0.5°C. Light from an incandescent lamp (*L*) passed via a system of converging lenses through the tube (*B*) and was received by a phototube (*P*), mounted in the casing (*C*). The 12 volt lamp was usually run at 9 or 10 volts, this voltage being supplied from the mains, stabilized by a Sorenson regulator, and reduced by a Variac.

The maximum in the relative energy distribution curve for the lamp was in the wavelength region 7000–10,000 Å and the phototube selected was an RCA No. 917, giving maximum response in the region 7000–9000 Å. The phototube was operated in conjunction with a two-stage d-c. amplifier, this being a modification of a circuit appearing in Phototubes Form PT20R1 by RCA. The plate current of the second-stage amplification, a function of the light intensity and wavelength, was metered. A 1 ma. graphic meter was used, suitably shunted to give a recordable range of 0–20 ma. in the photoelectric current.

Preparation of Materials

The stearic acid used was the Eastman Kodak White Label material (m.p. 69–70°C.). 12-Hydroxystearic acid (m.p. 75°C.) was supplied by the Baker Castor Oil Co. 10-Methylstearic acid (tuberculostearic acid) (m.p. 26°C.) and 9-keto-10-methylstearic acid (m.p. 25°C.) were prepared by the method of Schmidt and Shirley (4). Phenylstearic acid was prepared from oleic acid by Friedel-Crafts reaction with benzene in presence of aluminum trichloride. This material was undoubtedly a mixture of the 9- and 10-phenylstearic acids.

The alkali metal salts (soaps) were prepared by titration of a hot solution of the acid in ethyl alcohol with an alcoholic solution of the appropriate alkali metal hydroxide, using phenolphthalein as indicator. The resultant gel (Na,

Rb, Cs stearates; Na 9-CO-10-Me stearate) or precipitate (Li, K stearates; Na 12-OH stearate; Na 10-Me stearate; Na phenyl stearate) was dried in an air oven at 105°C. In each case the soap was then fused under vacuum to remove last traces of water and alcohol. The opinion has been expressed, by Ralston (3) and Lawrence (1), that this treatment is insufficiently drastic to remove last traces of water associated with soaps. However, it has been shown (5) that the dilatometric behavior of sodium stearate prepared in the above manner is identical to that of sodium stearate prepared from sodium and stearic acid under anhydrous conditions. It would therefore seem most likely that fusion of the soap under vacuum will render it anhydrous.

Experimental Procedure

The soap was crushed and placed in the cell, which was then evacuated, and the temperature raised above the "final melting point" of the soap—this term being used to signify the temperature at which the soap becomes optically transparent. Nitrogen at a pressure of one atmosphere was then admitted to the cell. In the absence of this positive gas pressure slight degassing of the glass cell took place at higher temperatures and gas bubbles rising through the soap affected the measurement of the transmitted light intensity. This effect could be considerably reduced by prior degassing of the cell but was more conveniently eliminated by the presence of the nitrogen.

The temperature was then lowered in stages of about 5°C. and in each case time was allowed for the system to come to equilibrium, the criterion taken being a steady reading of the graphic meter for at least 15 min. Each substance investigated was run twice on a cooling curve and also checked on a heating curve. The equilibrium photoelectric current readings, being a measure of the intensity of light transmitted through the soap, were plotted as a function of temperature.

RESULTS AND DISCUSSION

The intensity of light transmitted through the 2 mm. thickness of soap decreased as cooling proceeded. A series of marked discontinuities occurred in the curve obtained by plotting the photoelectric current as a function of temperature. The results obtained are shown in Figs. 2 and 3. In these figures the degree of translucency of the soap, as measured by the photoelectric current, has been expressed as a percentage of the transparency of the liquid above the final melting point, i.e.,

$$\%\ \text{transmission at } T°\text{C.} = \frac{\text{photoelectric current at } T°\text{C.} \times 100}{\text{photoelectric current above final melting point.}}$$

While it is not presumed that the absolute values of the photoelectric current can have much significance in this experimental arrangement, the above function provides a convenient means of comparing the discontinuities in the change of translucency with temperature, for the different soaps. The temperatures at which these discontinuities appear have been found to be very accurately reproducible (virtually within 1°C.), both on cooling and on heating. The actual values of the photoelectric current were fairly reproducible on

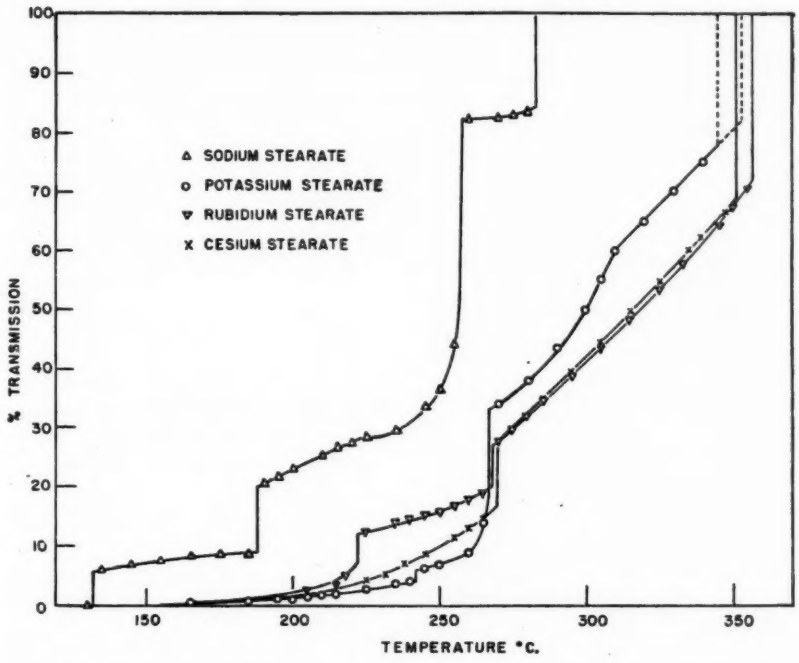

FIG. 2. Light transmission of alkali metal stearates as a function of temperature.

cooling curves but rather lower and less reproducible on heating curves, particularly at the lower temperatures. The reason for this is not perfectly clear but, in view of the excellent agreement between temperatures of discontinuities obtained on cooling and on heating, it would appear that supercooling is not responsible. One possible explanation may be that, on cooling from one phase to another where an appreciable density change is involved, microscopic cracking or vacuole formation may occur in the soap which will increase the light scattering and decrease the light transmission. On reheating it is to be expected that a hysteresis will exist in the closing of these cracks, leading to lower transmissions at any given temperature than those on cooling. Further, it is to be expected that the effect will be most marked in the lower temperature, more crystalline phases.

It should be mentioned here that one example of supercooling was observed in the case of lithium stearate. No results could be obtained for this soap below the temperature at which it melted to an optically clear liquid. The melting point was reproducible at 229°C. on heating. However, freezing occurred at temperatures between 229°C. and 218°C., depending on the rate of cooling. Below 229°C. the photoelectric current was irreproducible and no equilibrium was observed, even after two days had been allowed at each temperature.

A rather different phenomenon occurs in the case of potassium stearate

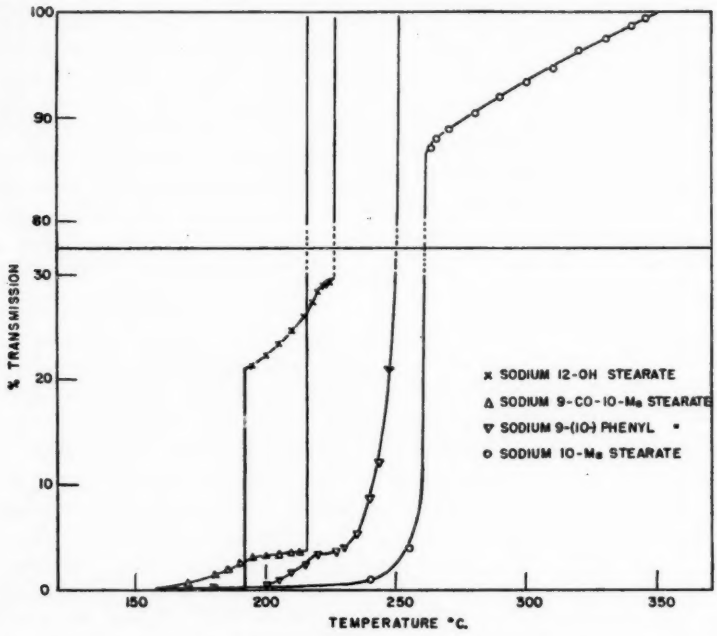

FIG. 3. Light transmission of some substituted sodium stearates as a function of temperature.

in the region of final melting. Between 345°C. and 353°C. two phases appear to be present, in stable equilibrium, and discrete lumps are visible to the naked eye. Above 353°C. the soap is optically clear and a maximum photoelectric current is obtained. Below 345°C. the homogeneous neat phase gives reproducible photoelectric current readings. Between these two temperatures, however, the reading depends on the position of the discrete lumps with respect to the optical path. For this reason, the final melting of potassium stearate is represented in two stages in Fig. 2.

A large non-equilibrium decrease in the intensity of transmitted light sometimes took place while a change was in progress. This was most probably caused by increased light scattering in the material while two phases were present.

A summary of the data obtained is given in Table II and comparison of the data for sodium stearate with those of Vold (8) and of Stross and Abrams (6) is given in Table I. It should be mentioned here that transition temperatures indicated by the optical method may not *necessarily* be true thermodynamic transition temperatures, since a change in translucency may be due to causes other than a phase transition. This may explain the discontinuity in the curve for sodium stearate at 188°C., which though doubtless a manifestation of the transformation from the superwaxy to the subneat phase is,

TABLE I

TRANSITION TEMPERATURES FOR SODIUM STEARATE

Transition	Temperature			
	Vold (8)	Vold (8)	Stross and Abrams (6)	This work
Curd–curd	89	90	88–96	—
Curd–subwaxy	114	117	112–118	—
Subwaxy–waxy	134	132	129–130	132
Waxy–superwaxy	—	167	—	165
Superwaxy–subneat	208	205	198	188 220
Subneat–neat	238	257	243–251 271–273	258
Neat–isotropic	280	288	280	283

TABLE II

SUMMARY OF OPTICAL TRANSITION TEMPERATURES

Soap	Final m.p., °C.					
Li stearate	229					
Na stearate	283	258	220†	188	165	132
K stearate	353, 345, 310†	267	242		160–165*	
Rb stearate	357	268	222		160–165*	
Cs stearate	351	270			160–165*	
Na 12-OH stearate	226		220†	192		
Na 9-(10-)phenyl stearate	250		220†		160–165*	
Na 10-Me stearate	*ca.* 350†	261			160–165*	
Na 9-CO-10-Me stearate	216		195†		160–165*	

**Temperature at which soap becomes opaque.*
†*Minor transitions.*

nevertheless, 10–15° lower than the previously reported temperatures of this transition. However, in general and where comparable, the agreement between the present data and transition temperatures determined by observation of other properties is very close.

It is apparent from Figs. 2 and 3 that the present transition data may be divided into two types, i.e. those transitions where an abrupt change occurs in the intensity of the transmitted light and those manifested by a change of slope in the light transmission – temperature curves. It is believed that the temperatures at which these latter minor changes occur are very much more accurately determined by the present technique than by the usual microscopic methods.

The final melting points of the alkali metal stearates are seen to rise from lithium to rubidium and then fall slightly in the case of cesium. This parallels the behavior of the palmitates (11). For sodium stearate in the neat phase the light transmission is nearly constant throughout the range of existence but shows a very large decrease at the transition neat to subneat at 258°C. In potassium, rubidium, and cesium stearates it decreases steadily as the neat phase is cooled and shows a very much smaller abrupt decrease at the transition neat to subneat. A small, but very definite and reproducible change is indicated within the neat phase, at 310–315°C., in the case of potassium stearate. Below the neat–subneat transition, the behavior of potassium,

rubidium, and cesium stearates is less closely similar. Between this transition and 165°C., where all three soaps become opaque, potassium stearate shows a transition at 242°C., rubidium stearate at 222°C., and cesium stearate none at all. A corresponding variation in sodium stearate,within the subneat phase, is found at 220°C., confirming the observation of Powell and Puddington (2) from viscosity determinations.

Below 165°C. only sodium stearate retains any degree of translucence and shows a minor transition at this temperature. The soap finally becomes abruptly opaque at 132°C., the accepted transition from the waxy to the subwaxy phase.

Turning to a consideration of the results obtained for the sodium salts of the substituted stearic acids, it is found that, with the exception of sodium 10-methyl stearate, a very much greater decrease in intensity of light transmitted through these soaps takes place at the melting point. A very large decrease does, in fact, occur in the sodium 10-methyl stearate at 261°C. but this temperature is not the final melting point. Optically clear liquid does not exist below about 340–350°C. It has not been found possible to fix a definite temperature; the photoelectric current starts to decrease slowly at approximately 350°C. Between 350°C. and 261°C. this soap definitely possesses considerable rigidity and will not, for example, flow under its own weight. The introduction of the methyl group into sodium stearate thus considerably strengthens the structure. The introduction of the phenyl group weakens it, (sodium phenyl stearate m.p. 250°C.). The methyl group has approximately the same dimensions as the cross-sectional area of the hydrocarbon chain and its presence might conceivably allow these chains to interlock instead of standing end to end, as is considered the case in the unsubstituted stearates. Such interlocking would not only increase the interaction between chains but would also increase the interaction between polar carboxylic end groups, in successive polar planes, since these would be brought closer together. The very much larger phenyl group would be more likely to affect the lateral chain spacings to such a degree that the result may be a reduction of chain interaction and probably even of polar interaction if similar over-all packing is exhibited.

The introduction of the carbonyl group in the 9-CO-10-Me stearate lowers the melting point to 216°C. and the 12-OH stearate melts at 226°C. This effect caused by the introduction of a second distal polar group in the molecule is consistent with the behavior of compounds such as octadecane dicarboxylates, although the strength and position of the second polar groups in the above compound is insufficient to eliminate the mesomorphic properties.

It is interesting to note that small discontinuities of the same type as that shown by sodium stearate are apparent at 220°C. in the 12-OH stearate and the phenyl stearate. Furthermore the 12-OH stearate shows an abrupt decrease in transmitted light at 192°C. to be compared with that in sodium stearate at 188°C.

Vold (11) has pointed out that, with the exception of lithium soaps, the temperature of formation of neat soap is essentially constant, being very nearly independent both of the nature of the cation, in the series of palmitates,

and of the length of the hydrocarbon chain. This is also seen to be true for the stearates. Vold concludes that the forces of interaction between the chains are therefore all important and it is especially interesting in this connection to consider the results obtained here for the substituted stearates.

In the neat phase of the unsubstituted soaps some type of micellar structure would seem to be involved. This micellar structure may still be possible in the case of the sodium methyl stearate, accounting for the transition at 261°C., but the large phenyl group is likely not to allow its formation, by virtue of both entropic and polar interactions. Also it is difficult to imagine a stable micellar structure in the cases where a second distal polar group is present in the hydrocarbon chain. The subneat–neat transition is that at which the soaps become appreciably electrically conducting and a study of this property, in progress at the moment, seems likely to give useful information regarding the structure of soaps in the high temperature phases. The results of this work will be given in a later paper in this series.

ACKNOWLEDGMENTS

We are indebted to Mr. J. K. Waterman for photometer construction and to Dr. A. M. Eastham for preparation of the substituted stearic acids.

REFERENCES

1. LAWRENCE, A. S. C. Trans. Faraday Soc. 34: 660. 1938.
2. POWELL, B. D. and PUDDINGTON, I. E. Can. J. Chem. 31: 828. 1953.
3. RALSTON, H. W. Fatty acids and their derivatives. John Wiley & Sons, Inc., New York. 1948. p. 889.
4. SCHMIDT, G. A. and SHIRLEY, D. A. J. Am. Chem. Soc. 71: 3804. 1949.
5. STAINSBY, G., FARNAND, R., and PUDDINGTON, I. E. Can. J. Chem. 29: 838. 1951.
6. STROSS, F. H. and ABRAMS, S. T. J. Am. Chem. Soc. 73: 2825. 1951.
7. VOLD, M. J. J. Am. Chem. Soc. 63: 160. 1941.
8. VOLD, R. D. J. Am. Chem. Soc. 63: 2915. 1941.
9. VOLD, R. D., MACOMBER, M., and VOLD, M. J. J. Am. Chem. Soc. 63: 168. 1941.
10. VOLD, R. D. and VOLD, M. J. J. Am. Chem. Soc. 61: 808. 1939.
11. VOLD, R. D. and VOLD, M. J. J. Phys. Chem. 49: 32. 1945.

THE ACTION OF PYRIDINE ON DULCITOL HEXANITRATE[1]

By G. G. McKeown and L. D. Hayward

ABSTRACT

A pyridine solution of dulcitol hexanitrate evolved gas and became highly colored when warmed to 50°C.; dilution with water caused the precipitation of 67% of the theoretical amount of a dulcitol pentanitrate. The product was characterized as D,L-galactitol-1,2,4,5,6-pentanitrate by methylation to a monomethyl dulcitol pentanitrate, denitration of the latter, and periodate oxidation of the monomethyl dulcitol obtained. The hexitol derivatives were all obtained in a pure crystalline form. The significance of the data now available on the selective partial denitration by pyridine of hexitol hexanitrates is briefly discussed.

INTRODUCTION

In a previous research (5) it was shown that excess pyridine at 35°C. selectively removed the third (or equivalent fourth) nitrate group from D-mannitol hexanitrate to give D-mannitol-1,2,3,5,6-pentanitrate in 73% yield. This reaction was first described in 1903 by Wigner (14) who also reported a good yield of a mannitol pentanitrate from the action of alcoholic pyridine on mannitol hexanitrate. Wigner also nitrated dulcitol (I) to obtain a hexanitrate melting at "about 95°" (3, 4, 13) and found that alcoholic pyridine had almost no effect on this product even at the boiling point. Warming a solution of the dulcitol hexanitrate in pure pyridine, however, caused a reaction accompanied by evolution of a gas, and, on pouring the reaction mixture into water, Wigner obtained a crystalline product which "sintered at 71° and melted at about 75°" after three recrystallizations from aqueous alcohol. Analysis indicated this product to be a dulcitol pentanitrate.

In the present research Wigner's results were confirmed and the dulcitol pentanitrate was characterized as the racemic D- and L-galactitol-1,2,4,5,6-pentanitrate (III) by a series of reactions parallel to that previously described (5) for the characterization of D-mannitol-1,2,3,5,6-pentanitrate.

Dulcitol hexanitrate (D- or L-galactitol-1,2,3,4,5,6-hexanitrate) (II) was prepared in 92% yield by direct nitration of dulcitol (galactitol) (I) with nitric–sulphuric acid mixture, and the pure, crystalline, optically inactive compound melted at 98–99°C. and had the correct nitrate nitrogen content. Hydrogenolysis of a sample of the hexanitrate produced dulcitol quantitatively (5, 6). The hexanitrate dissolved readily in pure pyridine at 30°C. to give an initially colorless solution which became orange-colored in five minutes. No gas evolution was observed until the solution was warmed to 50°C., whereupon an exothermic reaction commenced, brown fumes were observed in the open vessel, and fine, colorless, needle-like crystals appeared on the inner walls of the flask above the solution. The vigorous reaction subsided within a few minutes and after 24 hr. the dark-red solution was poured into

[1]*Manuscript received May 30, 1955.*
Contribution from the Department of Chemistry, University of British Columbia, Vancouver, B.C. This paper constitutes part of a thesis submitted by G. G. McKeown in partial fulfillment of the requirements of the degree of Master of Science in Chemistry, September 1952.

water which caused the separation of crystalline dulcitol pentanitrate (III) in 63–72% yield. The pure pentanitrate melted at 85–86°, was optically inactive, and did not reduce Fehling's solution (13). Hydrogenolysis again gave a nearly quantitative yield of dulcitol thus proving that the pyridine caused no structural or configurational changes in the hexitol skeleton. The pentanitrate was stable to the further action of pyridine under conditions which caused the partial denitration of the hexanitrate.

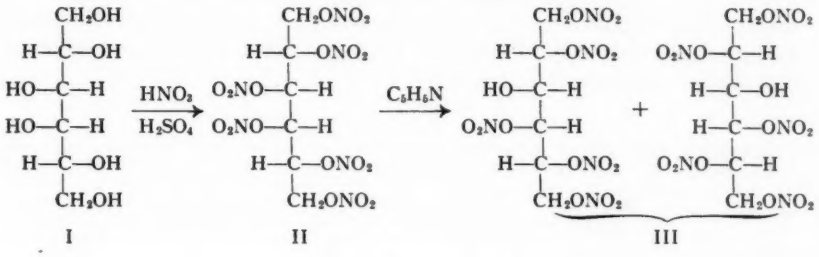

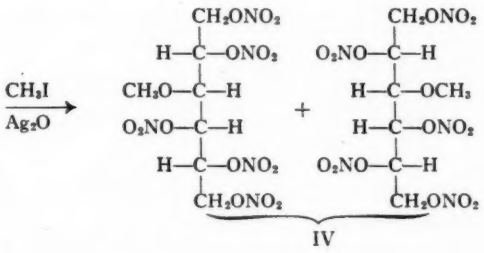

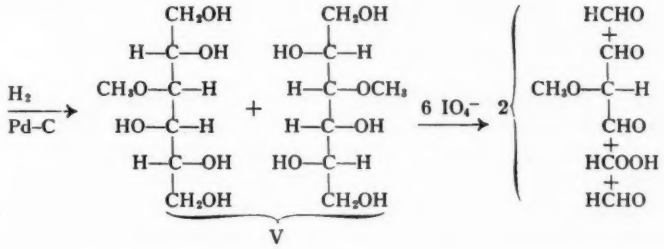

II or III $\xrightarrow{H_2,\ Pd\text{–}C}$ I (quantitative)

V $\xrightarrow[H_2SO_4]{HNO_3}$ IV (75%)

III + C_5H_5N ⟶ 94% recovery

IV + C_5H_5N ⟶ 89% recovery

Methylation of the pentanitrate gave a 67% yield of a new methyl dulcitol pentanitrate (IV), m.p. 99–100°C., with correct methoxyl and nitrogen analyses and this compound was also stable to pyridine at room temperature. Catalytic hydrogenolysis of the methylated pentanitrate yielded a crystalline

monomethyl dulcitol (V) melting at 149–150°. A sample of (V) was renitrated with mixed acids at −10°C. to give a 75% yield of the original methyl dulcitol pentanitrate (IV).

A literature search revealed no previous report of monomethyl derivatives of dulcitol and, apart from an independent synthesis, periodate oxidation appeared to be the most reliable means of locating the position of the methyl group. Taking account of the meso configuration of dulcitol our monomethyl hexitol was one of three possible compounds: a racemate of (1) D- and L-1-*O*-methyl galactitol, (2) D- and L-2-*O*-methyl galactitol, or (3) D- and L-3-*O*-methyl galactitol. The theoretical behavior of these compounds toward periodate oxidation is summarized in Table I.

TABLE I

THEORETICAL PRODUCTS OF THE PERIODATE OXIDATION OF HEXITOL MONOMETHYL ETHERS

	Position of OCH_3 group	Periodate consumed (moles)	Oxidation products (moles)		
			HCHO	HCOOH	Other
Case 1	1 or 6*	4	1	3	
Case 2	2 or 5*	3	1	2	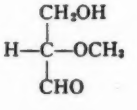
Case 3	3 or 4*	3	2	1	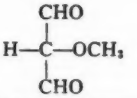

**Pairs of structural isomers although each compound has a unique configuration. Of the mannitol and iditol derivatives only one compound of the* D-*configuration and one of the* L-*configuration can exist in each case. For dulcitol and allitol derivatives the pair in each case is racemic.*

Oxidation of the monomethyl dulcitol with aqueous sodium periodate at room temperature showed a consumption of 4.9 moles of oxidant with the production of 2.1 moles of formic acid and 2.0 moles of formaldehyde per mole of methyl ether. Dulcitol under the same conditions gave the nearly theoretical values of consumption of oxidant (4.95 moles), formic acid (3.68 moles), and formaldehyde (1.98 moles). Comparison of the results for the monomethyl dulcitol with Table I showed Case 1 to be ruled out and that either Case 2 or Case 3 could have given these values if an additional oxidation requiring 2 moles of oxidant occurred with the concomitant formation of an extra mole of formaldehyde or of formic acid respectively. The rate of the periodate oxidation was therefore studied to determine the possibility of "overoxidation" at room temperature. The rates of oxidant consumption, and aldehyde and acid production at 23°C. for the monomethyl dulcitol (Fig. 1, Curves A, B, and C) indicated a rapid initial consumption of 3 moles of oxidant producing 2 moles of formaldehyde and approximately 1 mole of formic acid. The results at this stage conformed to Case 3. An hour later the aldehyde value was the same but the amount of

formic acid had increased to 2 moles and that of oxidant consumed to 5. A rate reaction run at 0°C. (Fig. 1, Curve D) in order to slow or halt the overoxidation clearly showed the rapid initial formation of 1 mole of formic acid followed by a slower secondary oxidation in which further quantities of

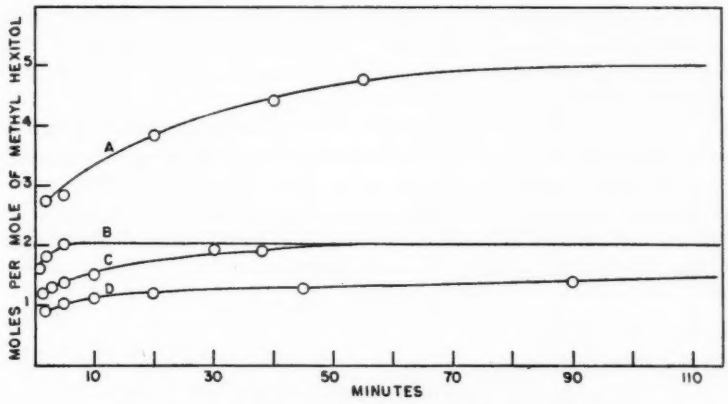

FIG. 1. Periodate oxidation of 3-*O*-methyl-D,L-galactitol.
A: Periodate consumption at 23°C.
B: Formaldehyde production at 23°C.
C: Formic acid production at 23°C.
D: Formic acid production at 0°C.

acid were produced to the final total of 2.0 moles of acid at 11 hr. These data indicated Case 3 to be involved and that the dialdehyde formed (Table I) in the first stages of the oxidation was oxidized further to produce a mole of formic or other acid. A similar reaction of the dialdehyde of malonic acid

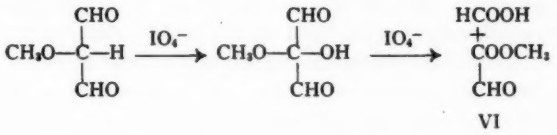

VI

(VII) was reported by Huebner, Ames, and Bubl (7) in which 3 moles of formic acid was produced with oxidant consumption of 3 moles. The methyl

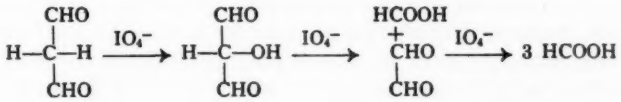

VII

ester of glyoxylic acid (VI) presumably formed in Case 3 could be expected to be comparatively stable to further oxidation. The unique correlation of the periodate oxidation data was for the monomethyl dulcitol to be the racemate,

3-*O*-methyl-D- and L-galactitol (V), and hence the structures and configurations of the compounds (III) and (IV) which preceded it were also established.

The reactions of mannitol and dulcitol hexanitrates with pyridine were analogous and consisted in the replacement of a nitric acid ester group by hydrogen at the 3 (or equivalent 4) position in about 70% of the hexanitrate molecules. No inversion of configuration occurred at the asymmetric center attached to the nitrate group and it may therefore be assumed that the O—N bond was cleaved through some type of nucleophilic attack of pyridine on the nitrate nitrogen (1, 2).

The selectivity of the reaction for one particular nitrate group among six in each molecule is intriguing. To test the hypothesis that this group must occupy a unique spatial environment we plan to treat the nitrates of other polyols with pyridine. Urbanski and Kwiatkowska (12) reported partial denitration of sorbitol hexanitrate when it was heated with alcoholic pyridine; however, the viscous product was not characterized.

EXPERIMENTAL

Materials and Methods

Since dulcitol hexanitrate and its partially nitrated derivatives are explosives (11), the scale of the preparations was restricted to 5 gm. or less and all evaporations were under reduced pressure with bath temperatures not exceeding 50°C.

Pure dulcitol (galactitol (I)) (m.p. 187–188°, optically inactive) (8) when nitrated with fuming nitric and concentrated sulphuric acids at −10°C., as described by Bechamp (3) and Patterson and Todd (9), gave a 92% yield of the crystalline dulcitol hexanitrate (II). After recrystallization from aqueous ethanol the colorless, needle-like crystals of hexanitrate were optically inactive and melted at 98–99°C. (corr.). The melting point was not altered by further recrystallizations. Previous workers (3, 13, 14) reported a melting point of 95°C. Found: N (nitrometer), 18.4, 18.8%. Calc. for $C_6H_8(NO_3)_6$: N, 18.6%. Hydrogenolysis of 0.685 gm. of the hexanitrate over palladized charcoal at 20–30 p.s.i. and room temperature as previously described (5, 6) yielded 0.289 gm. of crude product. Recrystallization from aqueous ethanol gave thick, colorless crystals melting at 185–187°C. A mixed melting point with authentic dulcitol showed no depression.

The analytical procedures for nitrate nitrogen, methoxyl, and periodate oxidation products were previously described (5, 6, 10).

Action of Pyridine on Dulcitol Hexanitrate

A 500 ml. Erlenmyer flask containing 3.11 gm. of pure dry dulcitol hexanitrate was immersed in a water-bath at 30°C. The hexanitrate dissolved immediately on addition of 25 ml. of pyridine (B.D.H. analytical reagent grade) to form a clear, colorless solution which became orange-colored within five minutes. No further change was observed until the water-bath was heated to 50°C. when the solution rapidly evolved small bubbles of gas and fine, colorless crystal-needles appeared on the neck of the flask. After the first vigorous reaction had subsided, the now dark-red solution was allowed to stand at room temperature for 24 hr. and was then poured with stirring into

300 ml. of water. The colorless sirup which separated crystallized readily and was recovered on a glass filter, washed thoroughly with water, and dried to constant weight *in vacuo*; yield 1.81 gm. (65%). Yields obtained in similar denitrations were 63, 65, 69, and 72%. Recrystallization of the product from aqueous ethanol, ether – petroleum ether, or carbon tetrachloride yielded colorless needles of pure dulcitol pentanitrate (D,L-galactitol-1,2,4,5,6-pentanitrate) (III); m.p. 85–86°C., optically inactive, soluble in alcohol, ether, benzene, and chloroform, insoluble in water and petroleum ether. The pentanitrate did not reduce Fehling's solution (13, 14). Found: N (nitrometer), 16.9, 17.0%. Calc. for $C_6H_8(OH)(NO_3)_5$: N, 17.2%.

A sample of the dulcitol pentanitrate (0.63 gm.) when treated with pyridine (4.0 ml.) under the conditions which caused denitration of the hexanitrate produced no gas, although the solution became dark-red in color. Unchanged pentanitrate, 0.59 gm. (94%), was recovered when the solution was worked up as described above. A 0.240 gm. sample of dulcitol pentanitrate yielded 0.110 gm. (100%) of crude dulcitol when hydrogenolyzed as described for the hexanitrate. The pure product melted at 185–188°C. and caused no depression in the melting point of pure dulcitol.

Methyl Dulcitol Pentanitrate (*3-O-Methyl-*D,L*-galactitol-1,2,4,5,6-pentanitrate*) (*IV*)

Dulcitol pentanitrate, 0.730 gm., was dissolved in 11 ml. of methyl iodide and 4 ml. of methanol and treated with 5 gm. of Drierite and 5 gm. of freshly-prepared silver oxide. After being refluxed for nine hours the mixture was filtered and the solids washed with dry acetone. Evaporation of the filtrate and washings and recrystallization of the colorless solid residue from aqueous ethanol yielded 0.508 gm. (67%) of monomethyl dulcitol pentanitrate (3-*O*-methyl-D,L-galactitol-1,2,4,5,6-pentanitrate) (IV); m.p. 99–100°C., soluble in alcohol, ether, acetone, and dioxane, insoluble in water. Found: N, 16.6, 16.5%; OCH_3, 7.34, 7.37%. Calc. for $C_6H_8(OCH_3)(NO_3)_5$: N, 16.6%; OCH_3, 7.37%. A sample of the methylated dulcitol pentanitrate was recovered unchanged in 89% yield from a pyridine solution after two days at room temperature.

Monomethyl Dulcitol (*3-O-Methyl-*D,L*-galactitol*) (*V*)

Monomethyl dulcitol pentanitrate, 1.42 gm., dissolved in 30 ml. dioxane diluted with 45 ml. ethanol and 5 ml. of water was hydrogenated at room temperature over 1 gm. of palladized charcoal at 45 p.s.i. After one hour the pressure became constant and the solution was free of nitrate by the diphenylamine test. The catalyst was filtered off, and evaporation of the solution left a colorless crystalline product. Recrystallization from boiling absolute alcohol gave 0.552 gm. (83%) of thick, colorless crystals; m.p. 149–150°C. Recrystallization from isoamyl alcohol or from water yielded the same product. Found: OCH_3, 16.1, 16.0%. Calc. for $C_6H_8(OCH_3)(OH)_5$: OCH_3, 15.8%. The monomethyl dulcitol did not react with Fehling's solution or bromine water.

Nitration of a sample of the monomethyl dulcitol with sulphuric–nitric acid mixture gave a 75% yield of the original 3-*O*-methyl-D,L-galactitol-

1,2,4,5,6-pentanitrate, identified by a mixed melting point and methoxyl analysis. Found: OCH_3, 7.39, 7.20%.

*Periodate Oxidation of Monomethyl Dulcitol (3-O-Methyl-*D,L*-galactitol) (V)*

Forty to fifty milligram samples of the monomethyl dulcitol were oxidized with aqueous sodium periodate solution by procedures previously described (6) which revealed the amount of periodate consumed and the amounts of formic acid and formaldehyde formed. At room temperature the amounts of formic acid obtained per mole of methyl dulcitol were 1.20, 1.30, 1.38, 1.51, 1.91, 2.06, and 2.11 moles after 1.5, 3, 5, 10, 38, 130, and 900 min. respectively. At 960 min. 4.93 moles of periodate had been consumed and at 1020 min. the formaldehyde production was found to be 1.98 moles. In two other runs under the same conditions the consumption of 2.76, 2.83, 3.86, 4.43, and 4.77 moles of periodate at 2, 5, 20, 40, and 55 min. was observed while the molar production of formaldehyde amounted to 1.61, 1.81, 2.02, 1.92, and 1.98 after 1, 2, 5, 30, and 1020 min. Oxidation of pure dulcitol under the same conditions formed 3.53, 3.63, and 3.68 moles of formic acid after 5, 15, and 25 hr. At 25 hr. the periodate consumption was found to be 4.95 moles and formaldehyde production 1.98 moles.

An oxidation of methyl dulcitol conducted in an ice bath revealed formic acid production as 0.91, 1.04, 1.12, 1.20, 1.27, 1.40, 1.70, 2.06, and 2.11 moles after 2, 5, 10, 20, 45, 90, 300, 660, and 1440 min.

The data for the oxidation of the monomethyl dulcitol are plotted in Fig. 1; theoretical values for the different structural isomers are listed in Table I.

ACKNOWLEDGMENT

The authors wish to thank the National Research Council of Canada for Grant G249 which helped to defray the cost of this research. One of them (G.G.M.) also thanks the Standard Oil Company of British Columbia Limited for a Fellowship which enabled him to complete the work.

REFERENCES

1. Anbar, M., Dostrovsky, I., Samuel, D., and Yoffe, A. D. J. Chem. Soc. 3603. 1954.
2. Baker, J. W. and Neale, A. J. J. Chem. Soc. 608. 1955.
3. Bechamp, A. Compt. rend. 51: 255. 1860.
4. Champion, P. Compt. rend. 78: 1150. 1874.
5. Hayward, L. D. J. Am. Chem. Soc. 73: 1974. 1951.
6. Hayward, L. D. and Purves, C. B. Can. J. Chem. 32: 19. 1954.
7. Huebner, C. F., Ames, S. R., and Bubl, E. C. J. Am. Chem. Soc. 68: 1621. 1946.
8. Lohmar, R. and Goepp, R. M., Jr. *In* Advances in carbohydrate chemistry. Vol. 4. *Edited by* W. W. Pigman and M. L. Wolfrom. Academic Press, Inc., New York. 1949. p. 219.
9. Patterson, T. S. and Todd, A. R. J. Chem. Soc. 2876. 1929.
10. Segall, G. H. and Purves, C. B. Can. J. Chem. 30: 860. 1952.
11. Taylor, C. A. and Rinkenbach, W. H. J. Franklin Inst. 204: 369. 1927.
12. Urbanski, T. and Kwiatkowska, S. Roczniki Chem. 25: 312. 1951.
13. Vignon, L. and Gerin, F. Compt. rend. 133: 540. 1901.
14. Wigner, J. H. Ber. 36: 794. 1903.

COEXISTENCE PHENOMENA IN THE CRITICAL REGION

III. COMPRESSIBILITY OF ETHYLENE AND XENON FROM LIGHT SCATTERING[1]

By F. E. Murray[2] and S. G. Mason

ABSTRACT

Turbidity measurements in the region immediately above the critical temperature are used to calculate values of $(\partial p/\partial v)_T$. These results show that $(\partial p/\partial v)_T$ is a continuously variable function of the density to within 0.02°C. above the critical temperature. The experiments indicate that there exists no region above T_c throughout which $(\partial p/\partial v)_T = 0$ in ethylene or xenon.

INTRODUCTION

In 1938 Mayer and Harrison (9, 10) concluded from a statistical treatment of a real gas that the phase transition at the critical point did not occur in the manner proposed by Andrews (1, 2). Their prediction of a "derby hat" region between two characteristic temperatures has stimulated a great deal of experimental work.

Maass (6) has summarized the evidence for the existence of anomalous behavior. Zimm (19), from a series of light-scattering measurements, concluded that the region predicted by McMillan and Mayer (8) did not exist in the case of a binary liquid system. From a theoretical viewpoint, Zimm (20) has discussed the probability of a single critical temperature. Weinberger and Schneider (16, 17) and Habgood and Schneider (4) found no evidence of a "derby hat" region in xenon. Other results observed in unstirred systems are of questionable value in settling this question, as it is doubtful if equilibrium can be attained without mechanical mixing. The experimental work described here was undertaken to obtain information regarding the validity of conclusions by Mayer and Harrison.

To account for the turbidity in the critical region of a pure gas, Smoluchowski (15) and Einstein (3) derived an equation from the theory of density fluctuations which may be written

$$[1] \qquad \frac{I_\theta}{I_0'} = \frac{AT\rho^2}{\lambda^4}\left[\frac{1+\cos^2\theta}{-(\partial p/\partial v)_T}\right].$$

Here I_θ is the intensity of the radiation scattered at angle θ from the incident beam, I_0' is the incident intensity, and λ the wavelength of the incident light beam. A is a constant for a particular gas and a fixed distance of observation, T is the absolute temperature, ρ is the density, and p and v are the pressure and specific volume of the fluid.

When the angular dependence of I_θ is given by the factor $(1+\cos^2\theta)$, the turbidity τ is related to the transversely scattered light by the equation

$$[2] \qquad \tau = b\, I_{90°}/I_0',$$

[1]*Manuscript received May 9, 1955.*
Contribution from the Chemistry Department, McGill University, Montreal, Quebec.
[2]*Holder of a Fellowship from the National Research Council of Canada. Present address: Chemistry Department, University of Manitoba, Winnipeg, Manitoba.*

where b is a constant. Equations [1] and [2] may be combined to yield:

$$[3] \qquad \tau = \frac{BT\rho^3}{\lambda^4} \Big/ -\left(\frac{\partial p}{\partial v}\right)_T.$$

Equation [3] predicts that I_θ becomes infinite when $(\partial p/\partial v)_T = 0$, i.e. at the classical critical point. This result is obtained because the derivation predicts infinite density fluctuations at the critical point. Physically, it is of course impossible for I_θ to be infinite. In a modified treatment of the problem by Ornstein and Zernicke (12, 13), the density fluctuations at the critical point are infinite, but I_θ is kept finite owing to optical interference between wavelets scattered from different volume elements in the fluid.

In a more detailed analysis, which neglects optical interference, Rocard (14) derived the equation

$$[4] \qquad \tau = \frac{BT\rho^3}{\lambda^4} \Big/ \left(-\left(\frac{\partial p}{\partial v}\right)_T + c\right),$$

where c is a constant for any particular gas and light source.

In the development of Eq. [4], both the density fluctuations and the value of I_θ are kept finite when $(\partial p/\partial v)_T$ becomes zero. Klein and Tisza (5) have shown that both Eq. [3] and Eq. [4] as well as that of Ornstein and Zernicke follow from their work.

At constant λ and over a small temperature range, Eq. [4] may be rearranged to the form

$$[5] \qquad \tau^{-1} = \frac{K}{\rho^3}\left[-\left(\frac{\partial p}{\partial v}\right)_T + c\right],$$

where K is virtually constant.

From Eq. [5] it follows that

$$[6] \qquad -\left(\frac{\partial p}{\partial v}\right)_T = \frac{\rho^3\tau^{-1}}{K} - c.$$

If K and c are known, $(\partial p/\partial v)_T$ may be calculated using Eq. [6]. In any case, $(\partial p/\partial v)_T$ is a linear function of $\rho^3\tau^{-1}$ over the temperature range in which K may be considered constant. Equation [6] indicates that if $(\partial p/\partial v)_T$ becomes zero, $\rho^3\tau^{-1} = Kc$, i.e. $\rho^3\tau^{-1}$ should be constant within the "derby hat" region predicted by Mayer and Harrison (9, 10).

In this investigation, the turbidity τ was calculated from measurements of transmitted light using the relation (for 1 cm. light path in the fluid)

$$\tau = 2.30 \log(I_0'/I'),$$

where I' is the intensity of the transmitted beam.

A polychromatic light source was used to give high intensity illumination which could be measured with a 929 photocell. Since the total intensity of such a beam may be written as the sum of intensities at various wavelengths in the incident light, then the total intensity is

$$I_0' = \sum I_0'(\lambda),$$

where the sum is taken over all wavelengths in the spectrum of the incident beam. $I_0'(\lambda)$ is the incident intensity over a small wavelength interval. For the scattered intensity in a single wavelength interval, Rocard's equation predicts that

$$I_\theta(\lambda) = \frac{I_0'(\lambda)}{\lambda^4} A T \rho^3 \left[\frac{1+\cos^2\theta}{-(\partial p/\partial v)_T + c} \right].$$

For the total intensity scattered from the polychromatic beam at angle θ,

[7] $$\sum I_\theta(\lambda) = \sum \frac{I_0'(\lambda)}{\lambda^4} A T \rho^3 \left[\frac{1+\cos^2\theta}{-(\partial p/\partial v)_T + c} \right].$$

When both sides of [7] are divided by $\sum I_0'(\lambda)$, the intensity of transversely scattered light becomes

[8] $$\frac{I_{90°}}{I_0} = \frac{A T \rho^3}{\sum I_0'(\lambda)} \sum \frac{I_0'(\lambda)}{\lambda^4} \left[\frac{1}{-(\partial p/\partial v)_T + c} \right].$$

Combining equations [2] and [8] yields

[9] $$\tau = \frac{B T \rho^3}{I_0} \sum \frac{I_0'(\lambda)}{\lambda^4} \left[\frac{1}{-(\partial p/\partial v)_T + c} \right].$$

For any stable light source, where the distribution of $I_0'(\lambda)$ remains constant throughout the spectrum of the beam, $\sum I_0'(\lambda)/\lambda^4$ is constant and equation [9] may be written

[10] $$\tau = D T \rho^3 / (-(\partial p/\partial v)_T + c)$$

or in a form similar to Eq. [6],

[11] $$-\left(\frac{\partial p}{\partial v} \right)_T = \frac{\rho^3 \tau^{-1}}{K'} + c.$$

Equation [11] is the form applicable to the following experimental results.

T_c is defined as the highest temperature (°C.) at which visible droplets form on slow cooling of the fluid; $\Delta T = (T - T_c)$ and may be positive or negative. The mean density $\bar{\rho}$ equals total mass of gas divided by volume of bomb.

EXPERIMENTAL

Apparatus

Except for modifications made to obtain transmission measurements, the apparatus was the same as that previously described (11). These modifications included the addition of a 929 photocell to the optical measuring assembly of Fig. 2 in Reference (11) to measure the intensity of the transmitted light. Except for a small round opening (about $\frac{1}{4}$ in. diameter) upon which the incident beam was aligned, the glass envelope of the photocell was painted black. The entire optical assembly could be moved to any desired level along the glass bomb.

The fluid sample was contained in a long (about 35 cm.) glass bomb (11). The bomb used in these experiments was sealed off at a point approximately

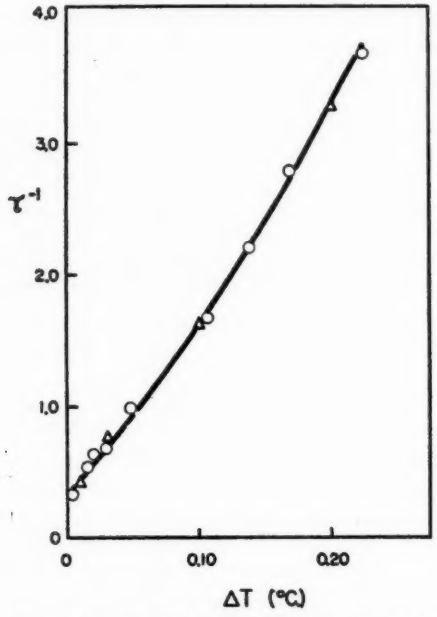

FIG. 1. Variation of τ^{-1} with $\Delta T = T - T_c$ at the density of maximum turbidity of xenon. The circles are measured values and the triangles values calculated from $(\partial p/\partial v)_{min}$ values of Habgood and Schneider (4) using the Rocard equation.

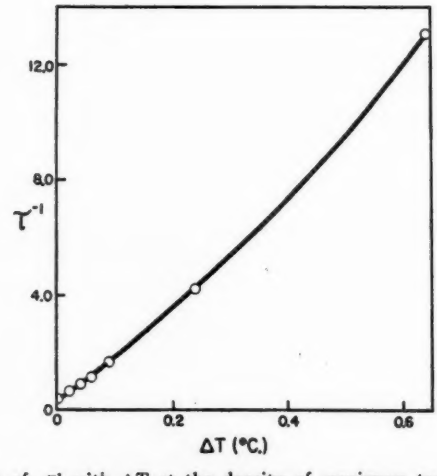

FIG. 2. Variation of τ^{-1} with ΔT at the density of maximum turbidity in ethylene.

10 cm. from the extreme top. This sealed-off portion was filled with methanol and was used at one fixed point to check and maintain a constant incident light intensity. The light source and 929 photocell combination had extremely good stability.

Procedures

The ethylene sample was Phillips research grade and contained 99.9 mole per cent ethylene before fractionation in the glass filling apparatus. The xenon was obtained from Linde Air Products and showed only the xenon spectrum when analyzed in a mass spectrometer. The xenon and ethylene samples were purified and distilled into the glass bomb in the manner previously described (11).

All transmission measurements were obtained immediately after vigorous stirring of the fluid and at one level near the center of the bomb. In this way,

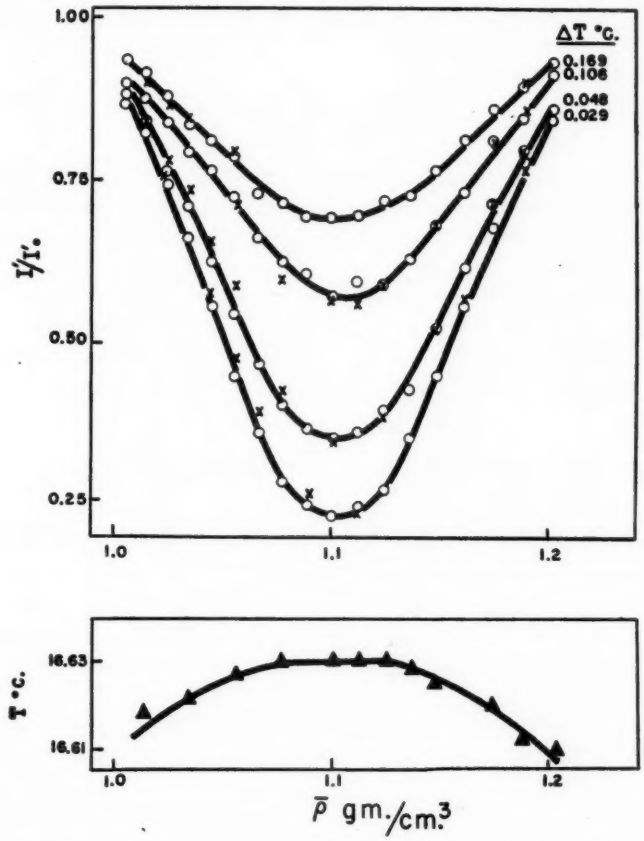

FIG. 3. Variation of transmittance with density along isothermals above T_c (upper curves) and liquid–vapor coexistence curve (lower curve) of xenon.

no appreciable time was allowed for establishment of a vertical density gradient and the density at the point of observation was virtually equal to the mean density. Under these conditions, the mean density $\bar{\rho}$ was used in the calculations from equation [11].

Points on the coexistence curves (lower parts of Figs. 3 and 5) were obtained by observing the first formation of visible droplets when the quiescent system was slowly cooled from above T_c as previously described (11, 18). The observed temperatures at any value of the average density were reproducible within ± 0.002°C. on a Beckmann thermometer.

RESULTS

Variation of Turbidity with Temperature

Xenon

Fig. 1 shows the variation of τ^{-1} with ΔT in xenon. All measurements were taken at the density of maximum turbidity ($\bar{\rho} = 1.100$ gm./cc.) and after the fluid had been efficiently stirred.

Using the equation

$$[12] \qquad \tau^{-1} = \frac{45.1}{\rho^3}\left[-\left(\frac{\partial p}{\partial v}\right)_T + 0.0059\right],$$

values of τ^{-1} were calculated from the $(\partial p/\partial \rho)_{\min}$ data of Habgood and Schneider (4). K' and c in Eq. [12] were chosen to give best correspondence between these calculated values and those obtained from our transmission measurements.

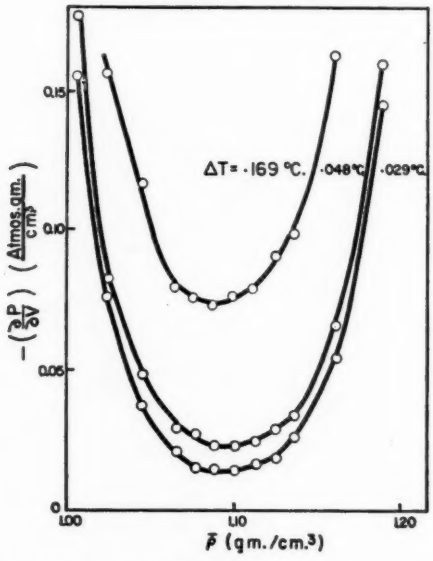

FIG. 4. Variation of $-(\partial p/\partial v)_T$ with density in xenon on isotherms immediately above T_c. Temperatures shown are values of ΔT.

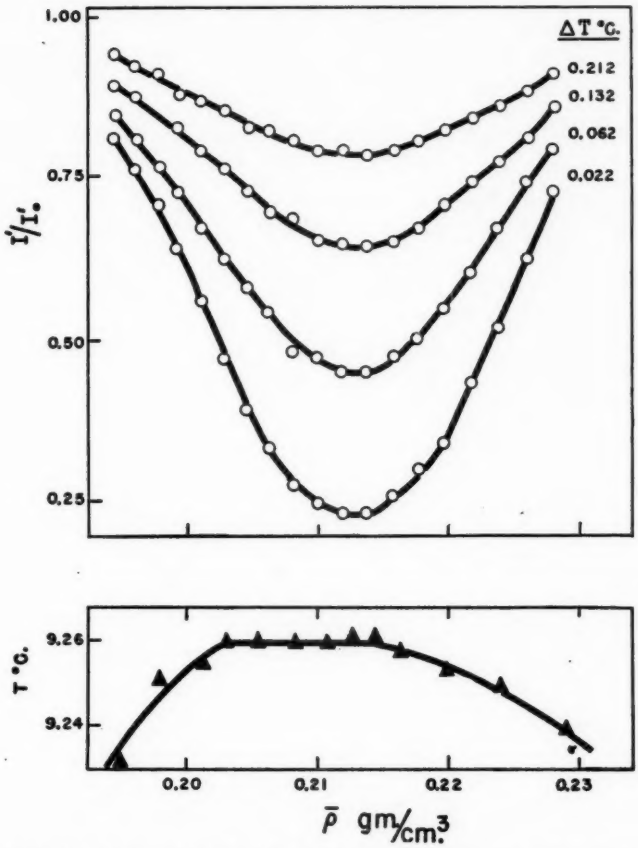

FIG. 5. Variation of transmittance with density along isothermals above T_c (upper curves) and liquid–vapor coexistence curve (lower curve) of ethylene.

Having, in this manner, established the values of K' and c for xenon, Eq. [12] was used to obtain $(\partial p/\partial v)_T$ from transmission measurements at other densities.

Ethylene

Fig. 2 shows values of τ^{-1} as a function of ΔT in ethylene. The curve obtained is almost identical with that obtained for xenon. The available PVT data on ethylene (7) are not sufficiently accurate for comparison of calculated and experimental values of τ^{-1}; consequently K' and c cannot be evaluated in this case.

Transmittance Isothermals

Figs. 3 and 5 show variation of transmittance with density in the systems xenon and ethylene and, in the lower portions, coexistence curves for these two

systems. The value of T_c observed for ethylene was 9.26±0.02°C. and that for xenon 16.63±0.02°C. The flat apexes on the coexistence curves have been attributed to gravity gradients by Weinberger and Schneider (17) and Mason *et al.* (11, 18).

The transmittance data are well fitted by continuous curves which show no indication of a discontinuity in τ.

Calculated $(\partial p/\partial v)_T$ *Isotherms*

Fig. 4 shows values of $(\partial p/\partial v)_T$ calculated from Eq. [12] at various densities in xenon.

Since K' and c of Eq. [11] could not be obtained for ethylene, $\tau^{-1}\rho^3$ is shown as a function of density in Fig. 6.

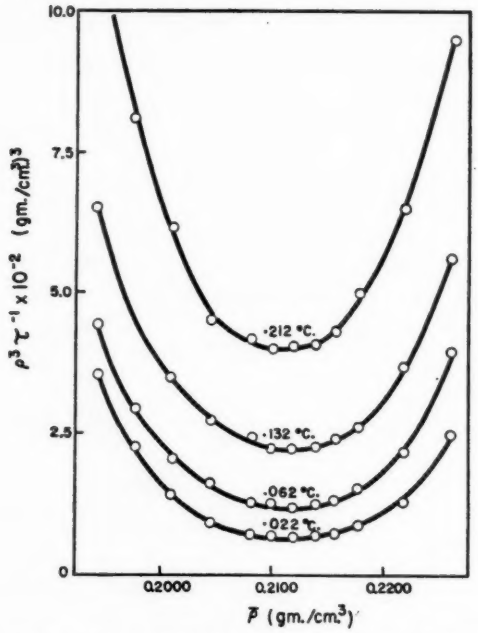

FIG. 6. Variation of $\rho^3\tau^{-1}$ with density in ethylene on isotherms immediately above T_c. Temperatures shown are values of ΔT.

CONCLUSIONS

The results of these experiments indicate that $(\partial p/\partial v)_T$ is a continuous function of the density and not equal to zero within 0.02°C. above T_c in ethylene and to within 0.03°C. above T_c in xenon.

Our results for xenon confirm the conclusion of Habgood and Schneider (4) based on PVT measurements. They are in disagreement with the conclusions of McIntosh, Dacey, and Maass (7) which were based on rather insensitive PVT data obtained for ethylene.

It appears that the "derby hat" region predicted by Mayer and Harrison

(9, 10) does not exist for the two systems studied. Other experiments, which are discussed in the following paper, indicate, however, that considerable molecular clustering may occur above T_c. This extensive molecular clustering is predicted by Mayer and Harrison (9, 10) at low values of $(\partial p/\partial v)_T$ and follows more rigorously from their theory than does the "derby hat" region.

ACKNOWLEDGMENTS

The authors are indebted to Dr. H. I. Schiff of McGill University for analyses of xenon in the mass spectrometer.

REFERENCES

1. ANDREWS, T. Trans. Roy. Soc. (London), A, 159: 583. 1869.
2. ANDREWS, T. J. Chem. Soc. 23: 74. 1870.
3. EINSTEIN, A. Ann. Physik, 33: 1275. 1910.
4. HABGOOD, H. W. and SCHNEIDER, W. G. Can. J. Chem. 32: 98. 1954.
5. KLEIN, M. J. and TISZA, L. Phys. Rev. 76: 1861.. 1949.
6. MAASS, O. Chem. Rev. 23: 17. 1938.
7. MCINTOSH, R. L., DACEY, J. R., and MAASS, O. Can. J. Research, B, 17: 241. 1939.
8. MCMILLAN, W. G. and MAYER, J. E. J. Chem. Phys. 13: 276. 1945.
9. MAYER, J. E. and HARRISON, S. F. J. Chem. Phys. 6: 87. 1938.
10. MAYER, J. E. and HARRISON, S. F. J. Chem. Phys. 6: 101. 1938.
11. MURRAY, F. E. and MASON, S. G. Can. J. Chem. 30: 550. 1952.
12. ORNSTEIN, L. S. and ZERNICKE, F. F. Physik. Z. 19: 134. 1918.
13. ORNSTEIN, L. S. and ZERNICKE, F. F. Physik. Z. 27: 761. 1926.
14. ROCARD, Y. J. phys. radium, 4: 165. 1933.
15. SMOLUCHOWSKI, M. Ann. Physik, 25: 205. 1908.
16. WEINBERGER, M. A. and SCHNEIDER, W. G. Can. J. Chem. 30: 422. 1952.
17. WEINBERGER, M. A. and SCHNEIDER, W. G. Can. J. Chem. 30: 847. 1952.
18. WHITEWAY, S. G. and MASON, S. G. Can. J. Chem. 31: 569. 1953.
19. ZIMM, B. H. J. Phys. & Colloid Chem. 54: 1306. 1950.
20. ZIMM, B. H. J. Chem. Phys. 19: 1019. 1951.

COEXISTENCE PHENOMENA IN THE CRITICAL REGION

IV. TIME-DEPENDENT BEHAVIOR IN VERTICAL DISTRIBUTION OF THE CRITICAL OPALESCENCE IN ETHYLENE AND XENON[1]

By F. E. Murray[2] and S. G. Mason

ABSTRACT

The variation with height of the transmittance in the critical region at various heights in long columns of xenon and ethylene continued to change for several hours after stirring. This change with time is attributed to gravitational settling of large molecular clusters. Other experiments also indicate that a region in which extensive molecular clustering occurs is necessary for an adequate description of phase transitions in the critical region.

INTRODUCTION

In a previous paper (4), it was shown that vertical gradients in the intensity of scattered light occurred in the system ethane in the region of the critical temperature. These gradients in turbidity were destroyed by stirring and re-formed only after a considerable time lag. In the experiments to be described, these time lags were the subject of extensive study in the systems xenon and ethylene.

Mayer and Harrison (2, 3) considered a gas to be made up of a mixture of single molecules and molecular clusters formed by molecular attraction. The rate of change of pressure with volume for any gas is given, according to their work, by the relation

$$[1] \qquad \left(\frac{\partial p}{\partial V}\right)_T = \frac{-kT}{V^2}\left(\sum_l l^2 V b_l Z^l\right)^{-1}.$$

In this equation, l is the number of molecules in any cluster and the summation is taken over all values of l; b_l is the cluster integral for clusters of l molecules each; V is the average volume per molecule; and Z is defined by the relation

$$\sum l V b_l Z^l = 1.$$

When l in Eq. [1] is small, $(\partial p/\partial V)_T$ remains large, but when the large molecular clusters begin to form, l becomes large and $(\partial p/\partial V)_T$ becomes small as in the region of the critical point.

According to fluctuation theory, density deviations in small volume cells of a fluid give rise to critical opalescence. A large positive deviation in density results if the number of molecules in a volume cell is much greater than the average number in that volume. Such a deviation must bring the molecules close enough together to render important the intermolecular forces between them. In this way, a large positive deviation in density corresponds, from a physical viewpoint, to a mathematical cluster of the theory of Mayer and Harrison.

[1]*Manuscript received May 9, 1955.*
Contribution from the Chemistry Department, McGill University, Montreal, Quebec.
[2]*Holder of a Fellowship from the National Research Council of Canada. Present address: Chemistry Department, University of Manitoba, Winnipeg, Manitoba.*

Since there is no essential conflict between fluctuation and cluster theory one can obtain an expression for the turbidity in a "cluster" gas using an equation derived by fluctuation treatment. For the turbidity τ of a gas, in terms of $(\partial p/\partial V)_T$, Rocard (6) derived an equation which we have (5) expressed in the form

$$\tau = \frac{BT\rho^3}{\lambda^4}[c-(\partial p/\partial V)_T]^{-1} \qquad [2]$$

where B and c are constants for given fluid and optical arrangements, T is the absolute temperature, and ρ and v are respectively the density and specific volume of the gas. Combining Eqs. [1] and [2] for a cluster gas yields

$$\tau = \frac{BT\rho^3}{\lambda^4}\left[c+\frac{kT}{V^2}(\sum l^2 V b_l z^l)^{-1}\right]^{-1}. \qquad [3]$$

Eq. [3] indicates that the high turbidity in the region above T_c is caused by the formation of numerous large molecular clusters.

The following symbols are used to denote experimental quantities:

T_c = the highest temperature at which visible aggregates form when the fluid is cooled slowly,
ΔT = $(T-T_c)$,
I'/I_0' = the optical transmittance of the fluid,
$(t-t_0)$ = time elapsed since cessation of stirring,
$\bar{\rho}$ = mean density, i.e. total mass/total volume,
$\bar{\rho}_m$ = mean density at which maximum turbidity was observed,
x = distance measured downward from the top of the fluid column.

EXPERIMENTAL

The apparatus and procedures were identical to those described in previous papers (4, 5). The xenon and ethylene systems were the same as those already described (5).

RESULTS

Transmittance Gradients in Xenon

Figs, 1, 2, and 3 show typical vertical gradients of transmittance in xenon. Results in Fig. 1 were observed at an average density less than $\bar{\rho}_m$. Results in Fig. 2 were obtained at average densities very near to $\bar{\rho}_m$ such that the transmittance was a minimum near the center of the fluid column. Fig. 3 shows gradients in transmittance at a density greater than $\bar{\rho}_m$.

To obtain these results, the fluid was well stirred and after cessation of stirring, measurements were recorded when the transmittance at various levels in the bomb remained virtually constant with time. Similar results were obtained with ethylene.

Time Lags after Stirring

When the fluid was stirred, the transmittance gradients such as shown in Figs. 1, 2, and 3 were destroyed. These gradients re-formed gradually during a period of at least one hour.

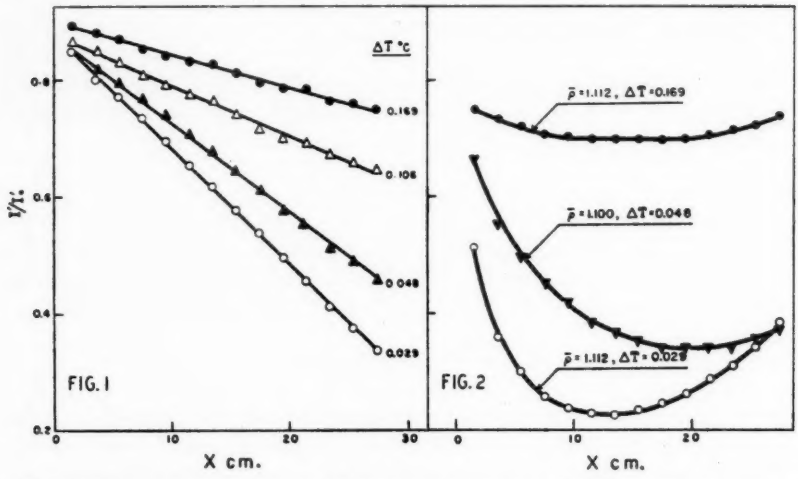

FIG. 1. Change in transmittance with distance (x) from top of vertical tube of xenon at various values of ΔT and at a mean density of 1.055 gm./cc., i.e. at $\bar{\rho} < \bar{\rho}_m$, $\bar{\rho}_m = 1.110$ gm./cc.
FIG. 2. Transmittance–height curves in xenon at $\bar{\rho} = \bar{\rho}_m = 1.110$ gm./cc.

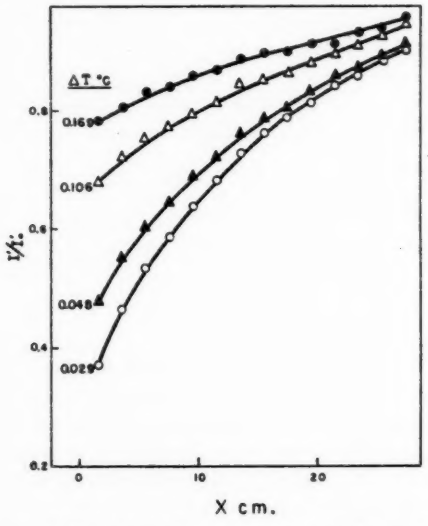

FIG. 3. Transmittance–height curves in xenon at $\bar{\rho} = 1.188$ gm./cc., i.e. $\bar{\rho} > \bar{\rho}_m$.

Fig. 4 shows the change of transmittance with time after stirring in xenon. These diagrams typify results obtained from numerous observations. Similar behavior was observed in ethylene but the times to equilibrium were greater.

The upper diagram in Fig. 4 shows change of transmittance with time at a number of levels in the bomb, at $\Delta T = 0.048$°C. and an average density less

than $\bar{\rho}_m$. The lower part of Fig. 4 shows results obtained at density greater than $\bar{\rho}_m$. These results illustrate the slow readjustment of the turbidity which appears visually to be due to a gravitational settling process.

Time Lags after a Turbidity Perturbation

When stirring in a fluid above T_c is stopped, rearrangement of material within the bomb takes place to establish the density gradients due to gravitational compression, which have been shown to exist (1, 4, 7, 8). The possibility of an extensive time lag in turbidity, not associated with redistribution of material, was investigated.

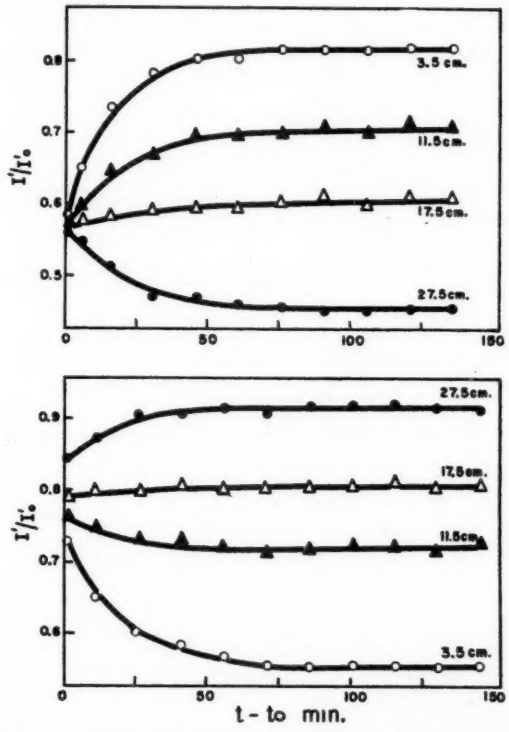

FIG. 4. Change in transmittance with time after cessation of stirring in xenon at $\bar{\rho} = 1.055$ gm./cc., i.e. $\bar{\rho} < \bar{\rho}_m$ (upper diagram) and at $\bar{\rho} = 1.188$ gm./cc., i.e. $\bar{\rho} > \bar{\rho}_m$ (lower diagram). Measurements made at various vertical heights indicated.

Xenon was allowed to attain vertical equilibrium, after stirring at $\bar{\rho} = 1.100$ gm./cc. and $\Delta T = 0.048$°C. The system was then rapidly compressed by means of the injector (4, 8) by a volume change of about 0.1%. This rapid compression caused a sharp increase in transmittance as shown in the lower part of Fig. 5. The transmittance was allowed to return to its precompression value and the system was rapidly expanded back to its original volume.

The rapid expansion caused a sharp decrease in transmittance. During the compression and expansion, the transmission was recorded continuously (at $x = 15.5$ cm.) on a Brush recording oscillograph.

Fig. 5 (lower part) shows a typical result of one of these experiments. The total perturbation by compression and expansion required slightly less than 1.5 min. In less than two minutes after the fluid was returned to its original volume, the turbidity had returned to its precompression value.

The upper portion of Fig. 5 shows the gradients observed at $\theta = 0$ min. (before the volume perturbation) and at $\theta = 10$ min. (after the volume

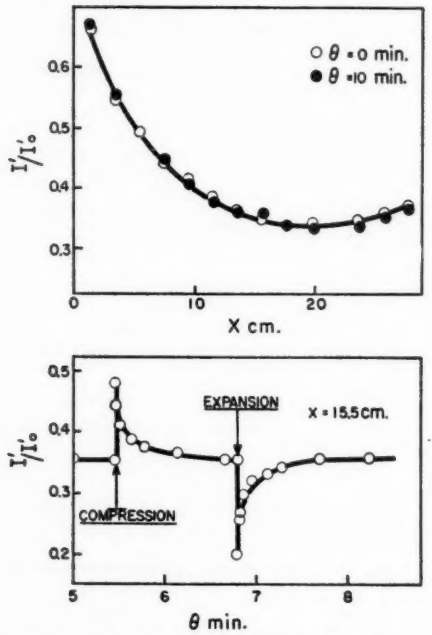

FIG. 5. The transmittance gradient in xenon immediately before (open circles) and after (solid circles) a rapid compression and expansion of xenon is shown in the upper curve. The lower curve shows the change in transmittance with time at $x = 15.5$ cm., $\bar{\rho} = \bar{\rho}_m = 1.100$ gm./cc., and $\Delta T = 0.048$°C.

perturbation). The total disturbance had no effect on the vertical transmittance gradient as shown by the coincidence of the open and closed circles.

From these results, it appears that the transmittance undergoes no protracted time lags when the vertical distribution of turbidity is not changing. Accordingly, the time lags after stirring must be associated with the slow redistribution of material in the gravitational field.

Miscellaneous Effects of Stirring

When a two phase system at $\bar{\rho} = \bar{\rho}_m$ is heated through T_c without stirring, the meniscus separating the two phases gradually becomes flat, but a visible

boundary persists over a positive interval of ΔT. A number of experiments were performed to show the result of stirring xenon after heating from below T_c without stirring. These experiments illustrate the increasing stability of a dispersion of the two phases as one approaches T_c from below. Above T_c, the two apparent phases are completely dispersible, by stirring, to a stable turbid fluid.

In the first of these experiments, xenon was heated, without stirring, from

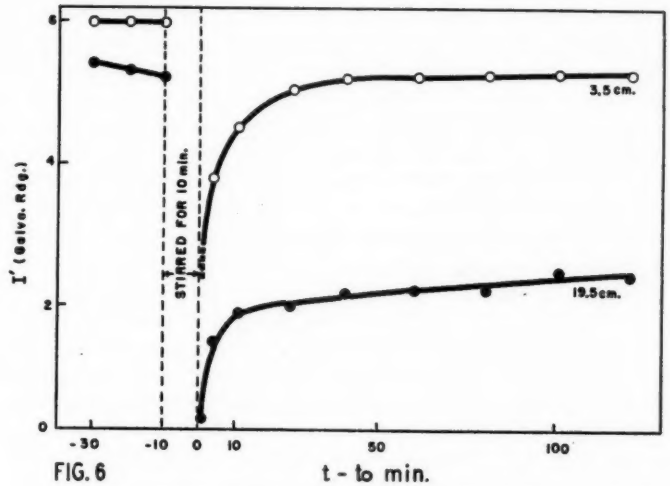

FIG. 6

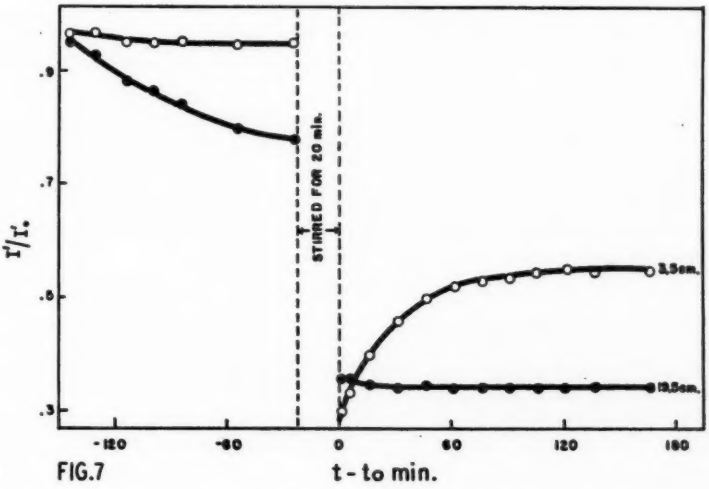

FIG.7

FIG. 6. Change in transmission readings before and after stirring xenon at $\bar{\rho} = \bar{\rho}_m = 1.100$ gm./cc. and $\Delta T = 0.027$°C.

FIG. 7. Change of transmittance before and after stirring xenon at $\bar{\rho} = \bar{\rho}_m$ and $\Delta T = 0.048$°C.

$\Delta T = -2$°C. and thermostatted at $\Delta T = -0.670$°C. No measurable change of transmission with time occurred at $\Delta T = -0.670$°C. and stirring was begun. Stirring caused complete mutual dispersion of the liquid and gas in the bomb. When stirring was stopped, the dispersion broke rapidly and the meniscus re-formed. There was no difference between transmission values observed before and after stirring.

As T_c was approached, the behavior of the dispersed system gradually changed. Fig. 6 shows the effect of stirring xenon, after heating without stirring from $\Delta T = -2$°C. to $\Delta T = -0.027$°C. Transmission readings, taken near the meniscus and near the top of the bomb, are shown as a function of $(t-t_0)$. When stirring was stopped, visible liquid droplets settled rapidly out of the gas phase to form a meniscus. This visible sedimentation was in progress during the observations at $(t-t_0) = 1$ and 4 min. At values of $(t-t_0)$ greater than five minutes, no discrete aggregates were visible above or below the meniscus and the opalescence which remained appeared visually to be identical in nature to that observed above T_c. At $(t-t_0) = 121$ min. a vertical gradient in transmission persisted throughout the fluid column.

In the experiment illustrated by Fig. 7, the xenon was heated from $\Delta T = -2$°C. through T_c, to $\Delta T = 0.048$°C. The fluid was thermostatted at this point. Before stirring, a clearly defined boundary persisted at the level $x = 20$ cm. During this time, the turbidity throughout the fluid column increased enormously. When stirring was stopped, the turbidity changed slowly throughout the bomb to reach an equilibrium distribution after about 90 min. The observed behavior resembled that which is seen when two liquid layers are dispersed by stirring to form a stable emulsion.

CONCLUSIONS

The experimental results discussed in this paper can be accounted for in terms of extensive molecular clustering in the region of T_c as was predicted by Mayer and Harrison (2, 3). The failure to observe any region within which $(\partial p/\partial V)_T$ remains zero (5) is not a serious contradiction of the more general cluster theory, but indicates that Mayer and Harrison (2, 3) may have made an erroneous assumption. This possibility is pointed out by Zimm (9) who contends that only one characteristic temperature is required to describe the phase change. In general, cluster theory, with the singular point modification of Zimm (9), seems best to describe the critical region.

REFERENCES

1. Atack, D. and Schneider, W. G. J. Phys. & Colloid Chem. 54: 1323. 1950.
2. Mayer, J. E. and Harrison, S. F. J. Chem. Phys. 6: 87. 1938.
3. Mayer, J. E. and Harrison, S. F. J. Chem. Phys. 6: 101. 1938.
4. Murray, F. E. and Mason, S. G. Can. J. Chem. 30: 550. 1952.
5. Murray, F. E. and Mason, S. G. Can. J. Chem. 33: 1399. 1955.
6. Rocard, Y. J. phys. radium, 4: 165. 1933.
7. Weinberger, M. A. and Schneider, W. G. Can. J. Chem. 30: 847. 1952.
8. Whiteway, S. G. and Mason, S. G. Can. J. Chem. 31: 569. 1953.
9. Zimm, B. H. J. Chem. Phys. 19: 1019. 1951.

TEMPERATURE COEFFICIENTS IN HYDROCARBON OXIDATION[1]

By Nan-chiang Wu Shu and J. Bardwell

ABSTRACT

The oxidation of gaseous butane has been investigated in the range 260°C. to 540°C. with reaction vessels differing greatly in surface to volume ratio. Increased surface area retards the reaction. The rate–temperature relation shows a maximum and a minimum. At low temperatures the rate is very sensitive to temperature, the apparent activation energy being greater than 100 kcal. The abnormal temperature coefficients are shown to arise in part from the differing response to temperature of the branching reactions and the initiation reactions, and in part from the occurrence of competing reactions.

The unusual effect of temperature on the rates of oxidation reactions has been pointed out by many investigators. Bodenstein (7) found that the oxidation of gaseous nitric oxide is slightly retarded by increased temperature. A similar but more pronounced effect, over a limited temperature range, was discovered by Pease in the oxidation of propane (18). Here the rate of reaction was found to pass through a maximum at 330°C. and then to decline, passing through a minimum at 380°C. The results of Pease were confirmed by Newitt and Thornes (16) and by Mulcahy (14). Anomalous temperature coefficients in oxidation reactions have been reported by others, for example by Beatty and Edgar with heptane (6), by Chamberlain and Walsh with diisopropyl ether (8), and by Bardwell and Hinshelwood with butanone (3, 4). The intervention of cool flames in hydrocarbon oxidation at certain temperatures and their disappearance at higher temperatures are related phenomena (3, 18).

When experiments are done at temperatures well below that at which a maximum occurs in the rate–temperature relation, it is frequently found that temperature now has an unusually large effect. The length of the induction period is particularly sensitive to changes of temperature. Aivazov and Neumann (1) reported that with pentane the apparent activation energy is in excess of 100 kcal. Abnormally high temperature coefficients have also been reported by Prettre (19) and by Mulcahy (14) with other hydrocarbons.

The oxidation of gaseous butane exhibits temperature effects similar to those cited for other fuels. In this paper these relations will be analyzed from the viewpoint of the theory of branching chains.

EXPERIMENTAL

Apparatus

The reaction vessel was supported vertically in a furnace and was connected to a manometer and an appropriate vacuum system. Close control of temperature was achieved by use of a "Merc-to-merc" thermoregulator and a Sunvic relay. The reactant gases were admitted separately to the vessel and the course of combustion was followed by pressure measurements.

Two reaction vessels were used, one with a low surface to volume ratio, the

[1]*Manuscript received May 17, 1955.*
Contribution from the Department of Chemistry, University of Saskatchewan, Saskatoon, Saskatchewan. This work was supported by a grant from the National Research Council of Canada

other with a high ratio. Both vessels were made of clear silica and were cylindrical in shape, 6 cm. in external diameter and 9 cm. in length. The first vessel was empty; the second was packed with 25 silica tubes each of 0.6 cm. inside diameter. The surface to volume ratio of the packed vessel was therefore more than 10 times that of the empty vessel.

RESULTS

Analysis of Pressure–Time Curves

The autocatalytic character of the reaction between oxygen and gaseous hydrocarbons necessitates the use of some arbitrary criterion of reaction rate. Two such criteria have found extensive use in previous kinetic investigations (2, 9, 15):

(*a*) the maximum rate, ρ_{max}, i.e. the slope of the pressure–time curve at its inflection point,

(*b*) the reciprocal induction period, $1/\theta$, the induction period being the length of time between the entrance of the reactants to the vessel and the attainment of some defined rate, often the maximum rate.

Theoretical treatments of hydrocarbon oxidation, for example that of Semenov (21), have ascribed the autocatalytic nature of the reaction to a slow multiplication of reaction centers by chain branching of a degenerate type. In a reaction where chain branching occurs the number of chain centers x increases with time according to the equation

$$[1] \qquad dx/dt = B' + Ax.$$

B' is the rate of production of chain centers independent of the branching process, for example by direct interaction of fuel and oxygen. A is the branching factor. Insofar as it is permissible to consider A and B' constant in the early part of the reaction, equation [1] may be integrated to yield:

$$[2] \qquad x = (B'/A)(e^{At} - 1).$$

Thus chain centers multiply in an approximately exponential fashion, and reaction rate increases accordingly. If it is assumed that the observed rate of pressure increase dp/dt is a valid measure of reaction rate, the increase in pressure, Δp, will be proportional to $\int x dt$, i.e. proportional to:

$$(B'/A^2)(e^{At} - At - 1).$$

Combining the proportionality constant and B' to give a new term B, we obtain

$$[3] \qquad \Delta p = (B/A^2)(e^{At} - At - 1).$$

When At is considerably greater than unity the exponential term dominates and a plot of log Δp against time should be linear.

The oxidation of butane provides abundant confirmation of this prediction. Plots of log Δp against time show excellent linearity during the first third or so of the reaction; i.e. before the consumption of reactants becomes excessive. This is true both with the empty vessel and with the packed vessel, and with

wide variations of vessel temperature and reactant concentration. The precision with which the pressure–time data conform to the predicted exponential relation compares favorably with that observed in studies of the oxidation of other gaseous fuels (4, 21). For calculation it is convenient to neglect all but the exponential term in Eq. [3], i.e. to take

$$\Delta p = (B/A^2)e^{At}. \quad [4]$$

A is thus the slope of the linear portion of the plot of the natural logarithm of the pressure increase against time of reaction. B is calculated from the intercept and slope of this plot, and has the units of mm./min^2. B will henceforth be called the initiation factor, whereas A will be called the branching factor. The units of A are min^{-1}.

The use of Eq. [4] rather than the more exact Eq. [3] for estimating A and B introduces an approximation, the magnitude of which is exemplified by the following data for an experiment with the empty vessel at 270°C. using 100 mm. each of butane and oxygen. Here Δp increased from 5.8 mm. at 8 min. to 20.1 mm. at 10 min. Calculated values of A and B are given in Table I. The errors introduced by use of the approximate but much more convenient Eq. [4] are not serious for present purposes, since discrepancies are always in the same direction and are small compared with the alteration of A and B with temperature (see below).

TABLE I

CALCULATION OF A AND B FROM PRESSURE–TIME DATA

	A (min.$^{-1}$)	B (mm./min.^{3})
By Eq. [3]	0.622	0.0156
By Eq. [4]	0.608	0.0172

Effect of Temperature on Maximum Rate and Reciprocal Induction Period

The general effect of temperature on oxidation rate with butane may be seen in Figs. 1–3, in which the logarithms of the usual criteria of reaction rate, ρ_{max} and $1/\theta$, are plotted against the reciprocal of the absolute temperature. Fig. 1 shows that with the empty vessel, the reciprocal induction period, $1/\theta$, passes through a maximum at about 350°C. and a minimum at about 430°C. The corresponding results for the maximum rate ρ_{max} are shown in Fig. 2. The curves resemble those in Fig. 1 in that the minima again occur at about 430°C. However, with the pressures used slow combustion gives way to cool flames over a considerable range of temperature and the curves for ρ_{max} are therefore not continuous.

When the packed vessel was used instead of the empty vessel, the reaction was considerably slower and cool flames appeared only in exceptional circumstances. Measurements of ρ_{max} and $1/\theta$ in the range 314°C. to 540°C. yielded the results shown in Fig. 3, which are qualitatively similar to those obtained using the empty vessel and lower pressures. The results also illustrate the two unusual temperature effects with which we are here principally concerned:

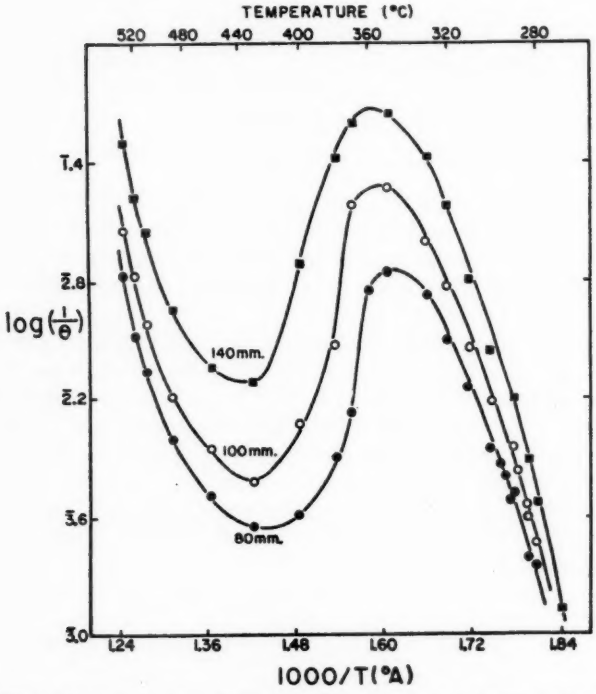

FIG. 1. Effect of temperature on the reciprocal induction period with equimolecular mixtures of butane and oxygen and an empty vessel 6 cm. in diameter. Total reactant pressure is shown

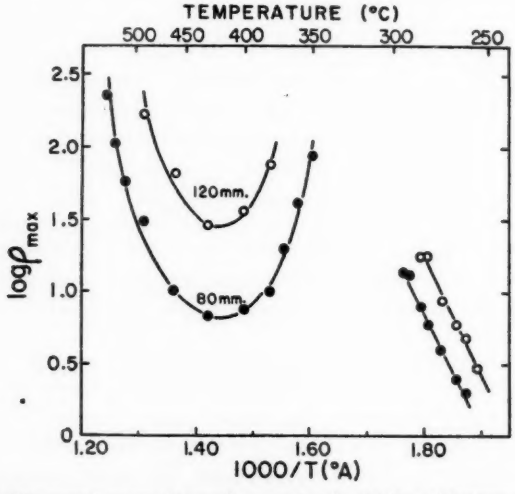

FIG. 2. Effect of temperature on the maximum rate of oxidation of butane with equimolecular mixtures of butane and oxygen and an empty vessel 6 cm. in diameter. Total reactant pressure is shown.

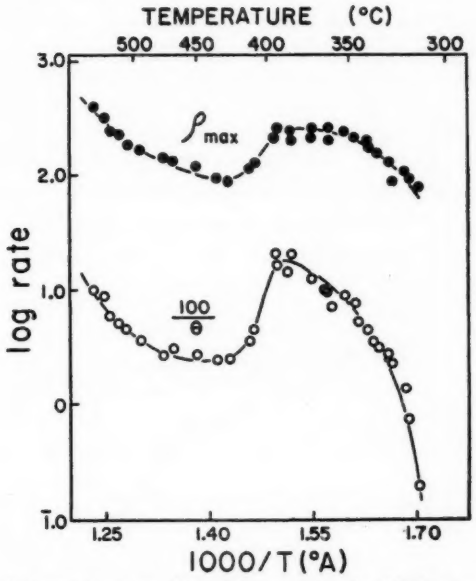

FIG. 3. Effect of temperature on the maximum rate of oxidation and on the reciprocal induction period using a packed vessel and equimolecular mixtures of butane and oxygen at a total pressure of 200 mm.

(*a*) The decline of reaction rate with rising temperature, which here occurs between 395°C. and 430°C. We shall henceforth refer to this negative effect of temperature as the anomalous temperature coefficient.

(*b*) The great sensitivity of the induction period to changes of temperature in the low temperature region. For example the data plotted in Fig. 3 show that on lowering the temperature from 324°C. to 314°C., the induction period increases from 50 sec. to 500 sec.

The Initiation Factor and the Branching Factor at Low Temperatures

Since the abnormal temperature coefficients noted above must arise from unusual sensitivity to temperature of the initiation factor, B, or of the branching factor, A, or of both, it is of interest to explore the effect of temperature on each of these factors. The exceptionally large temperature coefficient at low temperatures will be considered first.

When the pressure–time curves were analyzed by the method described above it was found that the initiation factor B was much more temperature-dependent than the branching factor A. For example, the results plotted in Fig. 3 in the temperature range 314°C. to 345°C. yield an apparent activation energy of 31 kcal. for A but a value of over 120 kcal. for B. In fact, the temperature coefficient of B becomes essentially infinite at about 314°C. with the pressure used.

The above relationships were investigated further in a series of experiments using 200 mm. each of butane and oxygen, again with the packed vessel. Convenient rates were obtained in the temperature range 260°C. to 305°C.

The results are shown in Fig. 4 and the calculated activation energies given in Table II. Of the four quantities plotted it is seen that the initiation factor B is by far the most sensitive to temperature, the values increasing by a factor of about 10^{13} for a temperature increase of 45°C. Considerable sensitivity to temperature is also shown by $1/\theta$, particularly in the range 260°C. to 270°C. In this 10-degree interval, $1/\theta$ increases by a factor of about five whereas ρ_{max} and A are approximately doubled. On the other hand B increases by a factor

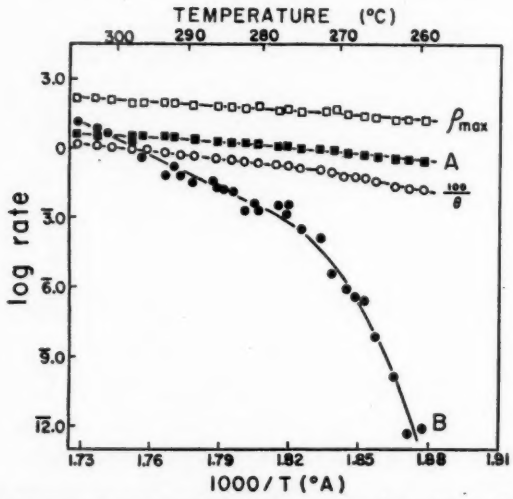

FIG. 4. Effect of temperature on maximum rate (ρ_{max}), reciprocal induction period ($100/\theta$), branching factor (A), and initiation factor (B) using a packed vessel and equimolecular mixtures of butane and oxygen at a total pressure of 400 mm.

of about 30 million. It may be concluded therefore that the large dependence of $1/\theta$ on temperature in this range is derived from the initiation factor rather than from the branching factor.

Experiments with the empty vessel gave results that confirmed the above conclusions for the packed vessel. For example, measurements in the temperature range 273°C. to 294°C. with 100 mm. each of butane and oxygen showed that the apparent activation energy of B was about 100 kcal. whereas that of A was about 68 kcal.

TABLE II

APPARENT ACTIVATION ENERGIES OF THE MAXIMUM RATE, RECIPROCAL INDUCTION PERIOD, BRANCHING FACTOR, AND INITIATION FACTOR

Butane pressure: 200 mm.; oxygen pressure: 200 mm.

Temperature range (°C.)	Activation energy (kcal.)			
	ρ_{max}	$1/\theta$	A	B
275° to 305°C.	30	49	38	220
260° to 270°C.	41	93	46	1000

Limiting Pressure for Finite Induction Periods

The large variation of induction period with temperature appears to be related to the existence of pressure limits in hydrocarbon oxidation. Here we shall not be concerned with the pressure limits delineating the regions of occurrence of slow combustion, cool flames, ignition, etc., but only with the low-pressure limit which marks the transition from finite to infinite induction periods. The existence of such a limit has been clearly demonstrated by Malherbe and Walsh (13) who showed that a plot at constant temperature of induction period against pressure yielded an asymptote of a definite positive pressure. Below this pressure the induction period was of infinite duration. Using a vessel with an effective diameter intermediate between those employed in the present investigation, Malherbe and Walsh showed that the low-pressure limit increased with decreasing temperature (13).

Our measurements have in general confirmed the above conclusions and have shown, furthermore, that the low-pressure limit increases with increasing surface to volume ratio (see Fig. 5). The low-pressure limit, P_c, is readily

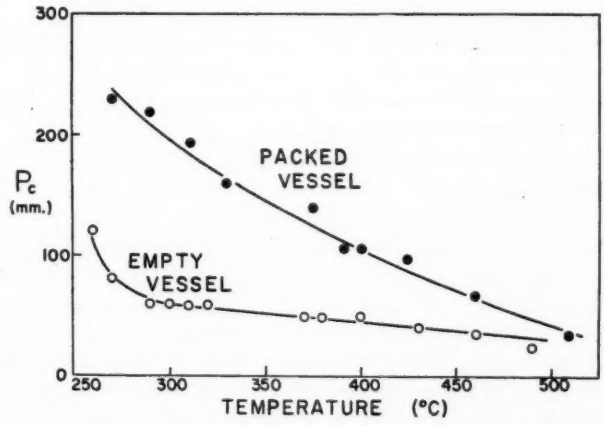

FIG. 5. Effect of temperature on the low-pressure limit. P_c is the total pressure of an equimolecular mixture of butane and oxygen at which the induction period becomes infinite.

determined by extrapolation of a plot of $1/\theta$ against pressure. Experiments with pressures slightly below this limit show that no perceptible reaction occurs even after many hours. Reaction can, however, be induced by the addition of a small amount of acetaldehyde (14) and it is of interest that the values of A and ρ_{max} then determined agree well with those obtained without acetaldehyde just above the pressure limit. Additions of acetaldehyde to reaction mixtures just above the low-pressure limit greatly increase B but have only a small effect on A. From these results it may be concluded that although favorable conditions for chain branching may still exist below the low-pressure limit the induction period is infinite because the effective rate of initiation is zero.

The Anomalous Temperature Coefficient

Attempts were made to analyze the sharp decline of reaction rate at about 400°C. by assessing the temperature coefficients of the branching factor and initiation factor. The empty vessel proved to be unsuitable for this purpose since the reaction rate was very high in the temperature range of interest (see Fig. 2). Even with the packed vessel where reaction was somewhat slower it was difficult to determine precise values of A and B over a considerable temperature range with any chosen constant pressure of reactants. The trends observed however are illustrated by the results given in Table III, which allow

TABLE III

EFFECT OF TEMPERATURE ON ρ_{max}, $1/\theta$, A, AND B IN THE REGION OF THE ANOMALOUS TEMPERATURE COEFFICIENT

Butane pressure: 70 mm.; oxygen pressure: 70 mm.

Temperature (°C.)	ρ_{max} (mm./min.)	$1/\theta$ (sec.$^{-1}$)	A (min.$^{-1}$)	B (mm./min.^{2})
368	83	0.030	8.9	6.7
382	20	0.0056	1.7	0.22

comparison of the behavior at 368°C. with that at 382°C. The latter temperature is approximately that for minimum reaction rate with the pressure employed. It is seen that here the sharp decline in ρ_{max} and $1/\theta$ is accompanied by substantial decreases in both A and B.

DISCUSSION

Temperature Coefficients

Although the experiments reported above have been confined to the oxidation of butane, comparison with other investigations shows that a wide range of temperature coefficient is a common property of the gas-phase oxidation of hydrocarbons (10, 12). Search for the origin of this behavior is considerably assisted by the exponential form of the pressure–time curve in butane oxidation, and by the opportunity thereby provided of estimating separately the branching rate and the initiation rate. It has been shown above that these two rates can differ greatly in their temperature dependence.

The large temperature coefficient of the induction period at low temperatures (Figs. 3 and 4) is apparently associated with the low-pressure limit (Fig. 5). Since this limit moves toward higher pressures as the temperature is lowered, it follows that when a series of experiments is done with constant pressures at successively lower temperatures the induction period will become infinite at (and below) some definite temperature. Comparison of Fig. 3 with Fig. 5 shows that it is just above this temperature that the induction period is most temperature-sensitive.

The Origin of the Low-pressure Limit

Malherbe and Walsh (13) have suggested that the low-pressure limit in hydrocarbon oxidation is similar in origin to that observed in the hydrogen–oxygen reaction, and represents the pressure above which the branching factor becomes positive and below which it is negative. Our results do not

support this explanation. Fig. 4 shows that the rapid lengthening of the induction period as the limit is approached, here by a decrease of temperature, is due to the approach to zero of the initiation factor B. It is also apparent from Fig. 4 and Table II that in this range the branching factor A is neither very small nor very temperature-sensitive. It seems very unlikely therefore that the branching factor would drop abruptly to zero when the temperature is lowered a few degrees more. The suggestion of Malherbe and Walsh also encounters difficulties in explaining the observed effect of adding small amounts of acetaldehyde along with the fuel and oxygen. As already noted, these additions to mixtures above the low-pressure limit greatly increase the initiation factor but have only a slight effect on the branching factor. The addition of acetaldehyde to mixtures just below the limit, i.e. where the induction period would normally be infinite, induces reaction which then displays a branching factor of substantial magnitude, and comparable to that observed just above the limit. These effects are not consistent with a vanishing of A at the limit but are quite in harmony with a vanishing of B.

The Anomalous Temperature Coefficient

It has been shown above that when the temperature approaches 400°C. the oxidation rate, as judged by either ρ_{max} or $1/\theta$, passes through a maximum and then declines. This behavior, as well as the resurgence of reaction at still higher temperatures, is similar to that reported in investigations of the combustion process with other paraffin hydrocarbons (18, 20). The customary interpretation is that at high temperatures the mechanism involves formaldehyde and relatively simple atoms and radicals, but that at lower temperatures complex molecules such as peroxides and higher aldehydes play an important part (11, 17). The decline of reaction rate with rising temperature at about 400°C. is taken as a sign of the decreasing importance of these compounds as combustion intermediates. Although the reactions responsible for this effect have not yet been firmly established, two reasonable possibilities exist:

(*a*) the combustion intermediate is wasted through its participation in reactions leading to inactive products (9, 20),

(*b*) the combustion intermediate is produced in smaller amounts because of pyrolytic destruction of one of its precursors in the chain sequence (22).

It has been shown in Table III that both the branching factor and the initiation factor are sharply reduced by a small rise of temperature in the region of the anomalous temperature coefficient. The decline of the initiation factor contributes to the lengthening of the induction period, but the decrease of the branching factor is more important since it affects both the induction period and the maximum rate, ρ_{max} (5).

Explanation by Competing Reactions

There remains the need for an explanation of the vanishing of the initiation factor and the branching factor at particular temperatures. For simplicity we may assume that a relatively stable combustion intermediate is formed which undergoes two modes of decomposition, one leading to its regeneration in increased quantity, the other leading to comparatively inert products. It may

be shown (5, 21) that when two such competing reactions occur the branching factor A is the difference of two terms, e.g. A_1-A_2. Each of these terms presumably increases with rising temperature, the rates of increase being determined by the respective activation energies E_1 and E_2. Now if $E_2 > E_1$, the variation of log (A_1-A_2) with $1/T$ will be as sketched in Fig. 6(*a*). At a sufficiently low temperature the apparent activation energy of the branching factor approaches that of A_1, but as the temperature is increased A_1-A_2 passes through a maximum and then falls off sharply. In this way the anomalous temperature coefficient at about 400°C. is accounted for, although the predicted vanishing of A is obscured by the intervention of the high-temperature mechanism of oxidation.

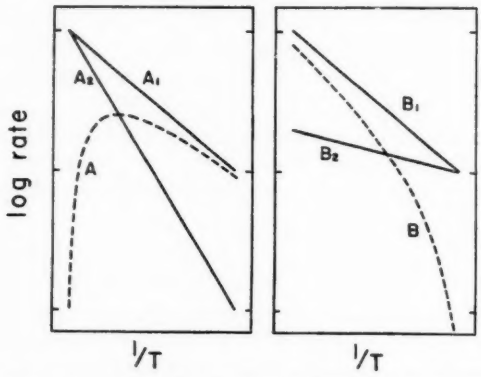

FIG. 6. Schematic diagrams explaining abnormal temperature coefficients.
Diagram (*a*), on left, $A = A_1-A_2$; activation energy of A_1 less than that of A_2.
Diagram (*b*), on right, $B = B_1-B_2$; activation energy of B_1 greater than that of B_2.

The extreme temperature-sensitivity of the initiation factor, B, at lower temperatures is explicable in a generally similar way. We may consider the measured initiation factor as being the difference of two terms, e.g. B_1-B_2, where B_2 represents inhibiting influences. If the activation energy of B_1 is greater than that of B_2 the variation of log (B_1-B_2) with $1/T$ will be as sketched in Fig. 6(*b*). The very large apparent activation energy of B (Table II) and the existence of a temperature below which the induction period is infinite (Fig. 5) are consistent with this diagram.

REFERENCES

1. AIVAZOV, B. and NEUMANN, M. Z. physik. Chem. B, 33: 349. 1936.
2. ANDREEV, E. A. Acta Physicochim. U.R.S.S. 6: 57. 1937.
3. BARDWELL, J. and HINSHELWOOD, C. N. Proc. Roy. Soc. (London), A, 205: 375. 1951.
4. BARDWELL, J. and HINSHELWOOD, C. N. Proc. Roy. Soc. (London), A, 207: 461. 1951.
5. BARDWELL, J. Proc. Roy. Soc. (London), A, 207: 470. 1951.
6. BEATTY, H. A. and EDGAR, G. J. Am. Chem. Soc. 56: 102. 1934.
7. BODENSTEIN, M. Z. physik. Chem. 100: 68. 1922.
8. CHAMBERLAIN, G. H. N. and WALSH, A. D. Third Symposium on Combustion, Flame and Explosion Phenomena. p. 368. 1949.
9. CULLIS, C. F. and HINSHELWOOD, C. N. Discussions Faraday Soc. No. 2: 117. 1947.
10. CULLIS, C. F. and SMITH, L. S. A. Trans. Faraday Soc. 46: 42. 1950.
11. EGERTON, A. C. Nature, 121: 10. 1928.

12. JOST, W. Explosion and combustion processes in gases. McGraw-Hill Book Company, Inc., New York. 1946. pp. 448–451.
13. MALHERBE, F. E. and WALSH, A. D. Trans. Faraday Soc. 46: 824. 1950.
14. MULCAHY, M. F. R. Trans. Faraday Soc. 45: 575. 1949.
15. MULCAHY, M. F. R. and RIDGE, M. J. Trans. Faraday Soc. 49: 1297. 1953.
16. NEWITT, D. M. and THORNES, L. S. J. Chem. Soc. 1669. 1937.
17. NORRISH, R. G. W. Discussions Faraday Soc. No. 10: 269. 1951.
18. PEASE, R. N. J. Am. Chem. Soc. 60: 2244. 1938.
19. PRETTRE, M. Compt. rend. 202: 1176. 1936.
20. PRETTRE, M. Compt. rend. 207: 576. 1938.
21. SEMENOV, N. Chemical kinetics and chain reactions. Oxford University Press, London, 1935.
22. WALSH, A. D. Trans. Faraday Soc. 43: 297. 1947.

SYNTHESES OF A SERIES OF 15-KETOGLYCOLS AND 15-KETO FATTY ACIDS FROM USTILIC ACID[1]

By A. T. Crossley[2] and B. M. Craig

ABSTRACT

Reaction of the methyl ester of ustilic acid A (15,16-dihydroxypalmitic acid) with a methyl Grignard, oxidation of the glycol grouping, bromination, and hydrogenolysis produced 15-methylhexadecanoic acid. A series of 15-keto acids resulted from reaction of the amide of ustilic acid A with the appropriate Grignard reagent followed by oxidation of the glycol grouping. Infrared absorption characteristics of these compounds are described.

Ustilagic acid has been produced by fermentation using a culture of *Ustilago zeae* (2). Ustilic acid A (15,16-dihydroxypalmitic acid) and ustilic acid B (2,15,16-trihydroxypalmitic acid) are produced by hydrolysis of ustilagic acid (4). These acids are easily separated from the remainder of the hydrolysis products and from one another and are potentially available in large quantities.

The ustilic acids possess a carboxyl group at one end of the molecule and an easily oxidizable glycol grouping at the other end and as such should constitute valuable starting materials for the synthesis of various new and naturally occurring long chain compounds. The present investigation deals with the synthesis of 15-methylhexadecanoic acid and a series of 15-keto acids.

A number of methyl branched fatty acids which are primarily concerned with the wool fats have been synthesized by a number of workers (1, 3, 7, 8, 9). These syntheses have involved the preparation of appropriate fragments followed by chemical coupling or anodic syntheses. Weitkamp (9) prepared 15-methylhexadecanoic acid from a lower homologue and Stenhagen *et al.* synthesized the same acid (1). Ustilic acid A is a convenient starting material for the synthesis of this acid by the following series of reactions:

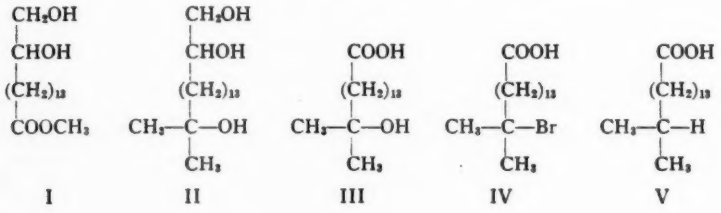

Methyl ustilate A (I) was converted in almost theoretical yield into the tertiary alcohol II, m.p. 55.5–56.0° C., by using a large excess of methylmagnesium bromide. Reaction of methyl isopropylidene ustilate A with the Grignard reagent followed by removal of the isopropylidene grouping with

[1]*Manuscript received May 24, 1955.*
Contribution from the National Research Council of Canada, Prairie Regional Laboratory, Saskatoon, Saskatchewan. Issued as Paper No. 197 on the Uses of Plant Products and as N.R.C. No. 3696.
[2]*National Research Council of Canada Postdoctorate Fellow 1952.*

methanolic hydrochloric acid gave a very poor yield of II. Oxidation of II with chromic oxide in acetic acid at low temperature gave 15-methyl-15-hydroxyhexadecanoic acid III, m.p. 70.5–71.5° C., which yielded *p*-bromophenacyl derivative, m.p. 80.6–81.0° C. This oxidation was also carried out using lead tetraacetate and oxygen as described below. The hydroxy acid III was treated with hydrogen bromide in acetic acid to give the tertiary bromo derivative IV, m.p. 45–46° C., which, on treatment with hydrogen and Raney nickel in ethanolic sodium hydroxide, gave 15-methylhexadecanoic acid V, m.p. 60.7–61.3° C. (reported m.p. 59.3–59.9° C. (1) and 60.2° C. (9)).

The synthesis of a series of 15-keto acids was carried out by the series of reactions given below. To favor the formation of the ketoglycol rather than the tertiary alcohol derivative, the amide of ustilic acid A was used as a starting material in the Grignard reaction. The reaction of amides with Grignard reagents has been investigated by Whitmore *et al.* (10, 11). To increase solubility the isopropylidene derivative (VII) was used. Reaction of the latter with 1.1 moles of methylmagnesium bromide gave a poor yield of the ketone (VIII) (R = CH_3), m.p. 40.0–41.0° C., semicarbazone m.p. 123.5–124.0° C., but the yield was increased by the use of 100% excess of the Grignard reagent. A small amount of the tertiary alcohol formed was separated on alumina. The corresponding ethyl, propyl, and butyl homologues (VIII) were also prepared by using the appropriate Grignard reagents. These had melting points, respectively, of 37° C. (R = C_2H_5), 43° C. (R = C_3H_7), and 48.5° C. (R = C_4H_9). Removal of the isopropylidene group afforded the free ketoglycols (IX) which are described in Table I. Purification of the latter compounds was greatly facilitated by a treatment with warm alcoholic alkali before crystallization from benzene.

TABLE I

MELTING POINTS AND ELEMENTAL ANALYSIS OF KETOGLYCOLS AND KETO ACIDS

Compound	Formula	M.p., °C.	Found		Calculated	
			C (%)	H (%)	C (%)	H (%)
1,2-Dihydroxy-16-ketoheptadecane	$C_{17}H_{34}O_3$	83.0–83.7	71.34	12.07	71.28	11.96
1,2-Dihydroxy-16-ketooctadecane	$C_{18}H_{36}O_3$	93.8	72.43	11.48	72.44	11.51
1,2-Dihydroxy-16-ketononadecane	$C_{19}H_{38}O_3$	92.5	73.39	11.59	73.02	11.61
1,2-Dihydroxy-16-ketoeicosane	$C_{20}H_{40}O_3$	93.9	73.08	12.07	73.11	12.27
15-Ketohexadecanoic acid*	$C_{16}H_{30}O_3$	82.3	70.86	11.10	71.07	11.18
15-Ketoheptadecanoic acid	$C_{17}H_{32}O_3$	85.7–86.1	71.73	11.44	71.78	11.34
15-Ketooctadecanoic acid	$C_{18}H_{34}O_3$	83.4	72.44	11.51	72.43	11.48
15-Ketononadecanoic acid	$C_{19}H_{36}O_3$	85.7	73.39	11.59	73.03	11.61

**Semicarbazone, m.p. 129.6° C. (C, 62.57; H, 10.22; N, 12.82%. Calc. for $C_{17}H_{33}O_3N_3$: C, 62.35; H, 10.16; N, 12.83%.)*

These ketoglycols (IX) were converted to 15-keto fatty acids (X) by simultaneous oxidation with lead tetraacetate and oxygen at 50° C. according to the method of Mendel and Coops (6). The oxidation products were purified by distillation and crystallization from alcohol. The melting points of these four, hitherto unprepared, keto fatty acids are given in Table I.

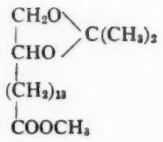

VI

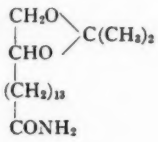

VII

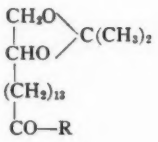

VIII

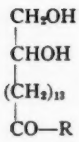

IX

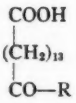

X

Infrared absorption determinations were made on all the compounds with a Perkin-Elmer Model 21 instrument equipped with a sodium chloride prism, and the crystalline samples were mounted in KBr. The 15-methyl-15-hydroxyhexadecanoic acid showed OH absorption bands at 3440 and 1152 cm.$^{-1}$, and also several poorly resolved bands between 1390 and 1300 cm.$^{-1}$ which might be caused by the $(CH_3)_2C-$ group. The 15-methylhexadecanoic acid showed two clearly resolved bands at 1385 and 1365 cm.$^{-1}$ which are characteristic for branched methyl groups. These bands were absent in the spectrum of pure hexadecanoic acid. The 1,2-dihydroxy-15-keto compounds showed the expected hydroxyl band between 3400 and 3200 cm.$^{-1}$ and also two absorption bands at 1100 and 1082 cm.$^{-1}$ which could be assigned to a secondary and a primary hydroxyl group respectively. They also showed the ketonic carbonyl absorption between 1710 and 1705 cm.$^{-1}$. The corresponding 15-keto acids showed absorptions in the 1700 cm.$^{-1}$ and the 900–700 cm.$^{-1}$ regions characteristic for carboxylic acids. Resolutions of the carboxyl C=O and ketone C=O were achieved in the 1720–1700 cm.$^{-1}$ region for 15-ketohexadecanoic and 15-ketoheptadecanoic acids but not for 15-ketooctadecanoic and 15-ketononadecanoic acids. The C=O absorption band in the latter was much wider than for the corresponding 15-keto-1,2-dihydroxy-nonadecane and -eicosane.

EXPERIMENTAL

NOTE: All melting points are corrected and determinations have been made in each case in the usual manner and also on a heating stage microscope.

Separation of the Ustilic Acids

A ustilic acid mixture (158 gm.), prepared by hydrolysis of ustilagic acid (4), was shaken for four hours with 1 liter of dry acetone containing 1% sulphuric acid. A small amount of inorganic material remained insoluble and the solution was filtered into a separatory funnel containing 3 liters of ice-cold water. The solution was extracted with 1.6 liters of petroleum ether (b.p. 60–80° C.) and the mother liquor was extracted with a further 1 liter. The combined petroleum ether extracts were washed three times with water. A cold solution of 60 gm. of potassium hydroxide in 420 ml. of water was then added and after

one minute's shaking, 450 ml. of 40% aqueous ethanol was added and the aqueous layer run off. The petroleum ether extract was then washed with 500 ml. of 3% aqueous potassium hydroxide and three times with 30% aqueous ethanol. The five aqueous ethanol washings were combined and diluted with 1 liter of water and re-extracted with 400 ml. petroleum ether, the extract being added to the main bulk of petroleum ether solution. The aqueous extract was acidified with sulphuric acid and extracted with chloroform to yield 163 gm. of crude isopropylidene ustilic acid A which was recrystallized from acetone to m.p. 64–65° C. The petroleum extracts gave 12 gm. of diisopropylidene ustilate B, m.p. 42–43° C., reported m.p. 42.5–43° C. (5).

The proportions of the ustilic acids in the mixture have been found to vary slightly and the present mixture represents the highest proportion of ustilic acid A which has been found. The amount may fall to about 70% of the mixture of acids.

Methyl Isopropylidene Ustilate A

Isopropylidene ustilate A (154 gm.) was esterified with diazomethane in dry ether to yield 160 gm. of the crude product as outlined in the procedure of Lemieux (5). Two crystallizations from acetone at 4° C. gave the pure methyl ester, m.p. 46.3–46.7° C., reported m.p. 46–47° C. (5).

Methyl Ustilate A

Isopropylidene ustilic acid A (20 gm.) was boiled under reflux with 4% methanolic HCl for two hours as outlined by Lemieux (5). The solution was poured into water and extracted with chloroform to give 16.2 gm. of crude methyl ustilate A, which after three crystallizations from ethanol had m.p. 85.2–86.1° C., reported m.p. 85.5–86.0° C. (5).

1,2,16-Trihydroxy-16-methylheptadecane

Methyl ustilate A (10 gm.) in 200 ml. of dry ether was added during one hour, with rapid stirring, to 23.5 gm. of methylmagnesium iodide in 300 ml. of ether, the mixture being allowed to reflux continuously during the addition. The semisolid reaction mixture was boiled under reflux for 10 hr. and was then decomposed with water and acetic acid. The crude tertiary alcohol, 10.1 gm., m.p. 54.0–55.0° C., was extracted with chloroform. The 1,2,16-trihydroxy-16-methylheptadecane purified by one crystallization from acetone had a m.p. 55.5–56.0° C. Calc. for $C_{18}H_{38}O_3$: C, 71.50; H, 12.60%. Found: C, 71.33; H, 12.50%.

15-Hydroxy-15-methylhexadecanoic Acid

The above tertiary alcohol (5.0 gm.) was dissolved in 140 ml. of acetic acid containing 7.0 gm. of chromic oxide and the solution allowed to stand for 12 hr. at 3° C., when it was diluted with ice-cold water (1 liter) and extracted with benzene. The benzene solution was washed with water until neutral and the benzene evaporated. The crude hydroxy acid was then taken up in 100 ml. of ether and the ether washed twice with 5% aqueous potassium hydroxide, and twice with water. The combined washings were acidified with sulphuric acid and extracted with ether to yield 2.63 gm. of 15-hydroxy-15-methyl-

hexadecanoic acid, which was purified by three crystallizations from acetone and crystallized as colorless needles, m.p. 70.5–71.5° C. Calc. for $C_{17}H_{34}O_2$: C, 72.10; H, 11.95%. Found: C, 72.45%; H, 12.06%.

15-Bromo-15-methylhexadecanoic Acid

The hydroxy acid (1.39 gm.) was dissolved in 10 ml. of a 50% solution of hydrobromic acid in acetic acid and left for 14 hr. at 22° C. The solution was then diluted with 100 ml. of ice-cold water and the product extracted with benzene. Yield, 1.71 gm.; m.p. 45.0–46.5° C. Calc. for $C_{17}H_{33}O_2Br$: Br, 22.6%. Found: Br, 22.5%.

15-Methylhexadecanoic Acid

The 15-bromo-15-methylhexadecanoic acid (1.65 gm.) was dissolved in 25 ml. of ethanol, and 50 ml. of ethanol containing 5 ml. of 4 *N* sodium hydroxide added, together with a small amount of Raney nickel. The mixture was shaken with hydrogen under a pressure of 25 p.s.i. for 14 hr. at 25° C. The solution was filtered, poured into dilute sulphuric acid, and the product extracted with ether. Unexpectedly this material contained a large proportion of unsaturated material (iodine value 40) and it was therefore hydrogenated, in a similar medium to that previously used, but at a temperature of 80° C. and a pressure of 800 p.s.i. of hydrogen, for four hours. The product was saturated (iodine value 0), and was purified by distillation followed by three crystallizations from ethanol. The pure 15-methylhexadecanoic acid had m.p. 60.7–61.3° C. (reported m.p. 59.3–59.9° C. (1) and 60.2° C. (9)). Calc. for $C_{17}H_{34}O_2$: C, 75.56; H, 12.59%. Found: C, 75.45; H, 12.72%. The *p*-bromophenacyl derivative had a m.p. 83.1–83.6° C. Calc. for $C_{25}H_{39}O_3Br$: C, 64.23; H, 8.41; Br, 17.1%. Found: C, 63.61; H, 8.64; Br, 17.4%.

Isopropylidene Ustilamide A

Methyl isopropylidene ustilate A (70 gm.), together with 1500 gm. of a 25% (wt.) solution of ammonia in methanol (prepared and kept below 0° C.), was heated to 180° C. in a sealed bomb for six and one-half hours. The product was poured into 3000 ml. of ice-cold water and the precipitated amide filtered off and washed with 1000 ml. of cold water. This material was dried and then boiled with 500 ml. of ether, and the slurry cooled to 5° C. when it was filtered. The precipitate was washed with 300 ml. of cold ether. Thirteen grams of unchanged methyl isopropylidene ustilate A were recovered from the ethereal filtrate and 55 gm. of crude amide were obtained, which crystallized from methanol as colorless plates, m.p. 99.7–100.3° C. Calc. for $C_{19}H_{37}O_3N$: C, 69.67; H, 11.39; N, 4.15%. Found: C, 69.62; H, 11.32; N, 4.17%.

Reaction of Isopropylidene Ustilamide A with Grignard Reagents

A solution of methylmagnesium bromide was prepared by slow addition of 236 gm. of a 17% solution of methyl bromide in dry ether (prepared by passing methyl bromide gas into dry ether at 0° C.) to 10.0 gm. of magnesium in 300 ml. ether. The Grignard reagent was allowed to settle, decanted, and its strength determined by titration.

A solution of methylmagnesium bromide in 440 ml. ether containing 47.5 gm.

(1.9 times theoretical) of the reagent was added to a solution of 33.9 gm. of isopropylidene ustilamide A, dissolved in 1500 ml. of a mixture of equal volumes of dry benzene and dry ether, with stirring, the solution being allowed to reflux during the addition. The solution was heated under reflux for a further eight hours, and the product was isolated in the usual manner. It was then dissolved in 50 ml. of ether and a small amount of unchanged amide was filtered off. The crude ketone (32.79 gm.) was dissolved in a small amount of benzene, transferred to an alumina column (14 cm. × 5 cm.), and eluted with benzene. The material in the first 150 ml. of eluate (0.3 gm.) was discarded and the pure ketone (25.0 gm.) was isolated from the next 8000 ml. of eluate. The isopropylidene ether of 1,2-dihydroxy-16-ketoheptadecane had m.p. 40.0–40.5° C. Calc. for $C_{20}H_{38}O_3$: C, 74.12; H, 11.74%. Found: C, 73.9; H, 11.85%. Its semicarbazone had m.p. 123.5–124.0° C. Calc. for $C_{21}H_{41}O_3N_3$: C, 65.75; H, 10.77; N, 10.96%. Found: C, 65.79; H, 10.71; N, 11.00%. Three homologous ketones were prepared in a similar manner by using ethyl-, propyl-, and butylmagnesium bromide Grignard reagents. These were purified by recrystallization and the melting points were respectively 37.0° C. (R = C_2H_5), 43.0° C. (R = C_3H_7), and 48.5° C. (R = C_4H_9).

1,2-Dihydroxy-16-ketoheptadecane

The 1,2-isopropylidene ether of 16-ketoheptadecane (8.0 gm.) was dissolved in 70 ml. of chloroform and the solution cooled to 5° C. Thirty milliliters of a 20% (wt.) solution of hydrochloric acid in 85% aqueous methanol was added and the solution allowed to stand at 20° C. for two hours. Water (100 ml.) was added and the product (m.p. 72–76° C.) extracted with chloroform. It was then dissolved in 50 ml. of 3% alcoholic potassium hydroxide solution and kept at 50° C. for 20 min. The solution was poured into 300 ml. of cold water and the methyl ketoglycol, 5.5 gm., m.p. 78–81° C., was filtered off and recrystallized three times from benzene, the pure product having m.p. 83.0–83.7° C. The products from the reaction of the ethyl, propyl, and butyl Grignards were treated in a similar manner to prepare the three other homologues whose constants are given in Table I.

15-Ketohexadecanoic Acid

Lead tetraacetate (300 mgm.) was dissolved in 25 ml. of dry benzene in a 50 ml. three-necked flask fitted with a stirrer, dropping funnel, and a condenser through which a glass tube passed and projected below the surface of the solution in the flask. 1,2-Dihydroxy-16-ketoheptadecane (500 mgm.) dissolved in 10 ml. of benzene (solution was maintained by the use of an infrared lamp) was added over a period of six hours from a dropping funnel. During addition the reaction mixture was stirred and maintained at a temperature of 50° C. and a stream of dried oxygen saturated with benzene was passed through the solution. At intervals of 45 min. 450 mgm. of lead tetraacetate was added to the solution. After the addition of ketoglycol was complete, the mixture was maintained at 50° C. with stirring for a further one and one-half hours, when 100 mgm. of ethylene glycol was added. After a further 10 min.

the warm solution was filtered and 10 ml. 30% acetic acid and then 100 ml. of water was added to the filtrate and the product extracted with benzene.

The benzene layer was washed once with water and the washings discarded. The keto acid was then extracted from the benzene layer by one washing with 50 ml. of 10% aqueous potassium hydroxide solution and two washes with water, disregarding emulsions formed owing to the rather low solubility of the potassium salt. The combined aqueous washings were acidified with sulphuric acid and extracted with benzene to yield 310 mgm. of the crude ketohexadecanoic acid. This was purified by conversion to its methyl ester, which was distilled and then reconverted to the free acid, which was crystallized four times from 95% methanol.

The ethyl, propyl, and butyl keto acids (Table I) were prepared similarly except that it was found unnecessary to convert to the methyl ester for the distillation of the crude product. The yield was found to decrease slightly as the molecular weight of the product increased.

ACKNOWLEDGMENT

The authors wish to express their thanks to J. A. Baignee for the microanalyses and to Miss Agnes Epp for the infrared studies.

REFERENCES

1. ARSENIUS, K. E., STALLBERG, G., STENHAGEN, E., and TAGASTROM-EKETORP, B. Arkiv Kemi Mineral. Geol. 26A. 1948.
2. HASKINS, R. H. and THORN, J. A. Can. J. Botany, 29: 585. 1951.
3. HAUGEN, F. W., ILSE, D., SUTTON, D. A., and DE VILLIEAS, J. P. J. Chem. Soc. 98. 1953.
4. LEMIEUX, R. U. Can. J. Chem. 29: 415. 1951.
5. LEMIEUX, R. U. Can. J. Chem. 31: 396. 1953.
6. MENDEL, H. and COOPS, J. Rec. trav. chim. 58: 1133. 1939.
7. MILBURN, A. H. and TRUTER, E. V. J. Chem. Soc. 3344. 1954.
8. VELICK, S. F. J. Am. Chem. Soc. 69: 2317. 1947.
9. WEITKAMP, A. W. J. Am. Chem. Soc. 67: 447. 1945.
10. WHITMORE, F. C., POPKIN, A. H., WHITAKER, J. S., MATTIL, K. F., and ZECH, J. D. J. Am. Chem. Soc. 60: 2462. 1938.
11. WHITMORE, F. C., NOLL, C. I., and MEUNIER, V. C. J. Am. Chem. Soc. 61: 683. 1939.

THE REACTION OF 2-ALKYLTETRAHYDROPYRANS WITH ANILINE OVER ACTIVATED ALUMINA[1]

By H. P. Richards[2] and A. N. Bourns

ABSTRACT

The vapor-phase reaction over activated alumina of 2-ethyltetrahydropyran with aniline gave 1-phenyl-2-ethylpiperidine, 1-phenyl-2-propylpyrrolidine, N-phenyl-4-heptenylamine, and N-phenyl-5-heptenylamine. 2-Methyltetrahydropyran with aniline gave 1-phenyl-2-methylpiperidine, 1-phenyl-2-ethylpyrrolidine, N-phenyl-4-hexenylamine, and N-phenyl-5-hexenylamine. The structures of the cyclic amines were confirmed by independent syntheses. The unsaturated secondary amines were reduced to known N-alkylanilines and degraded by ozonolysis. A mechanism has been proposed to account for the formation of these products.

INTRODUCTION

In an earlier communication the results of an investigation of the reaction of tetrahydropyran with primary aromatic amines were reported (1). N-Arylpiperidines were formed in almost theoretical yields with aniline, *m*-toluidine, and *p*-toluidine, while a lower yield (65%) was obtained when *o*-toluidine was used as the amine component. The investigation has now been extended to the reaction of aniline with 2-ethyltetrahydropyran (I) and 2-methyltetrahydropyran (II). In contrast to the results obtained with the parent ether, the 2-alkyl homologues produced a mixture of amine products suggestive of a carbonium ion mechanism.

Reaction of 2-Ethyltetrahydropyran (I) with Aniline

Careful fractional distillation of the product formed by passing aniline and the cyclic ether, in a molar ratio of 2: 1, over activated alumina at 300° C. gave three distinct fractions. These were identified as 1-phenyl-2-ethylpiperidine (III), 1-phenyl-2-propylpyrrolidine (IV), and a mixture (V) of N-phenyl-4-heptenylamine and N-phenyl-5-heptenylamine. The composition of the reaction product, the elemental analysis data, the boiling point and refractive index of each fraction, and the melting points of picrates prepared from the two cyclic amines are given in Table I.

TABLE I

PRODUCTS OF THE REACTION OF 2-ETHYLTETRAHYDROPYRAN WITH ANILINE

No.	Compound	Mole %[a]	b.p., ° C. at 8 mm.	n_D^{20}	Analyses[b]			Picrate m.p., ° C.
					Carbon	Hydrogen	Nitrogen	
III	1-Phenyl-2-ethylpiperidine	17	126–127	1.5502	82.67	10.36	7.16	178.2–178.8
IV	1-Phenyl-2-propylpyrrolidine	26	136–137	1.5518	82.65	10.40	6.95	137.0–137.5
V	N-Phenyl-4-heptenylamine and N-Phenyl-5-heptenylamine	57	145–146	1.5364	82.85	10.09	7.09	

[a] *The product composition figures are an average of three runs, the deviation of which did not exceed one per cent.*

[b] *Calculated for $C_{12}H_{19}N$, the molecular formula of all four compounds: C, 82.40; H, 10.11; N, 7.49.*

[1] *Manuscript received June 15, 1955.*
Contribution from the Department of Chemistry, McMaster University, Hamilton, Ontario.

[2] *Present address: Ontario Paper Company, Thorold, Ontario.*

The identity of the cyclic amines was established through independent syntheses involving reaction of dibromoheptanes with aniline. The reaction sequence and composition of products are shown in the following reaction scheme:

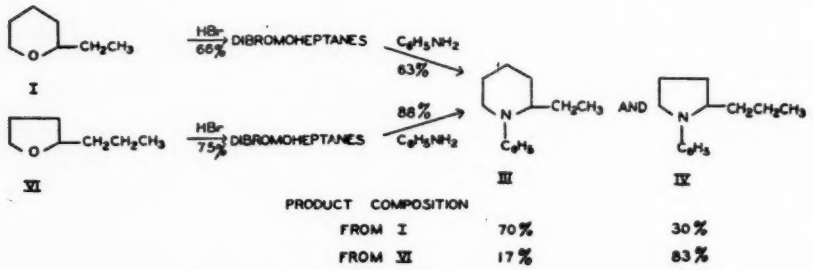

Treatment of 2-ethyltetrahydropyran (I) with hydrogen bromide converted it into dibromoheptanes, which on reaction with aniline gave a product 70% of which was shown to be identical with the lowest-boiling component (III) of the product of the catalytic reaction. The remaining 30% was identical with IV, the component of intermediate boiling point. On the other hand, conversion of 2-propyltetrahydrofuran (VI) to dibromoheptanes followed by reaction with aniline gave a product consisting of 17% III and 83% IV. In each sequence, ether → dibromide → amine, the major product was considered to be that resulting from direct substitution of oxygen by nitrogen without rearrangement, that is, the substituted piperidine from 2-ethyltetrahydropyran and the pyrrolidine from 2-propyltetrahydrofuran. This conclusion is based on the reasoning that if the major product of one sequence was that formed through a rearrangement, then this same compound would also have been the major product of the other sequence, since in this case it would have been formed directly without requiring a proton shift. Such clearly was not the case; the major product of one synthesis was the minor product of the other.* On the basis of these results, the lowest-boiling amine product of the catalytic reaction is considered to be 1-phenyl-2-ethylpiperidine; the component of intermediate boiling point, 1-phenyl-2-propylpyrrolidine.

The highest-boiling component (V) gave solid benzenesulphonamide derivatives, but these could not be recrystallized to constant melting point. Hydrogenation over Raney nickel converted V to N-heptylaniline. Ozonolysis of the benzoate of V produced volatile aldehydes identified as acetaldehyde and propionaldehyde by means of their 2,4-dinitrophenylhydrazones, which were separated chromatographically. The third component of the reaction of 2-ethyltetrahydropyran with aniline, therefore, consisted of a mixture of N-phenyl-4-heptenylamine and N-phenyl-5-heptenylamine. A separation of these unsaturated secondary amines was not attempted.

**The small amount of rearrangement occurring at the secondary carbon in these syntheses is considered more likely to occur in the reaction of the cyclic ethers with hydrogen bromide rather than in the subsequent reaction of the dibromide product with aniline.*

Reaction of 2-Methyltetrahydropyran with Aniline

Fractional distillation of the product formed by the reaction of 2-methyltetrahydropyran with aniline gave three distinct fractions identified as 1-phenyl-2-methylpiperidine (VII), 1-phenyl-2-ethylpyrrolidine (VIII), and a mixture (IX) of N-phenyl-4-hexenylaniline and N-phenyl-5-hexenylaniline. The composition of the product, the elemental analysis data, the boiling point and refractive index of each fraction, and the melting points of the picrates are shown in Table II.

TABLE II

PRODUCTS OF THE REACTION OF 2-METHYLTETRAHYDROPYRAN WITH ANILINE

No.	Compound	Mole %[a]	b.p., ° C. at 8 mm.	n_D^{20}	Analyses[b]			Picrate m.p., ° C.
					Carbon	Hydrogen	Nitrogen	
VII	1-Phenyl-2-methylpiperidine	42	113–114	1.5528	81.72	9.72	8.00	166.8–167.2
VIII	1-Phenyl-2-ethylpyrrolidine	27	125.5–126.5	1.5590	81.83	9.61	7.89	120.6–121.2
IX	N-Phenyl-4-hexenylamine and N-Phenyl-5-hexenylamine	31	131.5–132.5	1.5412	81.90	9.62	7.92	

[a] *Based on a single run.*
[b] *Calculated for $C_{12}H_{17}N$, the molecular formula for all four compounds: C, 82.23; H, 9.78; N, 7.99.*

The identity of the two tertiary amines (VII and VIII) was established by an independent synthesis. 2-Methyltetrahydropyran was converted to dibromohexane, which on treatment with aniline gave a product 87% of which was identical with VII. The remaining 13% was identical with VIII. This result is entirely analogous to that obtained in the corresponding synthesis of 1-phenyl-2-ethylpiperidine (III) and 1-phenyl-2-propylpyrrolidine (IV), discussed in the preceding section. Furthermore, there is a similar relationship in boiling points, refractive indices, and picrate melting points of the isomeric tertiary amines in the two cases. (See Tables I and II.)

The highest-boiling component (IX) of the catalytic reaction was converted into N-hexylaniline on reduction over Raney nickel. Ozonolysis of the acetate of IX gave the volatile aldehydes, formaldehyde and acetaldehyde. It is therefore concluded that IX was a mixture of the two unsaturated secondary amines, N-phenyl-4-hexenylamine and N-phenyl-5-hexenylamine.

Reaction Mechanism Considerations

The reaction of aniline with tetrahydropyran, which involves the displacement of oxygen at two primary carbon centers, gives almost theoretical yields of 1-phenylpiperidine. In contrast, the corresponding reaction of 2-alkyltetrahydropyran, in which one of the two carbons joined to oxygen is secondary, gives a mixture of products suggestive of a process proceeding through an intermediate carbonium ion. The following mechanism is proposed:

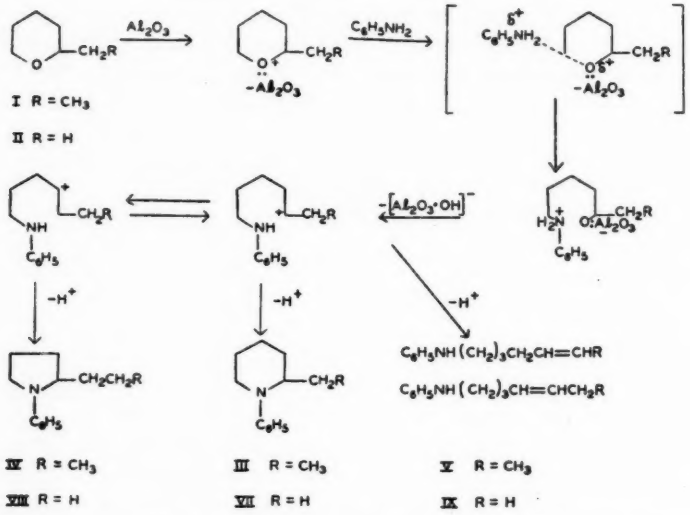

The alumina, acting as a Lewis acid, accepts a pair of electrons from oxygen, thus weakening the two carbon–oxygen bonds of the ether molecule (13).* Bimolecular attack of aniline at the primary carbon is followed by proton transfer from nitrogen to oxygen and then by unimolecular dissociation of the oxygen – secondary carbon bond. The resulting 'carbonium ion' may (*a*) interact with nitrogen to form the substituted piperidine, (*b*) rearrange to give a new 'carbonium ion', which on ring closure yields the pyrrolidine, or (*c*) lose a proton from a carbon atom adjacent to the center of electron deficiency and produce an unsaturated secondary amine.

It is possible that the initial cleavage occurs at the secondary rather than at the primary carbon. However, the fact that the 2-alkyltetrahydropyrans appear to be somewhat less reactive than tetrahydropyran itself would suggest that the bimolecular displacement at primary carbon is more facile, and therefore is the initial cleavage step. It is worthy of note in this connection that reaction of hydrogen iodide with *n*-butyl *sec*-butyl ether has been shown to give *n*-butyl iodide and *sec*-butyl alcohol (7). Ether fission in this reaction would appear to involve bimolecular attack of iodide ion at the primary carbon atom.

Reference to the composition data given in Tables I and II shows that there is a very much greater tendency for unsaturated secondary amine formation in the reaction of 2-ethyltetrahydropyran. It is suggested that hyperconjugation is one factor responsible for this. Of the two unsaturated amines formed in each of the two systems, one possesses the partial structure $-CH_2CH{=}CHCH_3$. The second unsaturated amine found in the product from 2-methyltetrahydropyran has the partial structure $-CH_2CH{=}CH_2$, and

**Although this is undoubtedly an oversimplification of the catalytic function (14), it seems reasonable to assume that it is in this capacity that alumina performs its key role in dehydration reactions.*

in the product from 2-ethyltetrahydropyran, $-CH_2CH{=}CHCH_2CH_3$. Since hyperconjugative stabilization is greater in the latter, the reaction of the 'carbonium ion' giving this product should compete more effectively with the ring closure forming the substituted piperidine. Analogous effects of hyperconjugation in determining product proportions have been observed in the solvolysis of alkyl bromides (3) and of sulphonium salts (5).

Steric effects (2) also may play a role in determining product proportions in the two cyclic ether – aniline reactions. Ring closure at the carbonium ion center, $-CH_2CH_2\overset{+}{C}HCH_3$, giving the substituted piperidine from 2-methyltetrahydropyran should have a somewhat higher entropy of activation, and therefore greater reaction rate, than closure at the center, $-CH_2CH_2\overset{+}{C}HCH_2CH_3$, required to produce a piperidine from the 2-ethyl homologue. On the other hand, the two reactions giving the substituted pyrrolidines involve the two ions of partial structures $-CH_2\overset{+}{C}HCH_2CH_3$ and $-CH_2\overset{+}{C}HCH_2CH_2CH_3$. These would be expected to show smaller differences in rate, since the increase in steric requirements resulting from the substitution of *n*-propyl for ethyl at the seat of displacement is not as great as that resulting from substitution of ethyl for methyl. This relationship between the steric requirements of *n*-alkyl groups has been demonstrated in bimolecular substitution reactions (6), and it might be expected to show up in processes involving interaction of a bulky nucleophilic reagent with carbonium ion centers.

If now it is assumed that the interconversion of the isomeric carbonium ions is rapid compared to their conversion to stable products, then these steric considerations lead to the prediction that more substituted piperidine and less unsaturated amines should be formed from 2-methyltetrahydropyran than from the 2-ethyl homologue. Reference to Tables I and II shows this to be the case.

A further factor which would tend to favor piperidine formation at the expense of the pyrrolidine from the 2-methyl ether is the somewhat greater stability and, if equilibrium between the isomeric carbonium ions is approached, greater concentration of $-CH_2CH_2\overset{+}{C}HCH_3$ compared to $-CH_2\overset{+}{C}HCH_2CH_3$, since in the former an extra C—H bond is available for hyperconjugation. The fact that the pyrrolidine is favored in the reaction of the 2-ethyl compound might be taken to mean a greater inherent stability of the five-membered heterocyclic system.

EXPERIMENTAL*†

Catalysis Procedure

The catalysis procedure has been described in detail in an earlier communication (1). The cyclic ethers and aniline, mixed in a molar ratio 1:2, were vaporized in a preheater and the vapors passed through 200 ml. of pretreated (1) Alcoa Activated Alumina (Grade F-1, 4-8 mesh) at 300° C. The

**All melting points are corrected; boiling points are uncorrected.*

†The microanalyses were performed at the Research Laboratories, Dominion Rubber Company, Guelph, Ontario, by Mr. Ralph Mills.

feed rate was 60 ml. of mixed liquid reactants per hour. A run consisted of 100 ml. of mixed reactants, following a prerun of 40 ml. during which temperature and feed rate were given final adjustment.

The organic product was separated from a water phase, dried over sodium hydroxide, and very carefully fractionated in a 30-plate modified Podbielniak column (8). A small amount of low-boiling alkadienes and unreacted cyclic ether was removed at atmospheric pressure, while excess aniline and the amine reaction products were distilled at 8 mm. pressure. Composition of amine products, properties, and elemental analysis data are given in Tables I and II. Combined yields of the amine products, based on cyclic ether charged, were 60% from 2-ethyltetrahydropyran and 76% from 2-methyltetrahydropyran.

2-Ethyl- and 2-Methyl-tetrahydropyran

The cyclic ethers were prepared from dihydropyran by the method of Paul (9) and purified by fractional distillation. 2-Ethyltetrahydropyran, b.p. 126.8–127.1° C., n_D^{20} 1.4262, was obtained in 63.4% yield, and 2-methyltetrahydropyran, b.p. 101.5–101.8° C., n_D^{20} 1.4180, in 76% yield.

Synthesis of 1-Phenyl-2-ethylpiperidine (III) from 2-Ethyltetrahydropyran (I) via 1,5-Dibromoheptane

2-Ethyltetrahydropyran, 30.0 gm., was added slowly to a cold mixture of 340 gm. of 48% hydrobromic acid and 18 ml. of concentrated sulphuric acid. Following a three-hour refluxing period, the reaction mixture was steam distilled, and the organic phase of the distillate extracted with ether, washed with sodium carbonate solution, and dried over calcium chloride. Fractionation gave 44.4 gm. (66.3%) dibromide, b.p. 112–116° C. (12 mm.), n_D^{17} 1.5010–1.5025. On the basis of the composition of the product formed in the subsequent reaction with aniline, this product is considered to consist of 70% 1,5-dibromoheptane and 30% 1,4-dibromoheptane.

A solution of 38.5 gm. (0.15 mole) of the dibromide and 62.2 gm. (0.68 mole) of aniline was warmed on a steam bath until it had formed into a brown cake. The reaction mixture was dissolved in hydrochloric acid and the free amines liberated by addition of sodium hydroxide solution. The organic phase was extracted with ether and dried over sodium hydroxide. Careful fractionation gave 12.5 gm. (44%) of 1-phenyl-2-ethylpiperidine (III), b.p. 125.5–126.0° C. (8 mm.), n_D^{20} 1.5505, picrate m.p. 177.6–178.2° C., and 5.3 gm. (19%) of 1-phenyl-2-propylpyrrolidine (IV), b.p. 132–136° C. (8 mm.), n_D^{20} 1.5534, picrate m.p. 135.6–136.1° C. A mixture of the picrate of III with the picrate formed from the lowest-boiling fraction of the product of the 2-ethyltetrahydropyran–aniline reaction showed no depression in melting point. Similarly, the melting point of the picrate of IV was not depressed in admixture with the picrate of the intermediate fraction of the catalysis product.

Synthesis of 1-Phenyl-2-propylpyrrolidine (IV) from 2-Propyltetrahydrofuran (VI) via 1,4-Dibromoheptane

Thirty-six grams (0.315 mole) of 2-propyltetrahydrofuran, b.p. 130–133° C., n_D^{20} 1.4215, prepared by the method of Paul (10, 11) from furfural in an over-all

yield of 65%, was dissolved in an equal volume of glacial acetic acid. The solution was saturated with anhydrous hydrogen bromide and heated in a sealed tube at 120° C. for three hours. The product was steam distilled and the organic phase extracted with ether and dried over anhydrous sodium sulphate. Fractionation gave 61 gm. (75%) dibromide, b.p. 108–110° C. (8 mm.), n_D^{20} 1.5010–1.5015. The results of the subsequent reaction with aniline indicated that this product consisted of 83% 1,4-dibromoheptane and 17% 1,5-dibromoheptane.

The dibromide, 57.6 gm. (0.22 mole), was treated with 84.3 gm. (0.91 mole) of aniline and the product worked up as described in the preceding section. Careful fractionation gave 30.7 gm. (73%) of 1-phenyl-2-propylpyrrolidine (IV), b.p. 137–138° C. (8 mm.), n_D^{20} 1.5518, picrate m.p. 136.0–136.5° C., and 6.3 gm. (15%) of 1-phenyl-2-ethylpiperidine (III), b.p. 126–129° C. (8 mm.), n_D^{20} 1.5502, picrate m.p. 177.2–177.6° C. Mixed melting point determinations on the picrates of these compounds with the picrates of corresponding fractions obtained from the catalysis reaction showed no depression.

Reduction of Mixed N-Phenylheptenylamines (V) to N-Heptylaniline

A solution containing 6.5 gm. of the highest-boiling fraction from the 2-ethyltetrahydropyrananiline reaction in 100 ml. of ethanol was treated with hydrogen in the presence of Raney nickel at room temperature and 50 p.s.i. pressure. Distillation, following removal of the catalyst, gave 5.1 gm. (79%) of product, b.p. 163–169° C. (24 mm.), n_D^{20} 1.5188, *p*-bromobenzenesulphonamide derivative m.p. 117–118° C. A mixture of this derivative with *p*-bromobenzenesulphonamide prepared from authentic N-heptylaniline showed no depression in melting point.

Ozonolysis of N-Benzoyl-N-phenylheptenylamines

To a solution of 3.8 gm. (0.02 mole) of the mixed heptenylanilines in 38 ml. of dry pyridine and 76 ml. of dry benzene was added dropwise 4.8 gm. (0.034 mole) of benzoyl chloride at 60–70° C. After an additional 30 min. at this temperature, the product was worked up in the usual way. Distillation gave 4.6 gm. (78.4%) of a thick straw-colored oil, b.p. 163–173° C. (0.3 mm.).

A stream of ozone (5%) was passed into a solution of 3.2 gm. of the benzoyl derivative in 50 ml. of aldehyde-free propionic acid until ozonization was complete. The ozonide was decomposed by hydrogenolysis for 10 hr. over palladium on calcium carbonate at room temperature and 63 p.s.i. pressure. Following removal of the catalyst, the volatile carbonyl products were swept out of the gradually-heated propionic acid solution and collected in ethanol cooled to dry-ice temperatures. These were then converted to 2,4-dinitrophenylhydrazones in the usual way and separated chromatographically on a silicic acid – Super Cel column (12). The less strongly absorbed hydrazone, on recrystallization from ethanol, melted at 153.3–154.8° C. and gave no melting point depression when mixed with authentic propionaldehyde 2,4-dinitrophenylhydrazone. The more strongly absorbed derivative, also recrystallized from ethanol, melted at 166–167° C., and did not depress the melting point of authentic acetaldehyde 2,4-dinitrophenylhydrazone.

Synthesis of 1-Phenyl-2-methylpiperidine (VII) from 2-Methyltetrahydropyran (II) via 1,5-Dibromohexane

2-Methyltetrahydropyran, 18.0 gm. (0.18 mole), was dissolved in glacial acetic acid and treated with anhydrous hydrogen bromide at 120° C., following the procedure previously described for the reaction of hydrogen bromide with 2-propyltetrahydrofuran. Fractionation of the product gave 35.7 gm. (82%) dibromide, b.p. 100.0–102.3° C. (12 mm.), $n_D^{13.5}$ 1.5077. The composition of the product formed in the subsequent reaction with aniline indicated that the dibromide consisted of 87% 1,5-dibromohexane and 13% 1,4-dibromohexane.

The conversion of the dibromide to cyclic amines by reaction with aniline was carried out following the procedure previously described. From 34.5 gm. of the dibromide was obtained 16.9 gm. (80%) of 1-phenyl-2-methylpiperidine (VII), b.p. 110.8–113.0° C. (8 mm.), n_D^{13} 1.5560, picrate m.p. 167.4–168.4° C., and 2.4 gm. (12%) of 1-phenyl-2-ethylpyrrolidine (VIII), b.p. 117.5–118.5° C. (8 mm.), n_D^{14} 1.5631, picrate m.p. 118–119° C. The melting points were not depressed when these picrates were mixed with picrates from corresponding fractions obtained from the reaction of 2-methyltetrahydropyran with aniline.

Reduction of Mixed N-Phenylhexenylamines (IX) to N-Hexylaniline

A sample of the mixed amines dissolved in ethanol was reduced at room temperature and 43 p.s.i. pressure over Raney nickel. Distillation gave a product, b.p. 163–165° C. (30 mm.), n_D^{20} 1.5230, *m*-nitrobenzenesulphonamide m.p. 79.6–80.2° C., and *p*-toluenesulphonamide m.p. 67–68° C. The melting points of these sulphonamides agree closely with literature values for the corresponding derivatives of N-hexylaniline (4). The *p*-bromobenzenesulphonamide melted at 96.2–97.2° C.

Ozonolysis of N-Acetyl-N-phenylhexenylamines

A solution of 4.5 gm. (0.026 mole) of mixed amines (IX) dissolved in 10.6 ml. (0.10 mole) of acetic anhydride and 70.8 ml. of piperidine was refluxed for one and one-half hours. Dilute sulphuric acid was added and the organic phase extracted with ether, dried, and distilled to give 4.75 gm. (85%) of liquid product, b.p. 115–120° C. (0.5 mm.), n_D^{21} 1.5223.

A stream of ozone (5%) was passed into a solution of 2 gm. of N-acetyl-N-phenylhexenylamines in 50 ml. of purified glacial acetic acid until ozonization was complete. The ozonide was decomposed by hydrogenolysis over palladium on calcium carbonate. Following removal of the catalyst, nitrogen was passed through the solution while its temperature was gradually raised. The aldehyde first swept from the solution was converted into *p*-nitrophenylhydrazone and 2,4-dinitrophenylhydrazone derivatives, the melting points of which corresponded to derivatives of acetaldehyde. Mixed melting point determinations showed no depression. The sweep gas passing through the solution at the higher temperatures was led into ethanol cooled in dry-ice, dimedone added, and the resulting derivative recrystallized from ethanol. Its melting point

corresponded to that of the dimedone of formaldehyde, and a mixed melting point determination with authentic compound gave no depression.

ACKNOWLEDGMENTS

Acknowledgment is made to the National Research Council of Canada for financial assistance which made this work possible.

REFERENCES

1. BOURNS, A. N., EMBLETON, H. W., and HANSULD, M. K. Can. J. Chem. 30: 1. 1952.
2. BROWN, H. C. and FLETCHER, R. S. J. Am. Chem. Soc. 72: 1223. 1950.
3. DHAR, M. L., HUGHES, E. D., and INGOLD, C. K. J. Chem. Soc. 2058. 1948.
4. HICKENBOTTOM, W. J. J. Chem. Soc. 1119. 1937.
5. HUGHES, E. D., INGOLD, C. K., and WOOLF, L. I. J. Chem. Soc. 2084. 1948.
6. IVANOFF, N. and MAGAT, M. J. chim. phys. 47: 914. 1950.
7. LIPPERT, W. Ann. 276: 148. 1893.
8. MITCHELL, F. W. and O'GORMAN, J. M. Anal. Chem. 20: 315. 1948.
9. PAUL, R. Compt. rend. 198: 1246. 1934.
10. PAUL, R. Compt. rend. 200: 1118. 1935.
11. PAUL, R. Bull. soc. chim. 5: 1053. 1938.
12. ROBERTS, J. D. and GREEN, C. Ind. Eng. Chem. Anal. Ed. 18: 335. 1946.
13. ROYALS, E. E. Advanced organic chemistry. Prentice-Hall, Inc., New York. 1954.
14. WALLING, C. J. Am. Chem. Soc. 72: 1164. 1950.

2,3-DIHYDROBENZO(*f*)-1,4-OXATHIEPIN AND DERIVATIVES[1]

By Marshall Kulka

ABSTRACT

A method has been developed for the synthesis of a new heterocyclic system III. When 2-β-chloroethoxybenzyl chloride (XI) was heated with thiourea in alcohol solution, S-(2-β-chloroethoxybenzyl)isothiuronium chloride (XII) was formed which on cleavage with aqueous alkali in high dilution yielded 2,3-dihydrobenzo(*f*)-1,4-oxathiepin (III). Derivatives of III with substituents such as methyl, *t*-butyl, chlorine, and nitro in the 7 and 9 positions were prepared in high yields from the corresponding substituted 2-β-chloroethoxybenzyl chlorides. The presence of substituents in the position ortho to the chloroethoxy group of XII had no retarding effect on the cyclization to XIV.

During the synthesis of aralkyl mercaptans required as intermediates in a synthetic insecticide research program, a new heterocyclic system, III, was discovered. The name for this new system is derived from oxepin (I) and 1,4-oxathiepin (II). The fusion of a benzene ring in the *f* position of 1,4-oxathiepin (II), followed by saturation of the 2,3-double bond, results in the new system, (III), for which the name 2,3-dihydrobenzo(*f*)-1,4-oxathiepin is appropriate.

The thiourea method for the preparation of alkyl (12) and aralkyl (8) mercaptans (VII) comprises heating the alkyl or aralkyl halide (IV) with thiourea (V) in alcohol solution followed by alkaline cleavage of the resulting isothiuronium chloride (VI). Sodium chloride, water, and cyanoguanidine (VIII) are formed along with the mercaptan (VII). It is well known (1,9) that mercaptans react with alkyl halides (IX) in the presence of aqueous or alcoholic alkali to form sulphides (X).

During the preparation of various benzyl mercaptans from the corresponding benzyl chlorides by the thiourea method, interest was aroused in regard to the behavior of 2-β-chloroethoxybenzyl chlorides (XI) in this reaction. Since phenyl 2-chloroethyl ether does not react with thiourea (V) under these conditions, the first product of the reaction between XI and V should be the S-(2-β-chloroethoxybenzyl)isothiuronium chloride (XII). This on treatment with alkali should yield the mercaptan XIII, which could theoretically undergo two reactions under these conditions. An intramolecular reaction would result in the 1,4-oxathiepin (XIV), while an intermolecular reaction would lead to the polymer (XV). Actually when an aqueous-alcoholic solution of S-(2-β-chloroethoxybenzyl)isothiuronium chloride (XII) was treated with excess sodium hydroxide in a small volume of hot water, the main product of

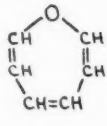

I

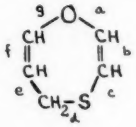

II

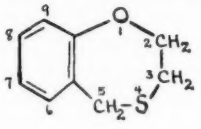

III

[1]*Manuscript received May 24, 1955.*
Contribution from the Dominion Rubber Company Limited Research Laboratories, Guelph, Ontario.

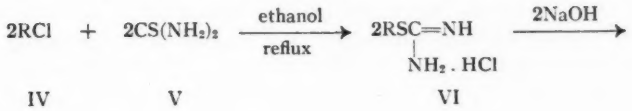

IV V VI

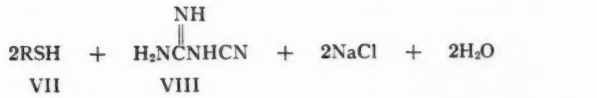

VII VIII

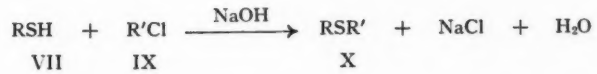

VII IX X

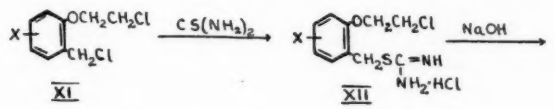

XI XII

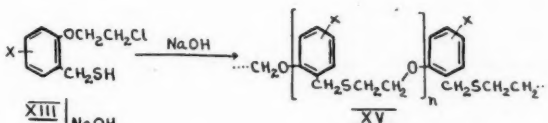

XIII XV XIV XVI XVII

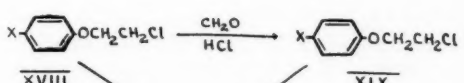

XVIII XIX XX

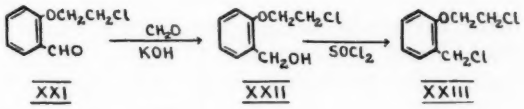

XXI XXII XXIII

NOTE: The formula for compound XIX should read

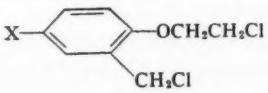

the reaction was the benzene-insoluble polymer (XV). On the other hand when the aqueous-alcoholic solution of XII was added dropwise to excess sodium hydroxide in a large volume of hot water, a benzene-soluble compound was obtained in high yield. This compound possessed a boiling point slightly lower than the corresponding 2-β-chloroethoxybenzyl chloride (XI), it was free of chlorine and contained a neutral sulphur which oxidized easily to the sulphone. On the basis of these properties together with analytic figures and molecular weight it must be presumed to be the intramolecular reaction product XIV.

The thiourea method has been successfully applied to the synthesis of several 2,3-dihydrobenzo(*f*)-1,4-oxathiepins (XIV) substituted in the benzene ring (Table II). These were oxidized to the corresponding sulphones (Table III). The method appears to have wide scope which is governed only by the availability of the benzyl chlorides (XI). Difficulties were expected in the preparation of nitroderivatives of XIV in view of the facts that S-(3-nitro-4-methoxybenzyl)isothiuronium chloride on treatment with aqueous alkali yields only resinous materials and no mercaptan and that *p*-nitrobenzyl mercaptan is sensitive to hot alkali (1). However XII (X = NO_2) was easily converted to XIV (X = NO_2) (Table II). A number of 3-substituted-5-alkyl-2-β-chloroethoxybenzyl chlorides (XI, X = 3-Cl, 3-NO_2, and 3-*t*-butyl) were also easily converted to the 1,4-oxathiepins (XIV, X = 9-Cl, 9-NO_2, and 9-*t*-butyl) via the corresponding isothiuronium chlorides (XII) showing that 3-substituents in XII have no retarding effect on the cyclization to XIV. This is in direct contrast to the behavior of 2-phenoxyphenylacetic acids (XVI) where substituents in the *ortho* position (R) sterically hinder the cyclization to the dibenzoxepinones (XVII) (6).

The 4-substituted-2-β-chloroethoxybenzyl chlorides (XIX) required in this investigation were prepared by chloroethylation of the phenols with ethylene dichloride according to the method of Harris and Stewart (4) followed by chloromethylation of the resulting 2-chloroethyl phenyl ethers (XVIII). A few failures were experienced when *p*-nitrophenol, 2,4-di-*t*-butylphenol (11), and 2-hydroxy-5-methylacetophenone (10) reacted poorly or not at all with ethylene dichloride and when 2,4,5-trichlorophenyl 2-chloroethyl ether failed to chloromethylate. The introduction by usual methods of such groups as chlorine, nitro, and *t*-butyl into the 4-substituted-phenyl 2-chloroethyl ethers (XVIII) either before or after chloromethylation yielded additional 2-β-chloroethoxybenzyl chlorides (XX) required in this investigation. *o*-β-Chloroethoxybenzyl chloride (XXIII) was prepared from salicylaldehyde by chloroethylation and reduction (crossed Cannizzaro) of the resulting aldehyde (XXI) to the benzyl alcohol (XXII) followed by thionyl chloride treatment. This compound (XXIII) proved to be extremely unstable and had to be used immediately without purification in the preparation of the isothiuronium salt.

EXPERIMENTAL

2-β-Chloroethoxybenzaldehyde (XXI)

A reaction mixture of *o*-hydroxybenzaldehyde (100 gm.), ethylene dichloride (100 ml.), and potassium hydroxide (50 gm.) in water (100 ml.) was heated

under reflux for five days. The organic layer was separated, diluted with ethylene dichloride, washed with aqueous sodium hydroxide and with water, and the solvent removed. The residue was distilled, the fraction boiling at 163–164° (12 mm.) being collected; yield, 61 gm. or 40%. The distillate crystallized from benzene as white prisms melting at 38–39°. Anal. Calc. for $C_9H_9O_2Cl$: C, 58.53; H, 4.88. Found: C, 58.34; H, 4.71.

2-β-Chloroethoxybenzyl Alcohol (*XXII*)

To a stirred solution of 2-β-chloroethoxybenzaldehyde (20 gm.), ethanol (100 ml.), and 40% formaldehyde (40 ml.) was added dropwise 50% aqueous potassium hydroxide (50 ml.), the temperature being kept at 35–40° by cooling. The reaction mixture was stirred at 40° for two hours and then about half the ethanol was removed *in vacuo*. The residue was extracted with ether, the ether solution was washed with aqueous sodium bisulphite, and the solvent was removed. The residue distilled at b.p. (12 mm.) = 166–167° as a colorless liquid, $n_D^{20} = 1.550$, yield, 17 gm. or 85%. Anal. Calc. for $C_9H_{11}O_2Cl$: C, 57.90; H. 5.89. Found: C, 57.34, 57.60; H, 5.76, 5.90.

2-β-Chloroethoxybenzyl Chloride (*XXIII*)

To a solution of 2-β-chloroethoxybenzyl alcohol (12 gm.) in dry benzene (50 ml.) was added portionwise thionyl chloride (10 gm.), the temperature being kept below 35° by cooling. The reaction mixture was allowed to stand at room temperature for five hours during which time hydrogen chloride and sulphur dioxide were evolved. About two-thirds of the benzene was removed *in vacuo without heat application* and the purple solution was used directly in the formation of the isothiuronium salt (see below). The 2-β-chloroethoxybenzyl chloride is extremely unstable and polymerizes on standing or on warming.

2-β-Chloroethoxy-5-methylbenzyl Chloride (*XIX*, $X = CH_3$)

A reaction mixture of *p*-tolyl 2-chloroethyl ether (100 gm.) (4), ethylene dichloride (150 ml.), concentrated hydrochloric acid (300 ml.), water (15 ml.), and paraformaldehyde (22 gm.) was stirred and heated at 55–60° for 24 hr. The organic layer was separated, washed with water, with aqueous sodium bicarbonate, and with water. The solvent was removed and the residue was distilled, yielding a colorless liquid (111 gm. or 88%) boiling at 158–160° (12 mm.) and melting at 25–27°. Anal. Calc. for $C_{10}H_{12}OCl_2$: C, 54.80; H, 5.48. Found: C, 54.77, 54.59; H, 5.70, 5.33.

2-β-Chloroethoxy-5-t-butylbenzyl Chloride (*XIX*, $X = C(CH_3)_3$)

This was prepared in 50% yield as above from *p-t*-butylphenyl 2-chloroethyl ether (2). The colorless liquid boiled at 170–173° (12 mm.), $n_D^{20} = 1.533$. Anal. Calc. for $C_{13}H_{18}OCl_2$: C, 59.80; H, 6.90. Found: C, 59.43, 59.48; H, 6.53, 6.60.

2-β-Chloroethoxy-3,5-dichlorobenzyl Chloride (*XX*, $X = Y = Cl$)

The preparation of this compound required considerably more drastic conditions than those used for the preparation of 2-β-chloroethoxy-5-chlorobenzyl chloride (7).

A suspension of paraformaldehyde (25 gm.), zinc chloride (150 gm.), and acetic acid (400 ml.) was saturated with hydrogen chloride. To the resulting solution was added 2,4-dichlorophenyl 2-chloroethyl ether (100 gm.) (2) and the solution was heated at 90–95° for four days. About half of the acetic acid was distilled off *in vacuo* from the reaction mixture, and the residue was treated with dilute hydrochloric acid and extracted with benzene. The benzene solution was washed with water, with aqueous sodium bicarbonate, and with water and the solvent was removed. The residue was fractionally distilled, yielding fraction 1 (52 gm.) boiling at 150–175° (12 mm.) and fraction 2 (18 gm.) boiling at 175–185° (12 mm.). Fraction 2 could not be purified further so the crude material was used in the preparation of the isothiuronium salt (see below).

2-β-Chloroethoxy-5-nitrobenzyl Chloride (*XIX*, $X = NO_2$)

This was prepared in 35% yield of crude material by the chloromethylation of *p*-nitrophenyl 2-chloroethyl ether (5) employing a method similar to that above except that 30 gm. of zinc chloride was used instead of 150 gm. The yellow liquid boiled at 170–175° (1 mm.). In view of the fact that this contained a small amount of difficultly separable *p*-nitrophenyl 2-chloroethyl ether, the crude material was used directly in the preparation of the isothiuronium salt where purification was easier.

2-Chloro-4-t-butylphenyl 2-Chloroethyl Ether

Into a solution of *p-t*-butylphenyl 2-chloroethyl ether (71 gm.) (2), sodium acetate (35 gm.), and acetic acid (200 ml.), chlorine gas was passed until 24 gm. were absorbed, the temperature being maintained at 35–40° by cooling. After it had been left at room temperature for 15 min., the reaction mixture was poured into water and extracted with benzene. The benzene extract was washed with water and the solvent was removed. The residue was distilled and the fraction boiling at 160–163° (12 mm.) collected. The yield of the colorless distillate was 56 gm. or 75%, $n_D^{20} = 1.532$. Anal. Calc. for $C_{12}H_{16}OCl_2$: C, 58.30; H, 6.48. Found: C, 58.72, 58.21; H, 6.60, 6.46.

2-β-Chloroethoxy-3-chloro-5-t-butylbenzyl Chloride (*XX*, $X = C(CH_3)_3$, $Y = Cl$)

Into a suspension of paraformaldehyde (10 gm.), zinc chloride (30 gm.), and acetic acid (250 ml.), hydrogen chloride was passed until saturated. To this was added 2-chloro-4-*t*-butylphenyl 2-chloroethyl ether (44 gm.) and the resulting solution was heated at 80–90° for three days. About half of the acetic acid was distilled off *in vacuo* and the residue was treated with dilute hydrochloric acid and extracted with benzene. The benzene extract was washed with water, with aqueous sodium bicarbonate, and with water. The solvent was removed and the residue was distilled, yielding 32 gm. (60%) of a colorless liquid, $n_D^{20} = 1.539$, boiling at 180–185° (13 mm.). Anal. Calc. for $C_{13}H_{17}OCl_3$: C, 52.80; H, 5.75. Found: C, 53.31, 53.17; H, 5.88, 5.61.

2-β-Chloroethoxy-3-nitro-5-t-butylbenzyl Chloride (*XX*, $X = C(CH_3)_3$, $Y = NO_2$)

To a solution of 2-β-chloroethoxy-5-*t*-butylbenzyl chloride (12 gm.) (XIX) in acetic acid (25 ml.) and acetic anhydride (10 ml.) was added dropwise fuming nitric acid (4 ml.) with stirring, the temperature being kept at 25–30° by

cooling. After it was allowed to stand at room temperature for two hours, the reaction mixture was poured into water and the precipitated oil was extracted with benzene. The benzene extract was washed with water and the solvent removed. The residue on crystallization from methanol yielded 9.8 gm. (70%) of white prisms melting at 77–78°. Anal. Calc. for $C_{13}H_{17}NO_3Cl_2$: C, 50.98; H, 5.55. Found: C, 50.93; H, 5.55.

2-t-Butyl-4-methylphenyl 2-Chloroethyl Ether

To a solution of *p*-tolyl 2-chloroethyl ether (150 gm.) (4) in *t*-butyl chloride (400 ml.) was added aluminum chloride (3 gm.) in three 1-gm. portions with cooling and swirling until dissolved. Then the reaction mixture was heated under gentle reflux for three hours. Because of the continuous evolution of hydrogen chloride the internal temperature remained at 35–40° for the first two hours and rose gradually to 50° during the last hour of the reaction. The dark red solution was washed with cold dilute hydrochloric acid, with water, with aqueous sodium bicarbonate, and with water. After the excess *t*-butyl chloride was distilled off, the residue was fractionally distilled, the fraction (106 gm.) boiling at 140–160° (13 mm.) being collected. This partially solidified on cooling and rubbing with a little methanol and was crystallized from methanol. The white prisms melted at 35–37° and weighed 58 gm. (30%). Anal. Calc. for $C_{13}H_{19}OCl$: C, 68.87; H, 8.39. Found: C, 68.94, 69.26; H, 8.16, 8.37.

2-β-Chloroethoxy-3-t-butyl-5-methylbenzyl Chloride (XX, $X = CH_3$, $Y = C(CH_3)_3$)

A suspension of 2-*t*-butyl-4-methylphenyl 2-chloroethyl ether (30 gm.), paraformaldehyde (6 gm.), and acetic acid (150 ml.) was saturated with hydrogen chloride and then heated at 78–80° for 18 hr. Most of the acetic acid was removed *in vacuo*, and the residue was treated with water and extracted with benzene. The benzene solution was washed with water, with aqueous sodium bicarbonate, and with water and the solvent was removed. The residue was distilled and the fraction boiling at 172–177° (13 mm.) collected. The yield of the colorless liquid was 20 gm. or 60%, $n_D^{20} = 1.534$. Anal. Calc. for $C_{14}H_{20}OCl_2$: C, 61.09; H, 7.25. Found: C, 61.48; H, 7.38.

2,4,5-Trichlorophenyl 2-Chloroethyl Ether

This was prepared in 72% yield from 2,4,5-trichlorophenol and ethylene dichloride according to the method of Harris and Stewart (4). The white needles melted at 52–53°. Anal. Calc. for $C_8H_6OCl_4$: C, 36.92; H, 2.31. Found: C, 37.37; H, 2.47.

2-Acetyl-4-methylphenyl 2-Chloroethyl Ether

This was prepared in 10% yield from 2-hydroxy-5-methylacetophenone (10) and ethylene dichloride (4). The white prisms melted at 61–62°. Anal. Calc. for $C_{11}H_{13}O_2Cl$: C, 62.14; H, 6.12. Found: C, 62.72; H, 6.24.

Preparation of S-Benzylisothiuronium Chlorides (*XII*) (*Table I*)

To a solution of the 2-β-chloroethoxybenzyl chloride (20 gm.) in ethanol (50 ml.) was added about 20% excess thiourea and the reaction mixture was

heated under reflux for three hours. The ethanol was removed *in vacuo* from the solution and the residual sirup was treated with hot water (20 ml.) (about twice as much water was required by the nitro derivatives of XII). The resulting solution was then extracted with benzene in order to remove any impurities, which were present only when crude 2-β-chloroethoxybenzyl chloride was used, and the aqueous solution was allowed to cool. The S-(2-β-chloroethoxybenzyl)isothiuronium chloride precipitated and could be crystallized from water or alcohol. Although S-benzylisothiuronium chloride is known to exhibit dimorphism (3), this was not observed with those chlorides listed in Table I.

TABLE I

THE PREPARATION OF S-(2-β-CHLOROETHOXYBENZYL)ISOTHIURONIUM CHLORIDES (XII) FROM THE CORRESPONDING BENZYL CHLORIDES (XI)

XII substituent(s)	Formula	M.p., °C.	Yield, %	Analyses			
				Calc.		Found	
				C	H	C	H
Unsubstituted	$C_{10}H_{14}N_2OCl_2S$		(Not purified)				
5-Chloro-	$C_{10}H_{13}N_2OCl_3S$	169–170	75	38.04	4.03	37.92	3.87
3,5-Dichloro-	$C_{10}H_{12}N_2OCl_4S$		(Not purified)				
5-Methyl-	$C_{11}H_{16}N_2OCl_2S$	180–181	82	44.75	5.42	44.76	5.13
5-*t*-Butyl-	$C_{14}H_{22}N_2OCl_2S$	199–200	69	49.85	6.53	49.93	6.30
5-Nitro-	$C_{11}H_{17}N_5O_5Cl_2S_2$[a]	158–159	80	32.84	4.23	33.02	4.29
3-Chloro-5-*t*-butyl-	$C_{14}H_{21}N_2OCl_3S$	194–195	79	45.22	5.65	45.28	5.50
3-Nitro-5-*t*-butyl-	$C_{14}H_{21}N_3O_3Cl_2S$	190–191	90	43.97	5.50	44.25	5.24
3-*t*-Butyl-5-methyl-	$C_{15}H_{24}N_2OCl_2S$	Sirup	(Not purified)				

[a]*Calc. N, 17.4. Found: N, 17.0. The analyses of this compound indicate that it possesses two molecules of thiourea instead of one.*

Preparation of the 2,3-Dihydrobenzo(f)-1,4-oxathiepins (XIV) (Table II)

The S-(2-β-chloroethoxybenzyl)isothiuronium chloride (30 gm.) (XII) was dissolved in ethanol (50 ml.) and water (100 ml.) and the solution was then

TABLE II

THE PREPARATION OF THE 2,3-DIHYDROBENZO(*f*)-1,4-OXATHIEPINS (XIV) FROM THE CORRESPONDING S-(2-β-CHLOROETHOXYBENZYL)ISOTHIURONIUM CHLORIDES (XII)

XIV substituents	Formula	M.p., °C.	B.p. (13 mm.)	Yield, %	Analyses			
					Calc.		Found	
					C	H	C	H
Unsubstituted	$C_9H_{10}OS$	35–36	130	47[a]	65.06	6.03	65.21	5.90
7-Chloro-	C_9H_9OClS[b]	70–71	160–162	80	53.84	4.49	54.15	4.35
7,9-Dichloro-	$C_9H_8OCl_2S$	114–115	*ca.* 180	10[a]	45.95	3.40	45.80	3.47
7-Methyl-	$C_{10}H_{12}OS$	45–46	146–147	90	66.66	6.67	66.67	6.55
7-*t*-Butyl-	$C_{13}H_{18}OS$	53–54	170	94	70.26	8.11	70.09	8.01
7-Nitro-	$C_9H_9NO_3S$	124–125		84	51.18	4.27	51.44	4.33
7-*t*-Butyl-9-chloro-	$C_{13}H_{17}OClS$		185–190	80	60.81	6.63	61.14	6.77
7-*t*-Butyl-9-nitro-	$C_{13}H_{17}NO_3S$	81–82		86	58.43	6.37	58.45	6.22
7-Methyl-9-*t*-butyl-	$C_{14}H_{20}OS$	61–62	175–180	53[a]	71.19	8.47	71.40	8.53

[a]*These yields are based on the 2-β-chloroethoxybenzyl chlorides and not on the corresponding isothiuronium salts as in the other cases.*

[b]*Molecular weight: calc., 200.5; found, 197 (Rast).*

added dropwise over one-half hour to a stirred solution of sodium hydroxide (20 gm.) in water (1 l.) heated on the steam bath. The stirring and heating was continued for another hour and the precipitated oil was then extracted with benzene. The benzene solution was washed with water and the solvent was removed. The residue was distilled and the almost odorless distillate crystallized from methanol. The results are shown in Table II.

Preparation of 2,3-Dihydrobenzo(f)-1,4-oxathiepin-4,4-dioxides (Table III)

To a solution of the 2,3-dihydrobenzo(*f*)-1,4-oxathiepin (XIV) (1 gm.) in acetic acid (5 ml.) was added 30% hydrogen peroxide (3 ml.). The reaction

TABLE III

THE PREPARATION OF 2,3-DIHYDROBENZO(*f*)-1,4-OXATHIEPIN-4,4-DIOXIDES BY THE OXIDATION OF XIV

2,3-Dihydrobenzo(*f*)-1,4-oxathiepin-4,4-dioxide substituent(s)	Formula	M.p., °C.	Analyses			
			Calc.		Found	
			C	H	C	H
Unsubstituted	$C_9H_{10}O_3S$	165–166	54.53	5.05	54.62	4.79
7-Chloro-	$C_9H_9O_3ClS$	194–195	46.45	3.87	46.56	4.00
7,9-Dichloro-	$C_9H_8O_3Cl_2S$	209–210	40.45	3.00	40.42	2.96
7-Methyl-	$C_{10}H_{12}O_3S$	175–176	56.60	5.66	56.77	5.64
7-*t*-Butyl-	$C_{13}H_{18}O_3S$	184–185	61.42	7.08	61.33	7.12
7-Nitro-	$C_9H_9NO_5S$	185–186	44.44	3.70	44.29	3.73
7-*t*-Butyl-9-chloro-	$C_{13}H_{17}O_3ClS$	158–159	54.07	5.89	54.43	6.03
7-*t*-Butyl-9-nitro-	$C_{13}H_{17}NO_5S$	187–188	52.17	5.68	52.31	5.80
7-Methyl-9-*t*-butyl-	$C_{14}H_{20}O_3S$	189–190	62.69	7.46	62.82	7.46

was exothermic and the temperature rose to about 80°. The solution was heated on the steam bath for one hour and then diluted with hot water and the sulphone allowed to crystallize. The white prisms were analytically pure and the yield was quantitative.

ACKNOWLEDGMENT

The author is indebted to Gisela von Stritzky for the microanalyses.

REFERENCES

1. BENNETT, G. M. and BERRY, W. A. J. Chem. Soc. 1666. 1927.
2. COLEMAN, G. H. and STRATTON, G. B. U.S. Patent No. 2,186,367. 1940. Chem. Abstr. 34: 3281. 1940.
3. DONLEAVY, J. J. J. Am. Chem. Soc. 58: 1004. 1936.
4. HARRIS, G. R. and STEWART, R. Can. J. Research, B, 27: 739. 1949.
5. KATRAK, B. N. J. Indian Chem. Soc. 13: 334. 1936. Chem. Abstr. 30: 7107. 1936.
6. KULKA, M. and MANSKE, R. H. F. J. Am. Chem. Soc. 75: 1322. 1953.
7. KULKA, M. and VAN STRYK, F. G. Can. J. Chem. 33: 1130. 1955.
8. LEWIS, T. R. and ARCHER, S. J. Am. Chem. Soc. 73: 2109. 1951.
9. PATTERSON, W. I. and DU VIGNEAUD, V. J. Biol. Chem. 111: 393. 1935. Chem. Abstr. 30: 80. 1936.
10. ROSENMUND, K. W. and SCHNURR, W. Ann. 460: 56. 1928.
11. STILLSON, G. H., SAWYER, D. W., and HUNT, C. K. J. Am. Chem. Soc. 67: 303. 1945.
12. URQUHART, G. G., GATES, J. W., JR., and CONNOR, R. Org. Syntheses, Collective Vol. III: 363. 1955.

NOTES

THE CRYSTAL STRUCTURE OF THE ALIPHATIC DIBASIC ACID $C_4H_4O_6.2H_2O$[1]

By M. P. Gupta[2]

The aliphatic dibasic acid $C_4H_4O_6.2H_2O$ has variously been described as having either the *cis-* or the *trans-* configuration. Chemical evidence against or in favor of either of these configurations has been presented by Hartree (2). In a previous communication, however, the present author (1) was able to show conclusively from X-ray diffraction data that the molecule in the crystalline state must have the *trans*-configuration since it crystallized in the monoclinic system, class $2/m$, space group $P2_1/c$ with two molecules in the unit cell of dimensions

$$a = 6.40, \quad b = 13.03, \quad c = 5.34 \text{ Å}, \quad \beta = 126.5°.$$

Thus the molecules were, tentatively, confirmed as molecules of dihydroxyfumaric acid and not dihydroxymaleic acid. The present note describes the results of a Fourier analysis of the X-ray diffraction data obtained from the crystals of dihydroxyfumaric acid dihydrate.

Reflections in the $\{0kl\}$ and the $\{h0l\}$ zones were obtained from Weissenberg photographs using Cu unfiltered radiation, and the intensities were estimated visually. Patterson projections were calculated for both these zones. The $\{h0l\}$ projection showed clearly the molecules to be lying in a plane perpendicular to the a axis which was the best axis for clear resolution of the atoms. The first Fourier map showed the rough orientation of the molecule as well as the position of the water molecule and this was refined in successive stages; the last Fourier map obtained is shown in Fig. 1 below. The figure shows the molecule as projected on a plane perpendicular to the a axis. Only one molecule is outlined together with parts of the neighboring molecules. All the atoms in this projection are clearly resolved. The structure has been confirmed by the $\{h0l\}$ projection in which, however, there is serious overlap—only two atoms out of the six in the asymmetric unit are clearly resolved in this projection.

There is no hydrogen bonding in the COOH groups of the adjacent molecules which form an extensive chain running roughly parallel to the [102] axis, and as in oxalic acid dihydrate, the crystal structure is held together mainly by the water molecules. No pronounced departure from a completely planar molecule is expected. The crystal structure is being refined using three-dimensional data, and full details of the intramolecular and intermolecular distances will be published later.

The author wishes to thank Dr. W. H. Barnes for providing all facilities for this research in his laboratory.

[1] *Issued as N.R.C. No. 3668.*
[2] *National Research Laboratories Postdoctorate Fellow.*

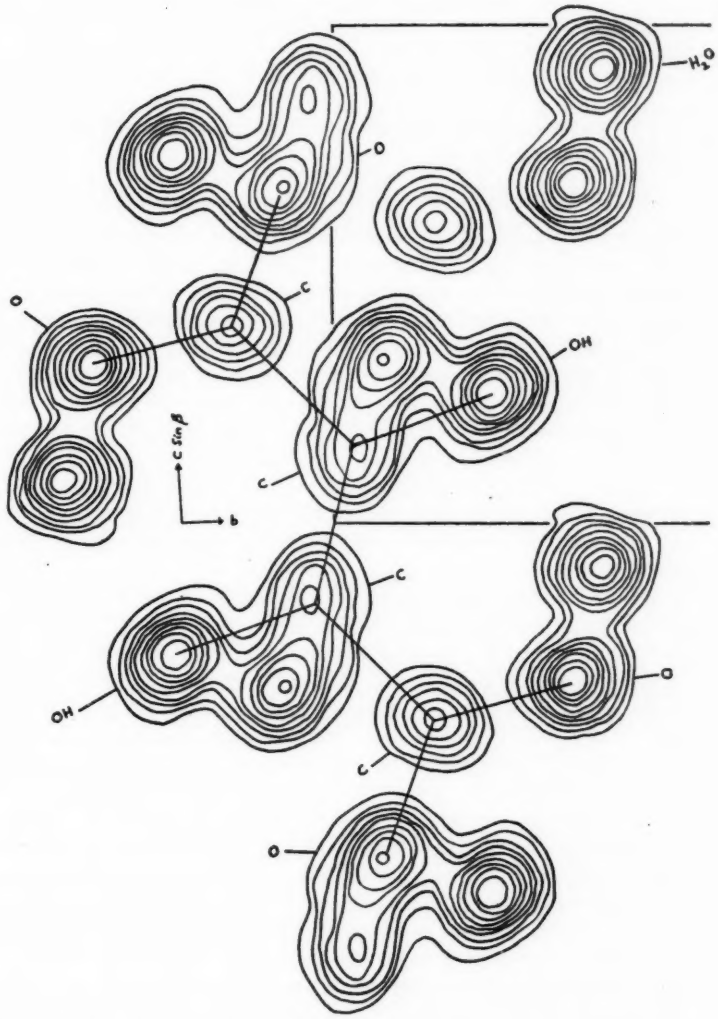

FIG. 1. Electron density projected on a plane perpendicular to the [100] axis. Contours drawn at arbitrary but equal levels of electron density.

1. GUPTA, M. P. J. Am. Chem. Soc. 75: 6312. 1953.
2. HARTREE, E. F. J. Am. Chem. Soc. 75: 6244. 1953.

RECEIVED MAY 17, 1955.
DIVISION OF PURE PHYSICS,
NATIONAL RESEARCH COUNCIL,
OTTAWA, CANADA.

THE ESTIMATION OF β-HYDROXY AMINO ACIDS BY A MICRODIFFUSION METHOD[1]

By L. Wiseblatt and W. B. McConnell

The periodic acid oxidation of β-hydroxy amino acids proceeds according to the following formula:

$$R—CHOH—CHNH_2—COOH \longrightarrow R—CHO + CHO—COOH + NH_3.$$

The reaction is rapid and quantitative and is used in analytical methods for determining serine and threonine (3, 5). It has also been used to estimate hydroxylysine, which occurs in a few proteins (6). Threonine yields acetaldehyde while serine and hydroxylysine give formaldehyde. Shinn and Nicolet (3) estimated threonine by aspirating the acetaldehyde into an excess of bisulphite, and Winnick (7) subsequently modified this to a microdiffusion method. Van Slyke, Hiller, and MacFadyen (6) have described a method for determining ammonia liberated by periodate oxidation (periodate ammonia) by aspirating it into boric acid and titrating in the usual way.

This communication describes a modified method for determining "periodate ammonia" which utilizes Conway Microdiffusion units (2).

To employ the method with protein hydrolyzates the following reagents are required:

1. Paraperiodic acid 0.5 *M* (114 gm. H_5IO_6 per liter).
2. Glycine solution (5% in *N* NaOH).
3. Potassium metaborate 5 *N* (410 gm. KBO_2 per liter).
4. Boric acid 2% containing 0.1% of bromcresol green – methyl red 2: 1.

One and one-half milliliters of boric acid solution are pipetted into the center well of a No. 1 Conway unit. One milliliter of sample solution, containing about 10 microequivalents of β-hydroxy amino acids, is added to the outer chamber. Immediately before the cell is sealed the following are added to the sample: 0.5 ml. periodic acid, 0.5 ml. glycine solution, 1.5 ml. potassium metaborate. After at least five hours at room temperature the contents of the center well are titrated with standard hydrochloric acid and the ammonia adsorbed is calculated. A control experiment with periodic acid omitted must be included to obtain a value for "preformed ammonia". Total ammonia less preformed ammonia is equal to periodate ammonia. Samples (10 microequivalents) of serine and threonine were analyzed as above. On individual determinations the percentage recoveries of the theoretical yield of ammonia were: serine—99.7, 100.4, 99.7, 100.1; threonine—99.5, 99.5, 100.3, 99.8. No interference from other common amino acids was found.

The total β-hydroxy amino acids in a protein hydrolyzate can be estimated in terms of periodate ammonia using the method outlined. If threonine is then estimated by Winnick's method (7) and "threonine ammonia" is subtracted from periodate ammonia, the difference should be a measure of serine content. Hydroxylysine glucosamine and ethanolamine give ammonia upon periodate oxidation and if present they would interfere with the estimation of serine.

[1]*Issued as N.R.C. No. 3692.*

Selected proteins were hydrolyzed for 20 hr. in refluxing 6 *N* hydrochloric acid. The hydrolyzates were freed from excess acid by repeated vacuum evaporation and dilution, made to suitable volumes, and 1-ml. aliquots were taken for "periodate ammonia" and threonine analyses. Aliquots were analyzed for total nitrogen by the micro-Kjeldahl method. Results are given in Table I.

TABLE I

SERINE AND THREONINE CONTENT OF PROTEIN
(In gm. per 16.0 gm. total nitrogen)

	Threonine			Serine		
	This investigation	Previously reported*		This investigation	Previously reported*	
Edestin	3.6	3.3	3.3	5.7	5.4	5.4
Casein	4.9	4.0	4.8	6.9	5.9	7.5
		4.9	4.6		6.0	6.8
Ovalbumin	4.2	4.3	4.1	9.3†	7.6	8.3
		4.7			9.5	
Gluten	2.7	2.7	2.3	5.7	4.7‡	

**Taken from a compilation by Block and Bolling (1).*
†Hydrolyzates of ovalbumin are known to contain glucosamine.
‡Reported by Pence et al. (4).

Triplicate determinations of periodate ammonia agreed to within less than two per cent; this is slightly better than the agreement reported by Winnick (7) for the threonine estimations.

1. BLOCK, R. J. and BOLLING, D. The amino acid composition of proteins and foods. 2nd ed. Charles C. Thomas, Publisher, Springfield, Ill. 1951.
2. CONWAY, E. J. Microdiffusion analysis and volumetric error. Revised ed. Crosby, Lockwood & Son, London. 1947.
3. NICOLET, B. H. and SHINN, L. D. J. Biol. Chem. 139: 687. 1941.
4. PENCE, J. W., MECHAM, D. K., ELDER, A. H., LEWIS, J. C., SNELL, N. S., and OLCOTT, H. S. Cereal Chem. 27: 335. 1950.
5. REES, M. W. Biochem. J. 40: 632. 1946.
6. VAN SLYKE, D. D., HILLER, A., and MACFADYEN, D. A. J. Biol. Chem. 141: 681. 1941.
7. WINNICK, T. J. Biol. Chem. 142: 461. 1942.

RECEIVED MARCH 30, 1955.
PRAIRIE REGIONAL LABORATORY,
NATIONAL RESEARCH COUNCIL OF CANADA,
SASKATOON, SASKATCHEWAN.

A NEW TYPE OF OSMOMETER FOR AQUEOUS SOLUTIONS

BY J. L. GARDON[1] AND S. G. MASON

INTRODUCTION

Most osmometers for determining molecular weights of macromolecules have metal plate membrane supports and solvent-filled manometers. These units are not convenient for use in aqueous solutions, because the high surface tension causes air bubbles to be trapped at the metal surfaces and also leads to large capillarity errors in the manometer.

[1]*Holder of the Anglo-Paper Research Fellowship and of a Studentship from the National Research Council of Canada. Present address: Industrial Cellulose Research Ltd., Hawkesbury, Ontario.*

The units described in this paper are inexpensive to construct, simple to operate, and have the following advantages:

(1) Measurements can be carried out reasonably fast, even with low porosity membranes, by making use of large membrane areas.

(2) In membranes as big as 200 sq. cm., membrane ballooning is eliminated.

(3) The membrane area per cc. half cell volume is 10 sq. cm., which compares favorably with other designs (2).

(4) The unit is transparent.

(5) Solutions can be changed readily without taking the unit apart.

The osmometer consists essentially of a cell and a manometer attachment. Two lucite disks and two rubber rings constitute the main body of the cell (Fig. 1). The membrane is clamped between two stainless steel screens and is

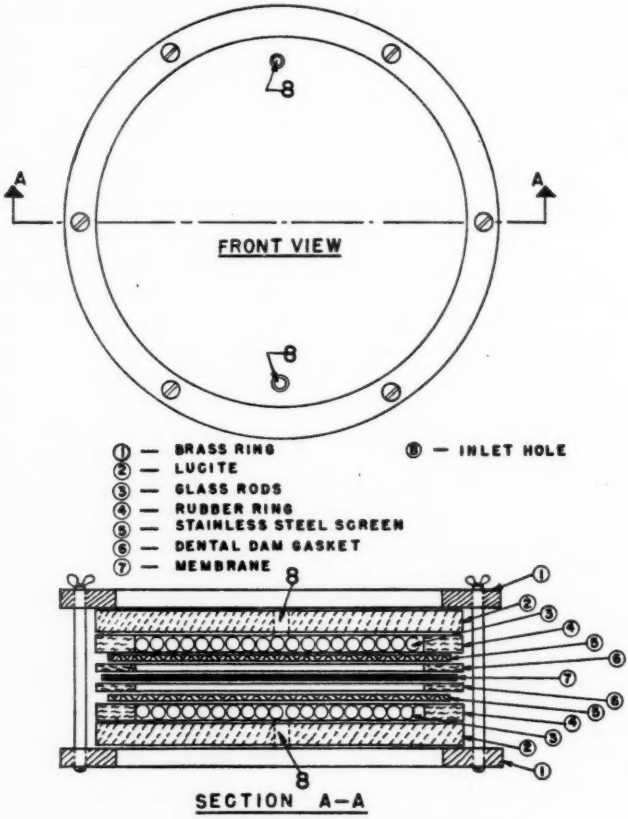

FIG. 1. Details of osmometer cell (exploded view).

supported by a layer of glass rods, closely packed parallel to one another in both cell compartments. The unit is sealed by means of the two rubber

rings mentioned above, which are compressed to the same thickness as the glass rods when the unit is assembled.

The osmotic pressure is measured in a capillary manometer which is connected to the solvent chamber. A syringe such as that from a glass syringe pipette acts as a levelling device.

All parts are individually clamped to a metal rod which forms the backbone of the unit.

CONSTRUCTION OF THE CELL

The stainless steel screens are placed between the rubber rings and the membrane. To avoid leakage through the screen meshes and to protect the membrane, two dental dam gaskets are placed between the screens and the membrane and the rubber rings are lubricated with silicone grease where they are in contact with the screens. As an additional precaution, Pyseal cement can be applied on the outside. If, for any reason, the use of silicone grease is to be avoided, four dental dam gaskets are used on each side of the screens, and Pyseal cement applied on the outside of the cell.

The components of three typical cells having active membrane areas of approximately 200, 60, and 20 sq. cm. are described in Table I. Standard

TABLE I

DIMENSIONS OF OSMOMETER CELL COMPONENTS

Active membrane area, sq. cm.	200	60	20
2 brass rings			
Inside diameter, cm.	18	11.5	6.5
Outside diameter, cm.	25.5	15	11.5
Number of holes for screws	8	6	4
2 lucite disks			
Thickness, 1 cm.			
Diameter, cm.	20.5	12.5	7.5
2 rubber rings			
Thickness, 3.1±0.1 mm.			
Inside diameter, cm.	15	10	5
Outside diameter, cm.	20.5	12.5	7.5
2 or 4 dental dam gaskets			
Inside diameter, cm.	15	10	5
Outside diameter, cm.	20.5	12.5	7.5
2 stainless steel screens			
125 mesh			
Diameter, cm.	16.5	11	6.0
Membrane			
Full diameter	17.5	11.5	6.5

pyrex rods with 3 mm. diameter are used as membrane supports. When these rods are initially packed into the cell, a 3 mm. clearance is left between them and the rubber rings to allow for expansion of the latter when the cell is tightened. The rods are vertical when the cell is in use.

There are two alternative methods of stabilizing the membrane and the stainless steel screen reinforcers.

(1) They can be supported by two disks of 12-mesh stainless steel screen instead of the glass rods. The diameters of these disks for the cells described in Table I are 14.5, 9.5, and 4.5 cm. The rubber rings for this design are cut

from sheets ½ to 1 mm. thick, corresponding to the thickness of the 12-mesh screens.

(2) Disks of 5 mm. diameter, cut out of the same rubber sheet as used to prepare the body of the cell, can also be used as stabilizers. These disks are placed in pairs opposite to each other on both sides of the membrane, using two to three such pairs per 10 sq. cm. membrane area. This method does not provide as firm a membrane support as the two others and should be used only for small cells.

The cell is clamped to the metal rod backbone through two short metal rods pressed into drilled holes in one of the brass rings.

When the largest cell is assembled, there is a tendency for the lucite and consequently for the membrane to balloon, since the pressure is applied only at the edges of the lucite disks. This can be overcome by providing additional compression at the center of the disks by means of a suitable clamp which is independent of the brass rings.

The lucite disks are simply and tightly connected with the stopcocks and the glass parts leading to the manometer attachment by tygon tubing without any cement. This tubing, of 1.5 mm. wall thickness and 10 mm. outside diameter, is placed into 8 mm. bore holes in the lucite. To introduce the tubing into the smaller hole, a piece of end is cut off conically along the length and using the tongue thus formed, the tubing is pulled into the hole. The tongue is finally cut away.

The lucite disks are equipped with the connectors before the cell is assembled, and for this purpose, each lucite disk has two holes near the opposite ends of its vertical diameter.

THE MANOMETER

The design of the glass parts assembled with the cell is shown in Fig. 2 and, as can be seen, the cells can be changed without taking the manometer unit apart. The different glass parts are connected by spherical ground-glass joints of 12 mm. sphere diameter. These joints are lubricated with silicone grease and clamped together. The glass parts can also be connected by tygon tubing. All connecting capillaries have 1 mm. bore. To ensure a constant capillary rise effect, the measuring capillary (E) should be of uniform bore; it was found that the most satisfactory bore diameter was 0.3 ± 0.003 mm. The tubes (A) and (B) are 1 cm. in diameter and are cut from the same piece of tubing. The syringe is lubricated with silicone grease and its plunger is firmly wired to a levelling screw. The toluene–water interface is in the 1.5 cm. diameter bulb below the measuring capillary. The ground-glass joint (D) is lubricated with toluene-insoluble lubricant (e.g. Fisher's Nonaq Grease) and waterproofed by coating the outside with Pyseal cement. All stopcocks have 1 mm. bore.

OPERATION

The measuring capillary is attached to the unit after the other parts have been filled with water. The bulb (D) is then filled with toluene, the capillary is sealed in, the stopcock (C) is opened, and toluene is allowed to rise into the dry capillary.

The unit is filled with solution from a pipette which is connected to the stopcock (H) by rubber tubing. To change solutions, the solution chamber is emptied and rinsed several times with the new solution. If necessary the water in the solvent chamber can be changed without disturbing the toluene–water interface, through stopcocks (G) and (F).

The measurements are carried out slightly above room temperature in a water thermostat controlled to 0.001° C. Temperature equilibrium is established in the cell within 0.5 to 1.5 hr.

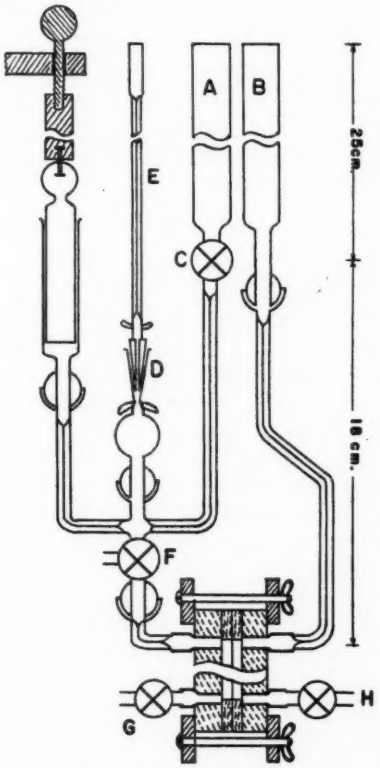

FIG. 2. Assembled osmometer unit showing details of the manometer system.

The readings are made on a scale with 0.5 mm. subdivisions behind the measuring capillary and are estimated to 0.01 cm. To avoid parallax, the scale is viewed through a cathetometer. The levels in tubes (A) and (B) are brought within 0.1 mm. of one another and the meniscus height in the measuring capillary is recorded. Stopcock (C) is then closed and the osmotic equilibrium is established by the half-sum method suggested by Fuoss and Mead (1). The difference between the original capillary meniscus reading and the one corresponding to the equilibrium is equal to the osmotic pressure

in centimeters toluene. No correction is necessary, since the density difference between water and the solution is negligible.

It is desirable to avoid excessive dilution of the solution by osmotic diffusion of solvent while the temperature equilibrium is being established. The measuring technique described above can be used only when the osmotic pressure of the solution is small, in our experience less than 3 cm. toluene. In the case of the larger osmotic pressures, it is preferable to adjust a level difference roughly corresponding to the expected osmotic pressure in tubes (A) and (B) when the instrument is being filled. Thus the driving pressure acting on the solvent is kept small until the actual measurement can be started. When temperature equilibrium is reached, stopcock (C) is closed and the osmotic equilibrium is established by the half-sum method. If the levels in tubes (A) and (B) are u and v respectively, and the meniscus levels in the capillary with stopcock (C) open and at equilibrium are w and z respectively, the osmotic pressure in gm./sq. cm. is given by

$$p = (v-u)d_{\text{solvent}} + (w-z)d_{\text{toluene}}$$

where d is the density.

The reproducibility of the capillary rise along the length of a 0.3 mm. bore capillary is ± 0.02 cm., if the precision of the bore is within 1%. If necessary, the accuracy can be improved by using larger capillaries; this however, can only be done at the expense of a longer time to osmotic equilibrium.

In addition, the accuracy of the measurements depends on the so-called "zero pressure", i.e. the finite apparent osmotic pressure existing when solutions of identical composition are placed on both sides of the membrane. In some instances, the solute may be adsorbed on the membrane thus leading to considerable difference in zero pressure before and after the measurement.

The speed of the measurements depends mainly upon the ratio of the capillary cross-section to membrane area. Using the small cell with 300 PT cellophane and the large cell with denitrated nitrocellulose and a capillary of 0.3 mm. bore, equilibrium osmotic pressures can be established to ± 0.02 cm. by the half-sum method within four hours after the temperature equilibrium is reached. This compares favorably with other designs of osmometer.

These units have been used for molecular weight determinations of fractionated samples of sodium ligninsulphonate; the results will be presented in a later communication.

1. Fuoss, R. M. and Mead, D. J. J. Phys. Chem. 47: 59. 1943.
2. Wagner, R. H. Technique of organic chemistry. Vol. I. Pt. I. *Edited by* A. Weissberger. Interscience Publishers, Inc., New York. 1949. pp. 518–540.

Received June 10, 1955.
Pulp and Paper Research Institute of Canada,
and
Chemistry Department,
McGill University,
Montreal, Quebec.

CANADIAN JOURNAL OF CHEMISTRY

Notes to Contributors

Manuscripts

(i) ***General.*** Manuscripts, in English or French, should be typewritten, double spaced, on paper 8½×11 in. **The original and one copy are to be submitted.** Tables and captions for the figures should be placed at the end of the manuscript. Every sheet of the manuscript should be numbered.

Style, arrangement, spelling, and abbreviations should conform to the usage of this journal. Names of all simple compounds, rather than their formulas, should be used in the text. Greek letters or unusual signs should be written plainly or explained by marginal notes. Superscripts and subscripts must be legible and carefully placed.

Manuscripts and illustrations should be carefully checked before they are submitted. Authors will be charged for unnecessary deviations from the usual format and for changes made in the proof that are considered excessive or unnecessary.

(ii) ***Abstract.*** An abstract of not more than about 200 words, indicating the scope of the work and the principal findings, is required, except in Notes.

(iii) ***References.*** References should be listed **alphabetically by authors' names,** numbered, and typed after the text. The form of the citations should be that used in this journal; in references to papers in periodicals, titles should not be given and only initial page numbers are required. All citations should be checked with the original articles and each one referred to in the text by the key number.

(iv) ***Tables.*** Tables should be numbered in roman numerals and each table referred to in the text. Titles should always be given but should be brief; column headings should be brief and descriptive matter in the tables confined to a minimum. Vertical rules should be used only when they are essential. Numerous small tables should be avoided.

Illustrations

(i) ***General.*** All figures (including each figure of the plates) should be numbered consecutively from 1 up, in arabic numerals, and each figure referred to in the text. The author's name, title of the paper, and figure number should be written in the lower left corner of the sheets on which the illustrations appear. Captions should not be written on the illustrations (see Manuscripts (i)).

(ii) ***Line Drawings.*** Drawings should be carefully made with India ink on white drawing paper, blue tracing linen, or co-ordinate paper ruled in blue only; any co-ordinate lines that are to appear in the reproduction should be ruled in black ink. Paper ruled in green, yellow, or red should not be used unless it is desired to have all the co-ordinate lines show. All lines should be of sufficient thickness to reproduce well. Decimal points, periods, and stippled dots should be solid black circles large enough to be reduced if necessary. Letters and numerals should be neatly made, preferably with a stencil (**do NOT use typewriting**) and be of such size that the smallest lettering will be not less than 1 mm. high when reproduced in a cut 3 in. wide.

Many drawings are made too large; originals should not be more than 2 or 3 times the size of the desired reproduction. In large drawings or groups of drawings the ratio of height to width should conform to that of a journal page but the height should be adjusted to make allowance for the caption.

The original drawings and one set of clear copies (e.g. small photographs) are to be submitted.

(iii) ***Photographs.*** Prints should be made on glossy paper, with strong contrasts. They should be trimmed so that essential features only are shown and mounted carefully, with rubber cement, on white cardboard with no space or only a **very** small space (less than 1 mm.) between them. In mounting, full use of the space available should be made (to reduce the number of cuts required) and the ratio of height to width should correspond to that of a journal page (4¾ × 7½ in.); however, allowance must be made for the captions. Photographs or groups of photographs should not be more than 2 or 3 times the size of the desired reproduction.

Photographs are to be submitted in duplicate; if they are to be reproduced in groups one set should be mounted, the duplicate set unmounted.

Reprints

A total of 50 reprints of each paper, without covers, are supplied free. Additional reprints, with or without covers, may be purchased.

Charges for reprints are based on the number of printed pages, which may be calculated approximately by multiplying by 0.6 the number of manuscript pages (double-spaced typewritten sheets, 8½ × 11 in.) and including the space occupied by illustrations. An additional charge is made for illustrations that appear as coated inserts. The cost per page is given on the reprint requisition which accompanies the galley.

Any reprints required in addition to those requested on the author's reprint requisition form must be ordered officially as soon as the paper has been accepted for publication.

Contents

Printed in Canada *by* University of Toronto Press